AN ABSTRACT OF THE THESIS OF

WALTER EARL BARNES for the Doctor of Philosophy
(Name of student) (Degree)

in Physics presented on June 8, 1970
(Major) (Date)

TITLE: THE DECAY OF Pd^{109}, Pd^{111g}, AND Pd^{111m}

Redacted for Privacy

Abstract approved: Dr. Harry T. Easterday

The decay of Pd^{109}, Pd^{111g}, and Pd^{111m} produced by thermal neutron irradiation of palladium targets has been investigated. Gamma ray energies and relative intensities have been measured with a high resolution Ge(Li) spectrometer. From energy sums and relative intensity considerations level schemes for Ag^{109} and Ag^{111} are constructed. On the basis of beta and gamma selection rules, spin-parity assignments are made for the levels of Ag^{109} and Ag^{111}.

The results of this study are compared with recent theoretical calculations.

The Decay of Pd^{109}, Pd^{111g}, and Pd^{111m}

by

Walter Earl Barnes

A THESIS

submitted to

Oregon State University

in partial fulfillment of
the requirements for the
degree of

Doctor of Philosophy

June 1971

APPROVED:

Redacted for Privacy

Professor of Physics
in charge of major

Redacted for Privacy

Chairman of Department of Physics

Redacted for Privacy

Dean of Graduate School

Date thesis is presented June 8, 1970

Typed by Opal Grossnicklaus for Walter Earl Barnes

ACKNOWLEDGEMENT

Dr. Harry T. Easterday deserves the sincerest thanks for his constant willingness to help, his sage advice, and his remarkable patience.

TABLE OF CONTENTS

LIST OF FIGURES

LIST OF TABLES

THE DECAY OF Pd^{109}, Pd^{111g}, AND Pd^{111m}

INTRODUCTION

A primary concern of low energy experimental nuclear physics is the determination of the properties of the ground and excited states of nuclei. These properties include the excitation energy, angular momentum, parity, mean life, and the electric and magnetic moments of the states. Certainly one of the most definitive methods employed to study these properties is the detection of gamma radiation emitted by nuclei as a result of transitions from one nuclear level to another. In the past the use of curved-crystal spectrometers and NaI scintillation crystals as gamma ray detectors has provided much fruitful information. However, the curved-crystal spectrometer with its excellent energy resolution of about 0.3% suffers from an exceedingly low detection efficiency, while the NaI detector has high efficiency but an energy resolution of about 7% at best. With the development of lithium-drifted germanium detectors in the early 1960's a particularly favorable compromise was struck between the requirements of resolution and efficiency, so that today the Ge(Li) spectrometer has largely replaced other types of detectors in gamma ray spectroscopy.

In the present study the excellent energy resolution of the Ge(Li) detector (0.3% at 1 MeV) has been employed in the study of the decay of Pd^{109} and Pd^{111}. Pd^{109} decays with a 13.5 hour half life by beta

emission to the excited levels of Ag^{109}, followed by gamma ray transitions to the ground state. Similarly, levels of Ag^{111} are populated by the beta decay of both the 22 minute ground state of Pd^{111} and the 5.5 hour Pd^{111m} state. Prior to the start of this investigation neither isotope had been studied with Ge(Li) detectors. Decay schemes, primarily based on NaI and beta spectrographic measurements (9, 18, 50 48, 5), showed numerous contradictions with regard to energy level and gamma transition placements. In addition it was evident that, particularly in the case of Pd^{111}, the gamma ray spectra were too complex to be adequately studied by NaI detectors.

Moreover, recent theoretical interest in the nuclei of mass $A \approx 100$ has been high, centering on the question of whether their properties are adequately described in terms of the "spherical" models: the vibrational, weak-coupling, and pairing-plus-quadrupole theories. For instance the initial failure of the pairing-plus-quadrupole model to account for the low-lying $7/2^+$ state in the odd-mass Ag isotopes (35) has led to several modifications of the theory (33, 31,59, 24). It therefore seemed evident that additional experimental information might prove useful in answering certain of these theoretical questions.

The findings of this study have revealed many new gamma ray transitions. The measurement of transition energies to within several tenths of a keV has allowed the construction of decay schemes in which

new levels are proposed. Spin-parity assignments have been made on the basis of gamma and beta branching ratios as deduced from gamma ray intensity measurements. The experimental results have then been compared to theoretical predictions.

Since the present study was begun, four papers have appeared describing Ge(Li) measurements of the Pd^{109} and Pd^{111} spectra (27, 4, 57, 3). Their results are generally in good agreement with those reported here. These papers are discussed in detail in the final chapter. In addition recent proton and alpha particle scattering and Coulomb excitation studies are discussed in conjunction with the results of the present study.

EXPERIMENTAL APPARATUS AND PROCEDURES

In the gamma ray spectroscopy system used in this study a photon is detected by the transfer of its energy to charged particles in a semiconductor detector. An electric field sweeps out the charge carriers to produce a pulse of charge proportional to the energy absorbed from the radiation. The pulse is then amplified and shaped by a preamplifier, a main amplifier, and biased amplifier to obtain at the output a pulse whose amplitude is proportional to the energy lost by the photon in the detector. The final component of the system, a multichannel analyzer, sorts the pulse according to its pulse height into one of many hundreds of energy intervals or channels. In this way the energy spectrum of a gamma emitting source may be determined.

Each of the components of the detection system will be discussed in detail.

Detector

The starting material for the lithium drifted germanium detector is p-type germanium. Lithium, which acts as a donor, is diffused into the crystal creating an intrinsic region. The p-i-n device is completed with the undrifted portion of the germanium serving as the p-type region. Because of the narrow band gap energy in germanium

and the extreme mobility of lithium ions, Ge(Li) crystals must be kept at liquid nitrogen temperature.

In order to collect free charges from the intrinsic region the n-type region is biased positively with respect to the p-type region. When a gamma ray interacts with the crystal, e.g., via the photoelectric effect, many electron-hole pairs (1 pair/3 eV) are produced as the primary and secondary electrons lose energy. The electrons are collected at the n-type region and the holes at the p-type region in a time of a few nanoseconds. The current pulse produced has a time integral or charge very nearly proportional to the energy lost by the gamma ray in the crystal (39).

The only truly fundamental limit to the energy resolution of the Ge(Li) detector is the statistical fluctuation in the number of electron-hole pairs created after an ionizing event (25). There would be no fluctuations at all if the entire energy lost by the ionizing particle were converted into ionization. On the other hand, if all the energy were mainly converted into thermal heating of the lattice, we would expect the number N of hole-electron pairs produced to have, for a Poisson distribution, a variance of N. In semiconductor detectors the situation lies between these two extremes with the result that the variance is FN, where F is a number between 0 and 1 called the Fano factor. Recent measurements suggest a Fano factor of approximately 0.12 (36), implying an ultimate resolution capability of 1.4 keV

for an energy loss of 1 MeV in germanium. However, noise in the associated electronics, particularly noise in the input stage of the preamplifier, is generally of the order of the statistical spread due to the basic charge production mechanism. The best detector systems presently available have a resolution of about 1.7 keV for 1 MeV gamma rays (47).

Detector efficiency, defined as the fraction of incident gamma rays which impart their total energy to the detector, is another important consideration. Photons interact with the detector primarily through the photoelectric effect, Compton scattering, and pair production (above 1.02 MeV). Only in photoelectric absorption, however, is the gamma ray certain to deposit its total energy in the detector. Compton scattering results in incomplete energy deposition if the scattered photon escapes from the crystal and hence contributes a lower energy continuum to the spectrum that unfortunately may mask the presence of other weak peaks. Following pair production, one or both of the annihilation gamma rays may escape the crystal, resulting in a peak whose energy is less than the full energy of the incident gamma ray by 511 or 1022 keV. Since full energy absorption does consist largely of photoelectric events, detector efficiency decreases rapidly with increasing gamma ray energy in correspondence with the photoelectric cross section. For this reason the high energy portion of the spectrum generally must be counted for

much longer periods than the low energy portion. Larger detector volumes mean greater efficiency because of an increase in single photoelectric events as well as in secondary events leading to total energy deposition, such as photoelectric absorption of Compton scattered photons. However, Ge(Li) crystals can rarely be fabricated with active volumes larger than 50 cc and hence compare poorly with the typical NaI detector as far as efficiency is concerned. For example the photopeak efficiency of a 50 cc Ge(Li) detector at 1 MeV is approximately 5% that of a 3" × 3" NaI crystal.

A figure of merit which characterizes the ability of a detector to show the presence of gamma rays in a complex spectrum is known as the peak to Compton ratio. This is the ratio of the height of the full energy peak due to gamma rays of a particular energy to the height of its mean Compton distribution. Generally this ratio is quoted for the 1.33 MeV gamma ray of Co^{60}. In a complex spectrum weak gamma rays appear as tiny bumps riding on the Compton distribution of higher energy gamma rays. The better the peak to Compton ratio, the more probable it is that these weak peaks will be observed. Clearly the peak to Compton ratio depends both upon the energy resolution and the efficiency of the detector and provides a valuable indication of the detector's performance. The best Ge(Li) detectors presently available have peak to Compton ratios of about 20/1 for 1 MeV gamma rays.

In this study a Ge(Li) detector fabricated by the Lawrence Radiation Laboratory was used. With dimensions of 1 cm^2 area × 6 mm depletion depth, it is of the planar type, i.e., a wafer of germanium whose faces are the n- and p-type regions. The resolution of the detector system was typically 3.6 keV for the 1.33 MeV gamma ray of Co^{60}. Its peak to Compton ratio at 1.33 MeV was 4.0. A ten liter dewar of the "chicken-feeder" type supplied liquid nitrogen to the backing plate of the crystal. To avoid condensation on the cold detector a Varian Associates eight liter/sec VacIon pump maintained a pressure of 10^{-7} Torr within the detector housing. A 510 volt reverse bias was applied to the detector by a RIDL Model 40-14 Power Supply.

Preamplifier

The signal from the detector consists of a pulse of charge collected on the capacitance between the detector electrodes. The preamplifier performs the function of amplifying this signal before it enters a long cable leading to the main amplifier, thus increasing the signal-to-noise ratio with respect to cable-induced noise. The preamplifier used in this study was a TMC Model 327 A. It is a charge-sensitive rather than a voltage-sensitive preamplifier, giving an output signal size independent of the input capacitance. This feature is convenient because any fluctuation in the bias voltage

applied to the detector causes the detector capacitance to vary. For low noise performance the Model 327A uses a room temperature field effect transistor in the input stage. Since preamplifier noise increases with input capacitance (52), the preamplifier is mounted as close as possible to the detector in order to minimize stray capacitance due to the lead-in wire from the detector. The output signal of the preamplifier has a rise time of about 100 nanoseconds and a decay time of about 100 microseconds.

Main Amplifier

Signals from the preamplifier were fed into an Ortec Model 440 Selectable Active Filter Amplifier. This amplifier uses active filter circuits for pulse shaping rather than passive networks. Pulse shaping has two purposes: preventing the overlap of pulses by making the pulse width short compared to the average spacing of the pulses and enhancing the signal-to-noise ratio by removing the relatively wide bandwidth noise components from the signal. Pulses of a Gaussian shape have been shown to give especially good signal-to-noise ratios (19). In the Model 440 an active RC filter produces pulses of approximately Gaussian shape, a task not easily performed by passive filter networks. In this study a 1 microsecond shaping time was used with a unipolar output wave form to obtain the optimum resolution at the typical counting rates encountered (20,000 counts per second).

Another useful feature of the Model 440 is pole-zero cancellation. In an amplifier without pole-zero cancellation the output pulse will have an undershoot that results from differentiation by the first clipping network of the exponential tail of the preamplifier output signal. Under overload conditions this undershoot is often sufficiently large to saturate the amplifier causing excessive deadtime. Furthermore, at high enough count rates the apparent amplitude of pulses overlapping such undershoots will be decreased. The result, known as baseline shift, is a smearing of the spectrum toward low energies. In pole-zero cancellation a dc path across the clipping capacitor of a differentiating network is provided in order to add an attenuated replica of the preamplifier pulse to just cancel the negative undershoot.

Biased Amplifier

The biased amplifier permits expansion of any portion of the pulse height spectrum. This it does by providing a continuously adjustable dc bias voltage to reduce the amplitude of all input pulses to the biased amplifier. The portion of the input signal above the bias level may then be amplified without saturating the amplifier. By this means the effective number of channels in the multichannel analyzer is multiplied by the biased amplifier gain.

Throughout much of this study two biased amplifiers, an Ortec

Model 408 and a RIDL Model 30-21, were used simultaneously in order that the combined capacity of two multichannel analyzers might be utilized. The Ortec Model 408 includes a baseline restoration network which forces the signal to return to baseline immediately after each pulse thus helping to reduce baseline shift at high count rates. This biased amplifier was used for expanding the low energy, high intensity portion of the spectrum. Since not all output pulses of the Model 408 Biased Amplifier may be wide enough to allow accurate amplitude analysis of the signal by the multichannel analyzer, an Ortec Model 411 Pulse Stretcher was employed to stretch the peak voltage of all pulses to a minimum pulse width.

Multichannel Analyzers

Two multichannel analyzers were used simultaneously in this study, providing a total capacity of 912 channels. Lower energy portions of the spectrum were recorded with a TMC Model 404 400-channel analyzer, while a Nuclear Data Model ND-130A 512-channel analyzer was used to record the higher energy portions. Integral linearity was stated to be 0.5% for the TMC and 0.25% for the Nuclear Data over the top 97% of the range.

THE DECAY OF Pd^{109}

First studied by Rall (53) in 1946 with the aid of a mass spectrometer, Pd^{109} was shown to beta decay to levels of Ag^{109} with a half life of about 13 hours. Siegbahn et al. (62) in 1949 made beta spectrographic measurements which indicated only a single beta component of ~1MeV end point energy feeding an isomeric level 88 keV above the Ag^{109} ground state. In 1957 Wapstra(76) reported for the first time the possibility that additional levels of Ag^{109} may be fed. Subsequent studies made with NaI spectrometers by Starner(66), Brandhorst and Cobble (9), and Eccles (18) have shown numerous gamma ray transitions in addition to the 88 keV isomeric transition. Approximately 99.9% of the beta decays of Pd^{109} proceed to the Ag^{109m} state, however (66). The decay scheme proposed by Brandhorst and Cobble (9) is shown in Figure 1.

Levels of Ag^{109} have also been studied by Coulomb excitation (1,44,5,54), (p, p') reactions (65, 21), (d, d') reactions (14), (n, n') reactions (73), and excitation by bremsstrahlung irradiation (12). The most useful of these studies are the Coulomb excitation investigations of Black and Gruhle (5) and Robinson et al. (54). The levels of Ag^{109} observed by Black and Gruhle (5) are shown in Figure 1.

During the course of this investigation several Ge(Li) studies of the Pd^{109} decay were published (27, 4, 57). A comparison of their results with the findings of this study will be found in a later section.

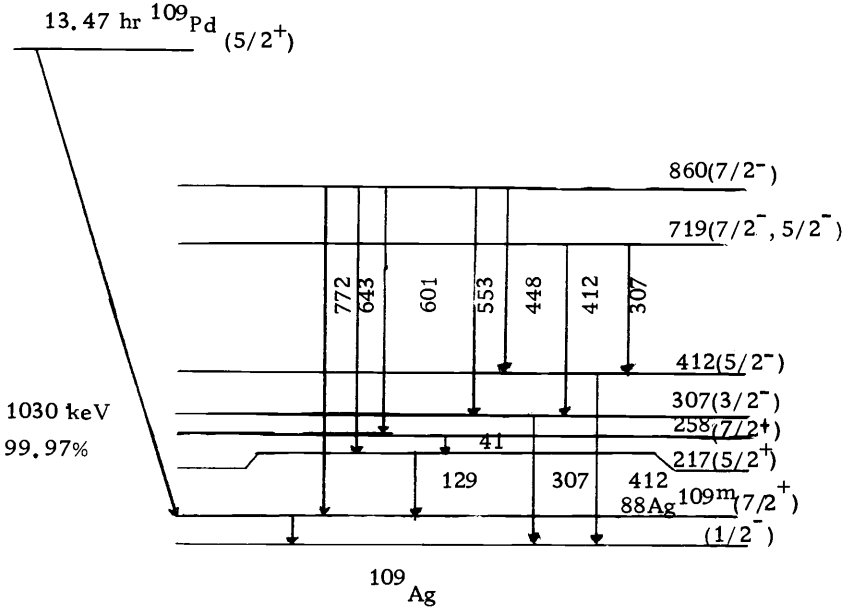

Figure 1. Decay scheme of Pd^{109}, adapted from Brandhorst and Cobble (9).

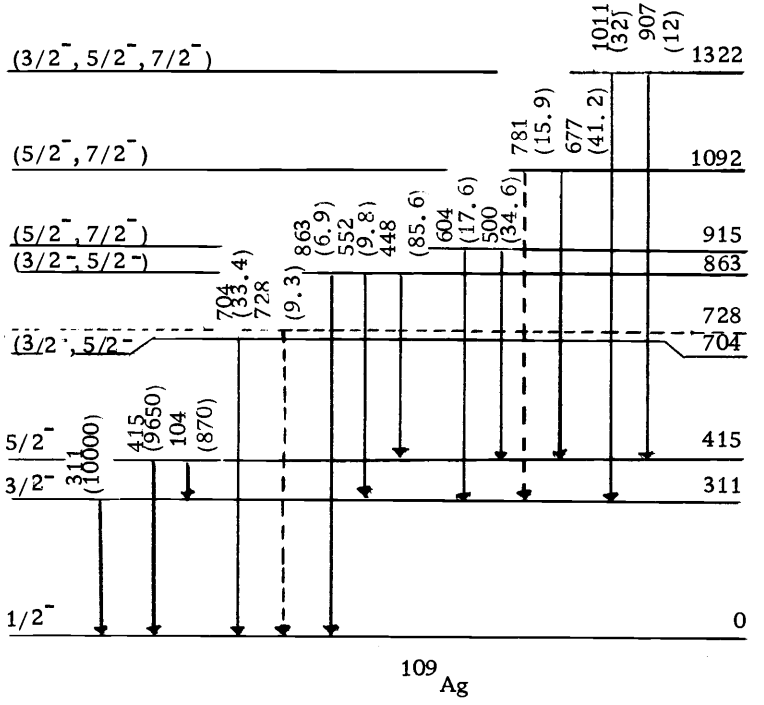

Energy levels of Ag^{109}, adapted from Black and Gruhle (5).

No use of this recent material is made in this section.

Sources of Pd^{109} were prepared by irradiating Pd^{108} in a thermal neutron flux of 10^{12} n/cm^2 sec in the Oregon State University Triga Reactor. A total of 27 irradiations of natural and isotopically enriched palladium targets were made. Irradiation times varied from 30 minutes to nine hours.

It was of great importance to identify any radioactive impurities that might be present in the source, especially since coincidence measurements could not be made, as is explained later in this section. Several steps were taken to insure the identification and, where possible, the removal of contaminants:

1. Three different types of target material were used with the assumption that any impurities would be present in varying proportions and hence could be identified by a simple comparison of spectra.

First, natural palladium was furnished by the Bureau of Mines, Albany, Oregon. Impurities were estimated to be as follows: copper (300-3000 ppm), iron (30-300 ppm), silicon (10-100 ppm). Six irradiations were made of targets of this material.

Isotopically enriched palladium (Pd^{106}, 2.8%; Pd^{108}, 94.2%; Pd^{110}, 2.1%) obtained from the Oak Ridge National Laboratories served as target material for 19 irradiations. The estimate of impurities was: silver (100 ppm), calcium (200 ppm), copper

(200 ppm), silicon (500 ppm), titanium (200 ppm).

Finally, natural palladium was obtained from Johnson, Matthey and Co., Limited, London. Estimates of impurities present were: iron (8 ppm), aluminum (1 ppm), and calcium, copper, magnesium, silicon (each less than 1 ppm). Two irradiations of this target material were made.

2. Natural palladium targets were chemically purified after irradiation by a procedure due to Glendenin (30). The target was dissolved in hot aqua regia, and silver and iron were removed by AgCl, AgI, and $Fe(OH)_3$ scavengings. Palladium was then precipitated with dimethyglyoxime, the residue filtered and allowed to dry.

No chemistry was performed on isotopically enriched targets so that they might be repeatedly re-irradiated.

3. Other radioactive isotopes of palladium which were present in the sources had to be accounted for. The natural abundance and, where applicable, the thermal neutron activation cross sections of the palladium isotopes are: Pd^{102} (0.8%, 4.8b), Pd^{104} (9.3%), Pd^{105} (22.6%), Pd^{106} (27.1%), Pd^{108} (26.7%, 12b), Pd^{110} (13.5%, 0.36 b - ground state, 0.02b - metastable state). Neutron irradiation of natural palladium produces activities of Pd^{103} (17d), Pd^{107} (7×10^6y), Pd^{109} (13h), Pd^{111} (22m), Pd^{111m} (5.5h).

Of these isotopes only Pd^{111} and Pd^{111m} are produced in sufficient quantity to interfere with the Pd^{109} activity. The isomers

of Pd^{111} subsequently decay to 7.5d Ag^{111}, which fortunately has only two major gamma ray transitions of energy 245 and 345 keV (56). To reduce the amount of Pd^{111} activity the majority of irradiations were made on isotopically enriched palladium (Pd^{108}, 94.2%; Pd^{110}, 2.1%). In any event the irradiated target was allowed to age until the most intense gamma ray of Pd^{111m}, the 175 keV isomeric transition, had disappeared.

4. A variety of bombardment times, ranging from 30 minutes to nine hours, were used to vary the relative yield of those contaminants with half lives different from that of Pd^{109}.

5. Care was taken to measure the relative intensity of the individual lines in the spectrum during a great variety of the stages of decay. In this way, any contaminant decaying at a different rate than Pd^{109} could be identified. This procedure was perhaps the most important in assigning gamma rays to the Pd^{109} decay.

6. The decay scheme (38) of every nuclide with a half life in the range of five to 20 hours was examined for correspondence with lines in the spectrum. Conversely, with the use of a table of gamma rays listed according to energy (64) it was possible to check the source of any suspicious lines in the spectrum.

Isotopically enriched targets gave spectra freest of impurities. With a few exceptions contamination lines appeared only after the Pd^{109} activity had largely decayed away. Impurities identified were

Na^{24}, Br^{82}, and Mn^{56}. Br^{82} was a major contaminant of the Johnson, Matthey and Co. sources. The Bureau of Mines material contained a host of impurities and no attempt was made to identify each of them.

The gamma ray spectrum of Pd^{109} appears in Figures 2, 4, 6. Figure 2 shows the low energy region from 50 to 320 keV. The intense 88 keV gamma ray depopulates the well known (77) 41 second first-excited state of Ag^{109}. A bremsstrahlung continuum accompanies the beta feeding of this state which, along with the Compton background from the higher energy transitions, tends to obscure the weak peaks at 104, 133, and 145 keV. By greatly expanding this region of the spectrum, sufficient peak and background definition could be obtained for energy and intensity measurements of these transitions (Figure 3).

Figure 4 shows the region from 350 to 680 keV. This and higher energy portions of the spectrum were usually recorded with a 60 mil cadmium absorber between source and detector to reduce the intensity of the 88 keV gamma ray and the problems associated with high count rate. The peak at 415 keV was found to have a line width consistently greater than that of other peaks of comparable energy, as is shown in Figure 5. This evidence is used to support the existence of two transitions of nearly the same energy in a discussion of the decay scheme below. The line at 511 keV is due to

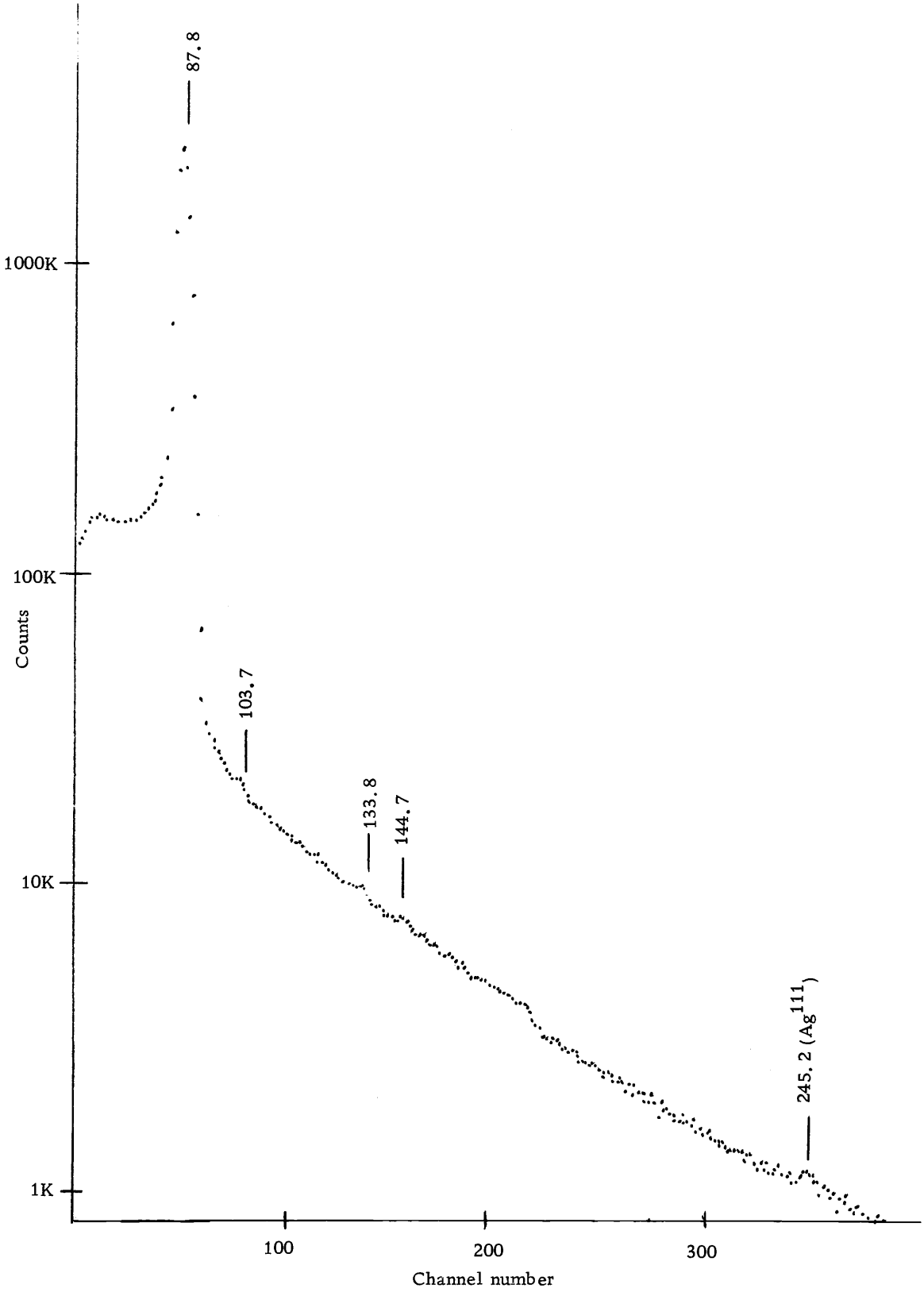

Figure 2. Low-energy gamma ray spectrum of Pd^{109}.

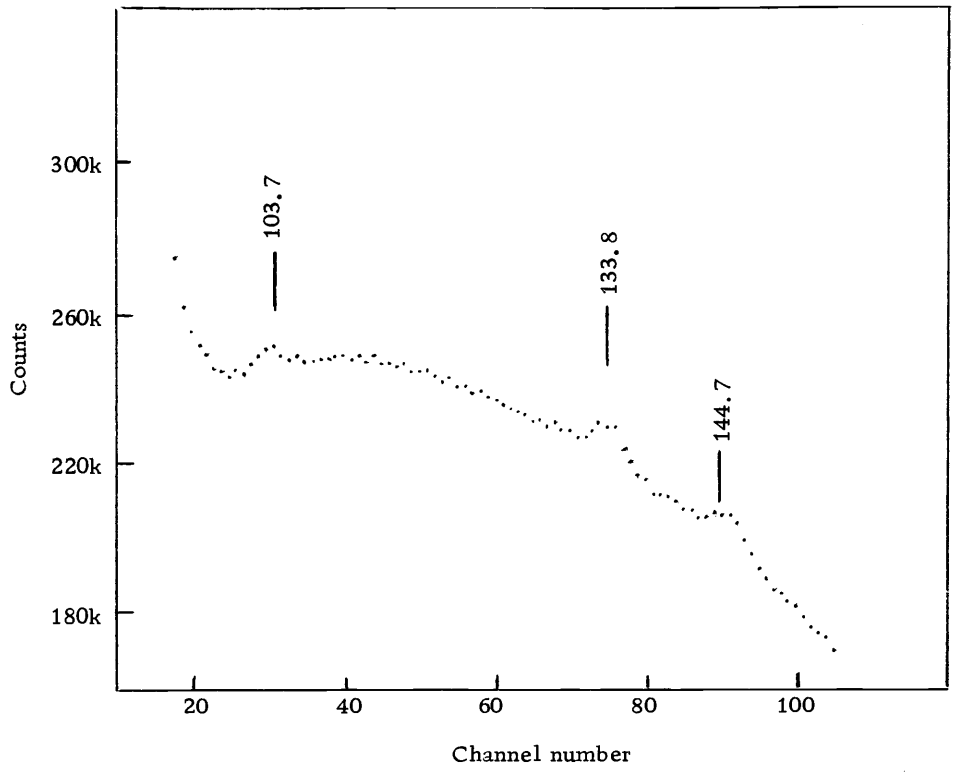

Figure 3. Detailed view of some of the low-energy peaks of Pd^{109}.

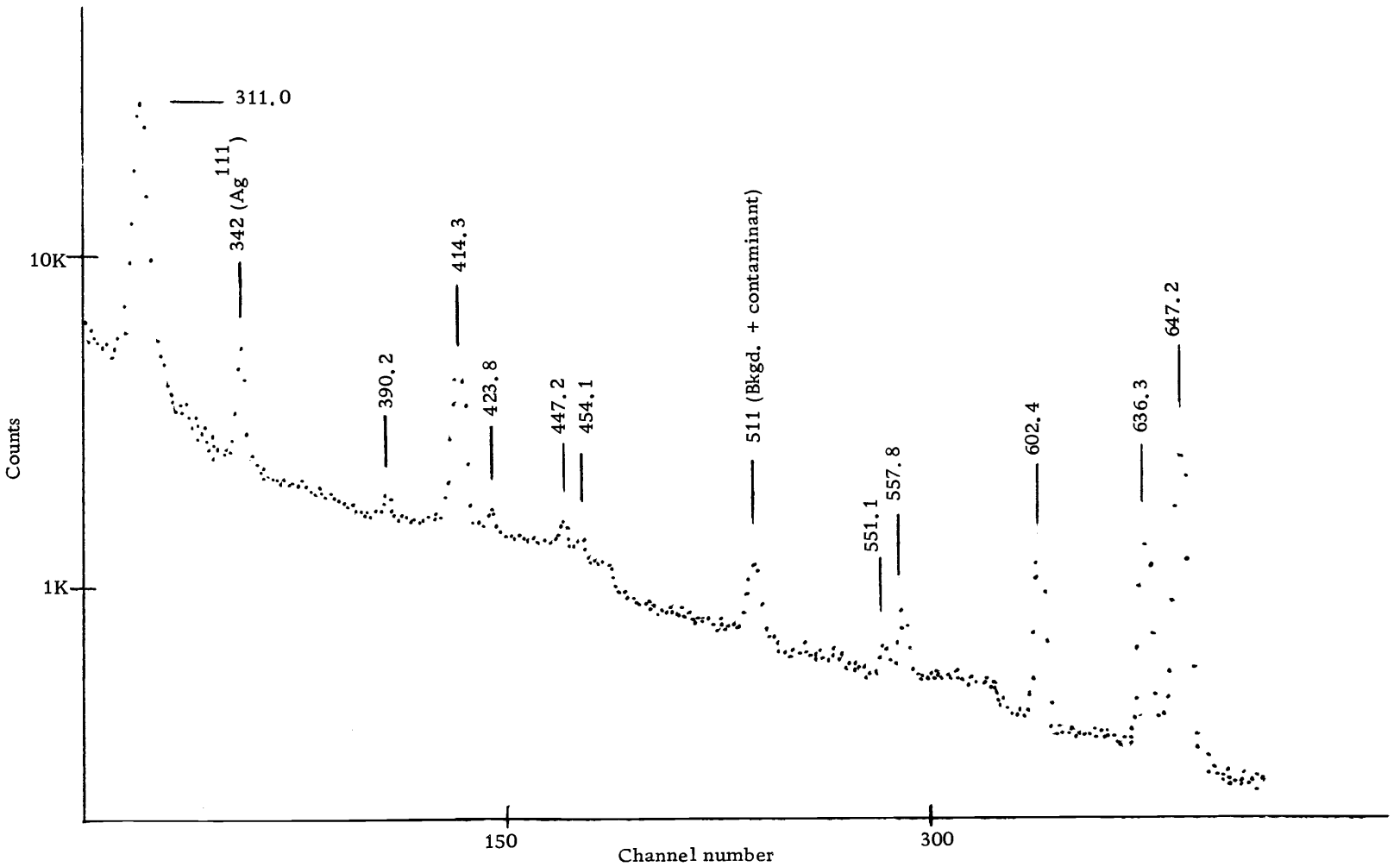

Figure 4. Intermediate-energy gamma ray spectrum of Pd^{109}.

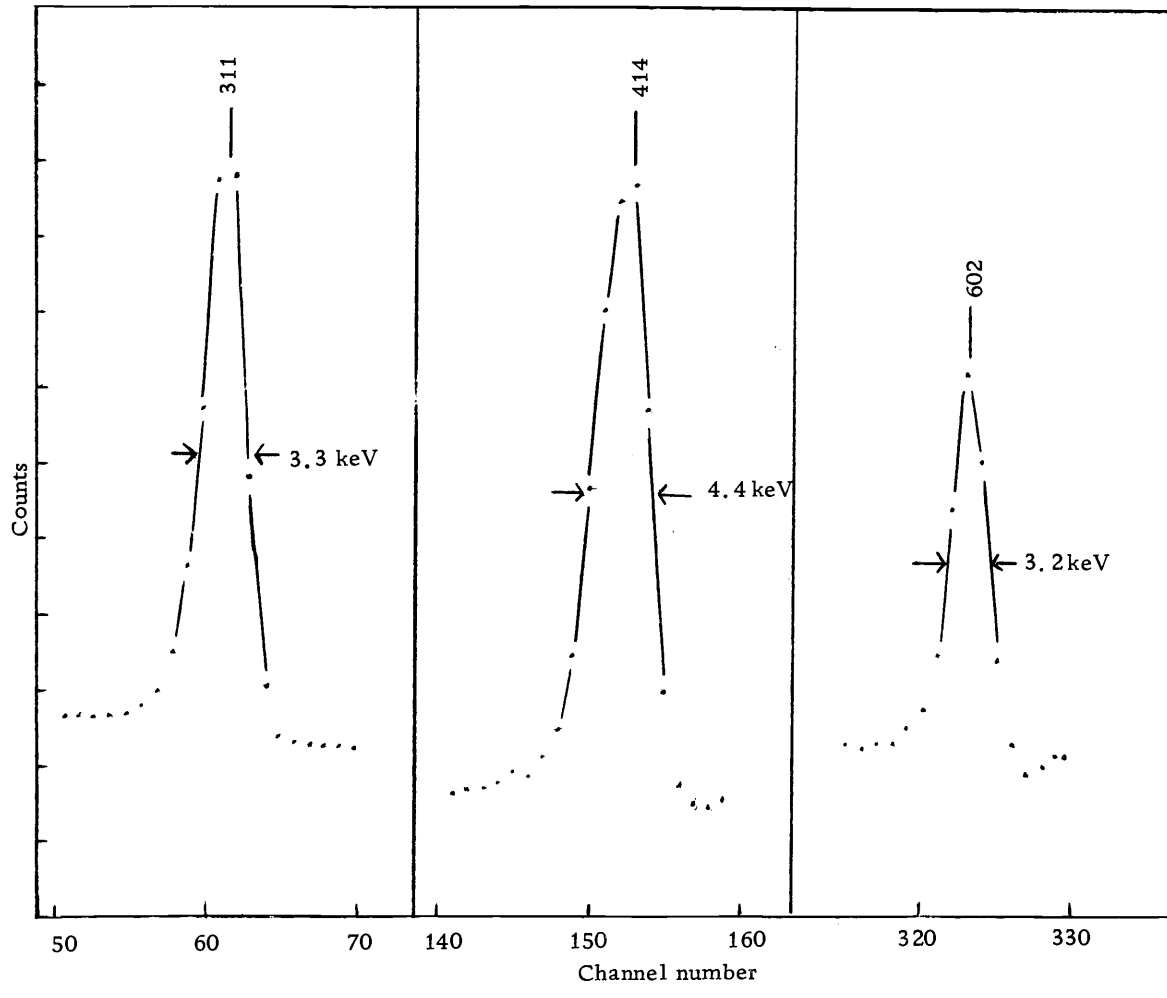

Figure 5. Comparison of the line widths (fwhm) of the 311, 414, and 602 keV peaks.

an unidentified contaminant of long half life.

The high energy portion of the spectrum from 700 to 1150 keV is shown in Figure 6. Because of the generally low intensity of transitions in this region and the poor efficiency of the detector for high energy photons, runs comparable in length to the half life of the decay were necessary. The resulting difficulty in determining accurately the relative intensity of these transitions as a function of time made assignments to Pd^{109} somewhat questionable for several high energy peaks. Above 780 keV, peaks at 823 keV and 865 keV repeatedly appeared with constant heights relative to other peaks and can be attributed to the Pd^{109} decay with reasonable certainty. The less intense peaks at 965 and 1010 keV were observed in 9 and 4 spectra respectively and also appeared to decay with a half life comparable to that of Pd^{109}.

A possible source of spurious lines is the summing of two irradiations which have been detected within the resolving time of the detector. Attempts to produce sum peaks in the recorded spectra of several standard sources failed, indicating that the detector efficiency is too small to produce summing effects at the count rates used.

An attempt to measure the gamma - gamma coincidence spectrum of Pd^{109} proved unsuccessful. A 3 in × 3 in NaI detector was gated on major peaks while observing the coincident energy spectrum with the Ge(Li) detector. Cross-over timing was employed with a

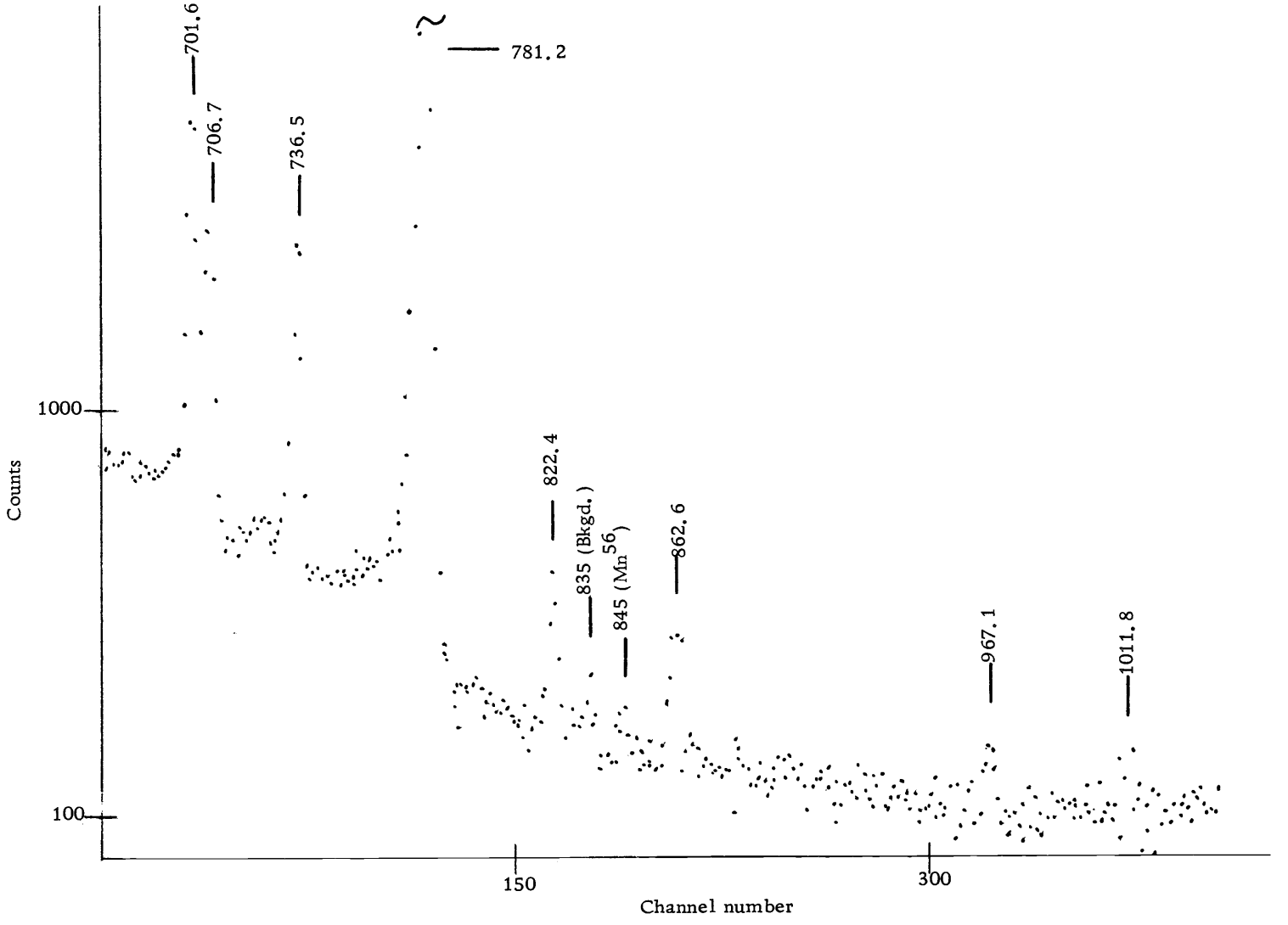

Figure 6. High-energy gamma ray spectrum of Pd^{109}.

resolving time of about 100 nsec. To prevent scattering from one detector to the other, Pb and Cd absorbers were placed between the detectors.

Even with very high singles count rates in each detector, the coincidence rate was too low to be useful. Several factors other than a lack of coincidence relationships were felt to be responsible. The first is a limitation on the maximum useable count rate due to signal degradation in the electronics. Probably the most serious cause of signal distortion at high count rates is the fluctuations in the base-line caused by random pulse bursts charging and discharging the coupling and bypass capacitors of the amplifier (29). Baseline shifts due to pulse pile-up also contribute to a smearing of the spectrum. Added to this limitation on count rate is the unfortunate circumstance that most counts result from radiation which provides no useful co-incidence information--the intense 88 keV isomeric transition, Compton scattered gamma rays, and bremsstrahlung. The use of a larger volume Ge(Li) detector and of such electronic devices (29) as long time constant amplifiers, baseline restorers, and fixed dead time circuits would mitigate these problems. A large capacity multi-channel analyzer operated in a two-parameter mode would make possible the acquisition of many coincidence spectra simultaneously.

In deducing the decay scheme, reliance was placed on the precision energy measurements made possible by the Ge(Li) detector.

Radionuclides whose gamma ray energies are accurately known were used to determine energy as a function of channel number for the multichannel analyzer at a particular amplifier gain setting. The energies of Pd^{109} lines in a spectrum recorded at the same setting were then computed by a least squares program. Peak positions were determined to within 0.1 channels by finding the mean position of the three highest points in each peak. In some cases it was necessary to correct for the steeply sloping continuum on which some peaks rode.

A serious source of systematic error associated with the energy measurements was pulse height shift with counting rate. To reduce its effect the calibration sources must be measured at the same count rate as the Pd^{109} source. For this purpose a scalar connected to the output of the amplifier served to monitor these rates. In this way shifts in the spectrum of as much as 2 keV were reduced to <0.3 keV. Shifts could not be entirely eliminated, possibly because the amount of shift depends on the character of the pulse height spectrum as well as on the count rate. An alternative method of avoiding problems connected with baseline shift is to record the calibration sources simultaneously with the Pd^{109} source. It has the disadvantage of complicating an already complex spectrum, however, thus requiring an additional series of runs to be made without the calibration sources.

Nonlinearity in the pulse height versus energy scale introduced by the amplifiers and multichannel analyzer posed an additional

problem. In principle calibration of even a nonlinear system can be done to any desired accuracy. But in practice the limited number of calibration lines that are available forces reliance on system linearity. It was found that by avoiding the lowest 100 channels of the multichannel analyzers nonlinearity could be significantly reduced. To allow for any remaining departure from linearity a quadratic equation, $E = a + bN + cN^2$ where E is the energy and N is the channel number, was least squares fit to the calibration points by the Oregon State University CDC 3300 computer. The least squares program was also weighted according to the precision with which each calibration energy was known. Typical values for the coefficients were b = 1 keV/channel, c = -0.0005 keV/(channel)^2.

Relative intensity measurements were obtained by correcting peak areas according to a detector efficiency curve established by Donald A. Walker (74). The relative efficiency curve was determined by the "pair-point" method (17) in which ratios of well-known gamma ray intensities are compared to corresponding ratios of measured peak areas in the spectrum. Some 44 data points from seven calibration sources were least squares fit in determining the curve. It is estimated to be accurate to about 10%.

In those cases in which a cadmium absorber was used, corrections of intensity data were made using the attenuation coefficients of White (79).

Table 1. Gamma ray energies and intensities observed in the decay of Pd^{109}.

Energy (keV)[a]	Relative intensity
87.8	9700 ± 1000
103.7	3.2 ± 1
133.8	3.2 ± 0.5
144.7	2.5 ± 0.7
311.0	100
390.2	2.3 ± 0.3
414.3 [b]	47.2 ± 5
423.8	1.6 ± 0.2
447.2	1.8 ± 0.3
454.1	0.92 ± 0.2
551.1	1.9 ± 0.2
557.8	6.4 ± 0.7
602.4	20.9 ± 2
636.3	31.1 ± 3
647.2	64.0 ± 6
701.6	9.3 ± 1
706.7	3.8 ± 0.5
736.5	4.4 ± 0.5
781.2	34.4 ± 3
822.4	0.47 ± 0.06
862.6	0.44 ± 0.06
967.1 ± 1 [c]	0.12 ± 0.03
1011.8 ± 1 [c]	0.11 ± 0.03

a) All errors are ±0.5 keV unless otherwise indicated

b) Complex peak

c) Not placed in decay scheme

The energies and intensities of the gamma rays observed in the decay of Pd^{109} are listed in Table 1. For all but the weakest lines, energy uncertainties are given as ±0.5 keV. This uncertainty is several times the standard error of the mean as calculated typically from at least 20 measurements and is intended to include systematic errors introduced, for example, by baseline shift. A shifting in energy of <0.3 keV is indicated by a comparison of the measured energies of several contaminant lines appearing in the spectra with their well known values. Since count rate shifts affect all energies to the same extent, it is expected that the Pd^{109} energy results have an internal consistency which is more nearly characterized by the standard errors of the mean, typically ±0.1 to 0.2 keV.

The intensities have been normalized to the area of the 311 keV peak which is taken to be 100. Uncertainties listed for the intensities include errors in measuring the areas of peaks as well as an estimated 10% error in the efficiency curve. The latter error usually accounted for the greater part of the total error.

The Decay Scheme

The proposed decay scheme appears in Figure 7. It is deduced in the following way: energy balance relationships are sought which indicate the presence of two or more cascade gamma rays and the corresponding crossover transition. Energy levels which would

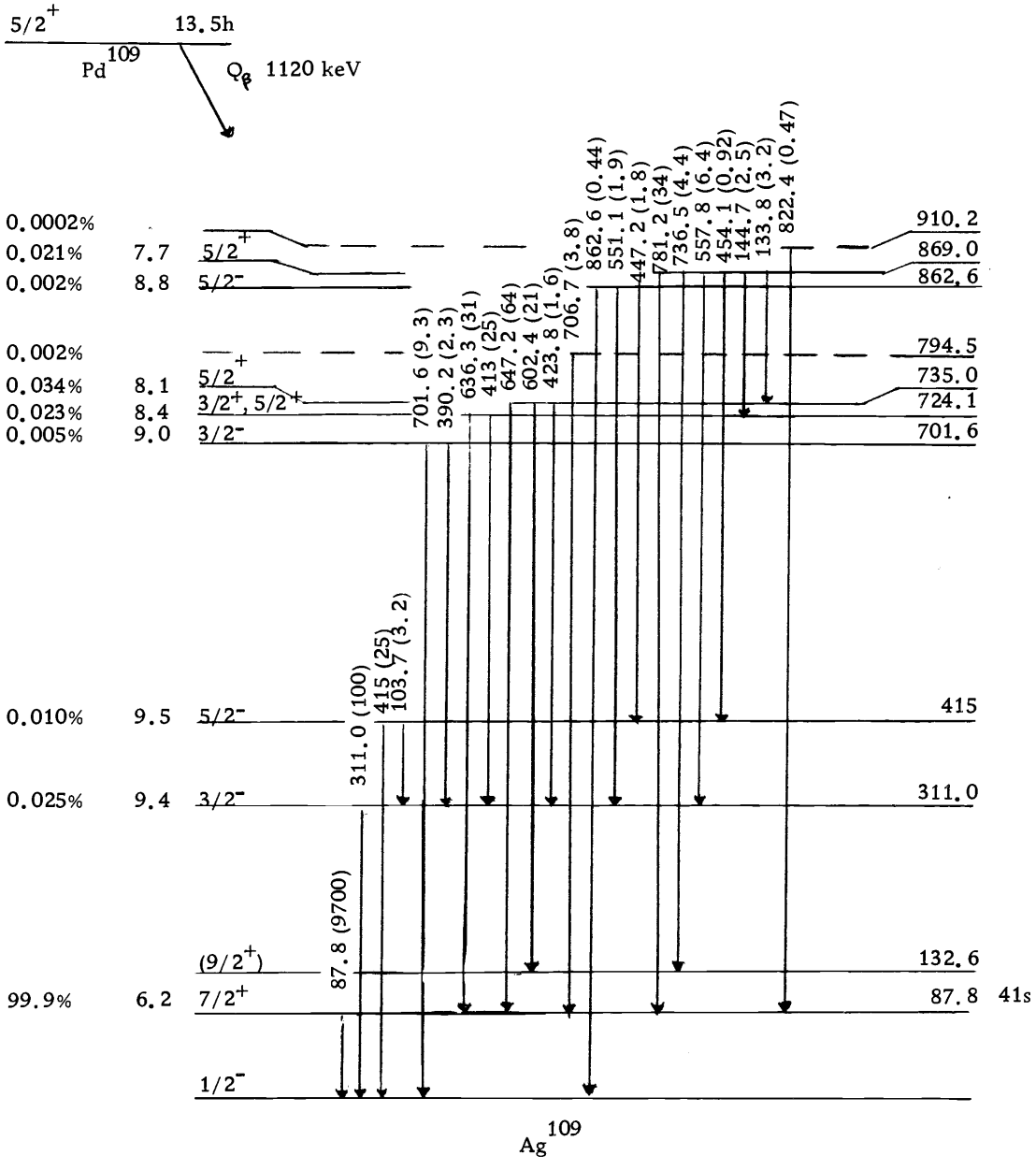

Figure 7. Decay scheme for Pd^{109}. Relative photon intensities are given by the numbers in parentheses.

accommodate these transitions are then proposed. To distinguish between bona fide and accidental energy relationships, recourse is made to previous well established gamma-gamma coincidence, Coulomb excitation, and reaction data.

The following groups of energies have the characteristic that the sum of the first two energies equals the third within the experimental error:

1) 103.7, 311.0, 414.3
2) 103.7, 447.2, 551.1
3) 103.7, 454.1, 557.8
4) 103.7, 602.4, 706.7
5) 103.7, 862.6, 967.1
6) 133.8, 423.8, 557.8
7) 133.8, 602.4, 736.4
8) 133.8, 647.2, 781.2
9) 144.7, 414.3, 557.8
10) 144.7, 557.8, 701.6
11) 144.7, 636.3, 781.2
12) 144.7, 822.4, 967.1
13) 311.0, 390.2, 701.6
14) 311.0, 551.1, 862.6
15) 311.0, 701.6, 1011.8
16) 390.2, 390.2, 781.2
17) 414.3, 447.2, 862.6
18) 414.3, 551.2, 967.1
19) 454.1, 557.8, 1011.8

From the extensive study of the electron capture decay of Cd^{109} (77), Ag^{109} is known to have an 88 keV, 41 second first excited state. The 88 keV gamma ray observed in the decay of Pd^{109} is taken to be this isomeric transition on the basis of the good energy agreement between the Pd^{109} and Cd^{109} gamma rays. In addition the relative intensity of the 88 keV transition is consistent with the

known spin and parity of the Pd^{109} ground state and the Ag^{109} ground and first excited states, as will be discussed later in this section.

Excited states at 311 keV and 415 keV have been established by (p, p'), (d, d'), and (n, n') reactions (65, 14, 73), by Coulomb excitation (1, 44, 5,54), and by beta decay studies (66, 9). These states will be assumed to give rise to the 311 keV transition and one member of the 415 keV complex. The 104 keV gamma ray of relation 1) is taken to be the transition between these two states. Supporting this assignment is the Coulomb exictation study of Black and Gruhle (5) which found a 104-311 coincidence relationship.

Relations 2) and 14) suggest the existence of a level at 863 keV accommodating the 447, 551, and 863 keV transitions. A state of approximately this energy has been established by previous studies (66, 9, 65,5,54). In particular the 863 keV level seen in Coulomb excitation (5,54) is depopulated by gamma rays whose energies and relative intensities agree closely with those of this study.

A level 558 keV above the 311 keV level, at 869 keV, is suggested by relation 3). This level also accommodates the 781 keV transition feeding the 88 keV state. The existence of the 863 and 869 keV levels is consistent with the gamma-gamma coincidence data of Starner (66) and Brandhorst and Cobble (19) which show 552-311 keV and 448-415 keV coincidence relationships. However, the

use of NaI detectors in these studies did not allow the 447, 454 keV and 551, 558 keV pairs to be resolved. That an 869 keV state is not observed in Coulomb excitation may be explained by the fact that because of the E2 character of the excitations only odd-parity states are populated.

As has been previously mentioned, the peak at 414 keV is complex as evidenced by its greater line width. Since all available gamma-gamma coincidence data (66, 9, 5) indicate a 310-415 cascade, it may be assumed that one of the 414 keV components feeds the 311 keV level from a state at 724 keV. Such a state would also accommodate the 145 keV transition between the 869 and 724 keV levels and the 636 keV transition between the 724 and 88 keV levels. Relation 11) bears on the latter of these transitions.

Relations 6) and 8) imply the existence of a level at 735 keV which is fed by the 134 keV transition originating at the 869 keV level and depopulated by the 424 and 647 keV transitions feeding the 311 and 88 keV states, respectively. The existence of this state as well as the 724 keV state is consistent with the coincidence data of Starner (66) and Brandhorst and Cobble (9) which show a 643-129 keV coincidence relationship. Since it was not possible for them to resolve the 636, 647 keV and 133, 145 keV pairs, however, their data does not provide conclusive proof of these assignments.

A level 602 keV below the 735 keV state, at 133 keV, is suggested by relation 7). The 602 keV transition must follow rather

than precede the 133 keV transition as a result of the 1113 keV excitation energy of the Pd^{109} ground state (9). Support is given to the existence of this level by coincidence data (66,9) which indicate a 601-129-45 keV relationship. No 45 keV line was observed in the spectra of this study. However, at this low energy contributions from Compton scattered gamma rays, bremsstrahlung, and electronic noise would obscure transitions were they of low intensity. Since the energy difference between the 88 keV first excited state and the proposed 133 keV state is 45 keV, a 133-602-45 keV cascade connecting the 869 keV and 88 keV levels seems likely in view of these energy and coincidence relationships.

Relation 13) suggests a level at 702 keV. There is no coincidence data bearing on either the 702 keV or the 391 keV transitions and so the existence of this state can only be considered plausible. The fact that the 702 keV gamma ray was not found to be in coincidence with the 311 keV transition (66,9)may be taken as evidence that a state at 1012 keV as suggested by relation 15) does not exist.

Two gamma rays remain to be fit into the decay scheme: the 707 keV and the 822 keV transitions. As no energy balance or coincidence relations apply, these transitions could conceivably feed the ground, first, second or, in the case of the 707 keV gamma ray, the third excited states in view of the beta disintegration energy of 1120 keV. These two transitions are taken to feed the 88 keV state for the

following reasons, which should be considered quite speculative. Since gamma rays of these energies were not observed in Coulomb excitation (5,54), it is likely that they proceed from positive-parity states. The spins of these states are $3/2^+$, $5/2^+$, $7/2^+$ unless the states are populated by gamma transitions from above or beta fed by second forbidden transtions, which is quite unlikely. Levels of spin $5/2^+$ and $7/2^+$ would preferentially decay to the 88 keV $7/2^+$ level. From a $3/2^+$ level one might expect to observe transitions to the $1/2^-$ ground state, the $7/2^+$ first excited state, and the $3/2^-$ third excited state, although it is entirely possible that only one of these transitions is intense enough to be observed.

Gamma rays of energy 967 and 1012 keV were observed in the spectra but with such low intensity that they could not be definitely assigned to the Pd^{109} decay. It is of interest to note that their energy difference is approximately that of the first and second excited states, suggesting that they might feed these states from a level at 1099 keV. These transitions are not included in the decay scheme.

In the decay scheme of Figure 7 the number in parentheses after each gamma ray energy indicates the relative intensity of the transition. The log ft values, which follow the percentage of beta branching to each state, were determined from the nomogram of Moszkowski (46). A total internal conversion coefficient of 24.2 was used for the 88 keV transition (58) and the Pd^{109} disintegration energy was taken

to be 1116 keV (9) in the calculations. In the decay scheme the intensity of the 415 keV complex has been divided equally between the (presumably) two members on the basis of the symmetric shape of the peak.

Spins and Parities in the Decay of Pd^{109}

Spin and parity assignments are based on the usual beta and gamma decay selection rules. Except for the 88 keV isomeric transition, it will be assumed that gamma ray transitions are limited to E1, M1, and E2 multipolarity.

Many of the spins and parities of the levels populated in the decay of Pd^{109} have been previously established. The ground state of Pd^{109} is known to be $5/2^+$ from the Pd^{108}(d, p) Pd^{109} reaction (13). This assignment is in agreement with the shell-model prediction which has the 13 neutrons past the closed shell of 50 in a $(2d_{5/2})^5 (1g_{7/2})^8$ ground state configuration. Hyperfine structure studies have shown the ground state of Ag^{109} to be $1/2^-$ (32) in agreement with the shell-model prediction of a $(2p_{1/2})^1 (1g_{9/2})^8$ configuration for 47 protons in the ground state. These assignments are consistent with measurements of the end point energy of the Pd^{109} beta spectrum which, when compared to the Pd^{109} disintegration energy (15), show no evidence of beta branching to the ground state of Ag^{109}.

The 88 keV Ag^{109m} isomer is known to be $7/2^+$ since the half-life and internal conversion coefficient (77) of the gamma ray transition imply an E3 multipolarity. The log ft value of 6.2 for the beta group feeding this level is consistent with an allowed ($5/2^+ \rightarrow 7/2^+$) transition.

Coulomb excitation studies have established the spin and parity of many of the excited levels of Ag^{109}. Table 2 lists those levels observed in Coulomb excitation which energy and intensity considerations imply are identical to those seen in this work. These are the levels at 311, 415, 702, and 862 keV, each of which will be discussed in detail.

The 311 keV level is assigned a spin of $3/2^-$ by Coulomb excitation studies (1, 44,5,54). This assignment is consistent with the log ft value of 9.4, indicating a first forbidden transition for the beta group associated with this level.

A $5/2^-$ spin is assigned to the level at 415 keV by the Coulomb excitation studies. The first forbidden log ft value of 9.5 is also consistent with this assignment.

Robinson et al. (54) were able to uniquely establish the spin of the 702 keV level as $3/2^-$ by measuring the angular anisotropy of the gamma rays emitted following Coulomb excitation. This assignment is supported by a first forbidden log ft value of 9.0 and gamma ray branching to the $3/2^-$ and $1/2^-$ levels but not to the $5/2^-$ 415 keV

level.

Black and Gruhle (5) indicate possible spins of $3/2^-$ or $5/2^-$ for the 863 keV level while Robinson et al (54) make the $5/2^-$ assignment. The log ft value of 8.8 associated with this level is consistent with either spin. Gamma ray branching to $5/2^-$ and $3/2^-$ levels but not to the $3/2^-$ 702 keV level and very weakly to the $1/2^-$ ground state, however, slightly favor the $5/2^-$ assignment of Robinson.

The spins and parities of the other Ag^{109} levels may be inferred from log ft values and gamma transition selection rules. Since these levels are not observed in Coulomb excitation, they are likely to have positive parity.

The 132 keV level is likely to have high spin since it is not fed from any of the $3/2^-$ or $5/2^-$ levels. There is no evidence for a 132.6 keV transition to the $1/2^-$ ground state, and so the level must decay by a 45 keV transition to the $7/2^+$ Ag^{109m} isomeric state, a gamma ray too low in energy to be detected in this study. Assignments of 7/2, 9/2, or 11/2 are possible. Of these alternatives the $9/2^+$ spin is chosen in analogy with the 126 keV second excited state in Ag^{107} whose spin has been established as $9/2^+$ (37). In view of the identical spins of the ground and first excited states of Ag^{107} and Ag^{109}, the very similar energy spacings of their three lowest levels, and the close correspondence in general between the level schemes of these isotopes (5,54), the $9/2^+$ choice seems the most plausible.

Presumably, this is the $1g_{9/2}$ state expected at low energy in the odd-mass Ag isotopes.

The level at 724 keV is depopulated by transitions to $7/2^+$ and $3/2^-$ levels. This suggests an assignment of $7/2^-$, $5/2^\pm$, or $3/2^+$ on the assumption that the gamma transitions have E1, M1, or E2 multipolarity. Choosing the positive parity members, we have $3/2^+$ or $5/2^+$ as possible assignments.

Levels at 735 keV and 869 keV both feed states whose spins range from $3/2^-$ to $9/2^+$. The only likely positive parity assignment under these circumstances is $5/2^+$.

Not enough is known about the proposed levels at 795 keV and 910 keV to make meaningful spin-parity assignments.

It is of interest to note the high log ft values encountered in the Pd^{109} beta decay. Beta transitions to the 724, 735 and 869 keV levels which are expected to be allowed have log ft values ranging from 7.7 to 8.4. The first forbidden transitions in Pd^{109} have log ft values which in all cases exceed 9.0. This phenomenon has been observed in the neighboring odd-A nuclei and is discussed in a later section.

Table 2. Gamma ray energies and branching ratios from levels observed in both Coulomb excitation and in the Pd^{109} decay.

Level (keV)	This work		Black and Gruhle (5)		Robinson et al. (54)	
	Eγ (keV)	γ-branching (%)	Eγ (keV)	γ-branching (%)	Eγ (keV)	γ-branching (%)
311	311.0	100	311	100	311.3	100
415	414	91	415	92	415.1	95.3
	103.7	9	104	8	103.5	4.7
702	701.6	80	704	100	701.7	81
	390.2	20			390.7	19
862	862.6	10	863	4	862.8	9
	551.1	46	552	51	551.1	41
	447.2	44	448	45	447.3	50

THE DECAY OF Pd^{111}

Only a few studies of the energy levels of Ag^{111} have been made and these have been largely limited to the investigation of the decay of Pd^{111} using scintillation detectors. In 1952 McGinnis (43) reported the production of 22 minute Pd^{111g} and 5.5 hour Pd^{111m} by a 20 MeV deuteron bombardment of natural palladium. His studies indicated a 2150 keV beta group and a 170 keV isomeric transition associated with the Pd^{111m} decay and a 2100 keV beta group feeding a low energy isomeric state in Ag^{111} in the decay of 22 minute Pd^{111g}. Shell model predictions give the following spin-parity assignments for these states: Pd^{111g} $(5/2^+)$, Pd^{111m} $(11/2^-)$, Ag^{111g} $(1/2^-)$, Ag^{111m} $(7/2^+)$. Scintillation spectrometer studies by Pratt and Cochran (50), Eccles (18), and Pandharipande et al. (48) have disclosed a complex gamma ray spectrum associated with the Pd^{111} decay. The decay scheme proposed by Pandharipande et al. (48) is shown in Figure 8. This complexity is not surprising in view of the large beta disintegration energy and the feeding of Ag^{111} levels from two states of widely different spin.

While this study was in progress, two investigations of the decay of Pd^{111} using Ge(Li) detectors were published (57, 3). A comparison of the results of these studies will be made in a later section and no reference to them will be made in the discussion

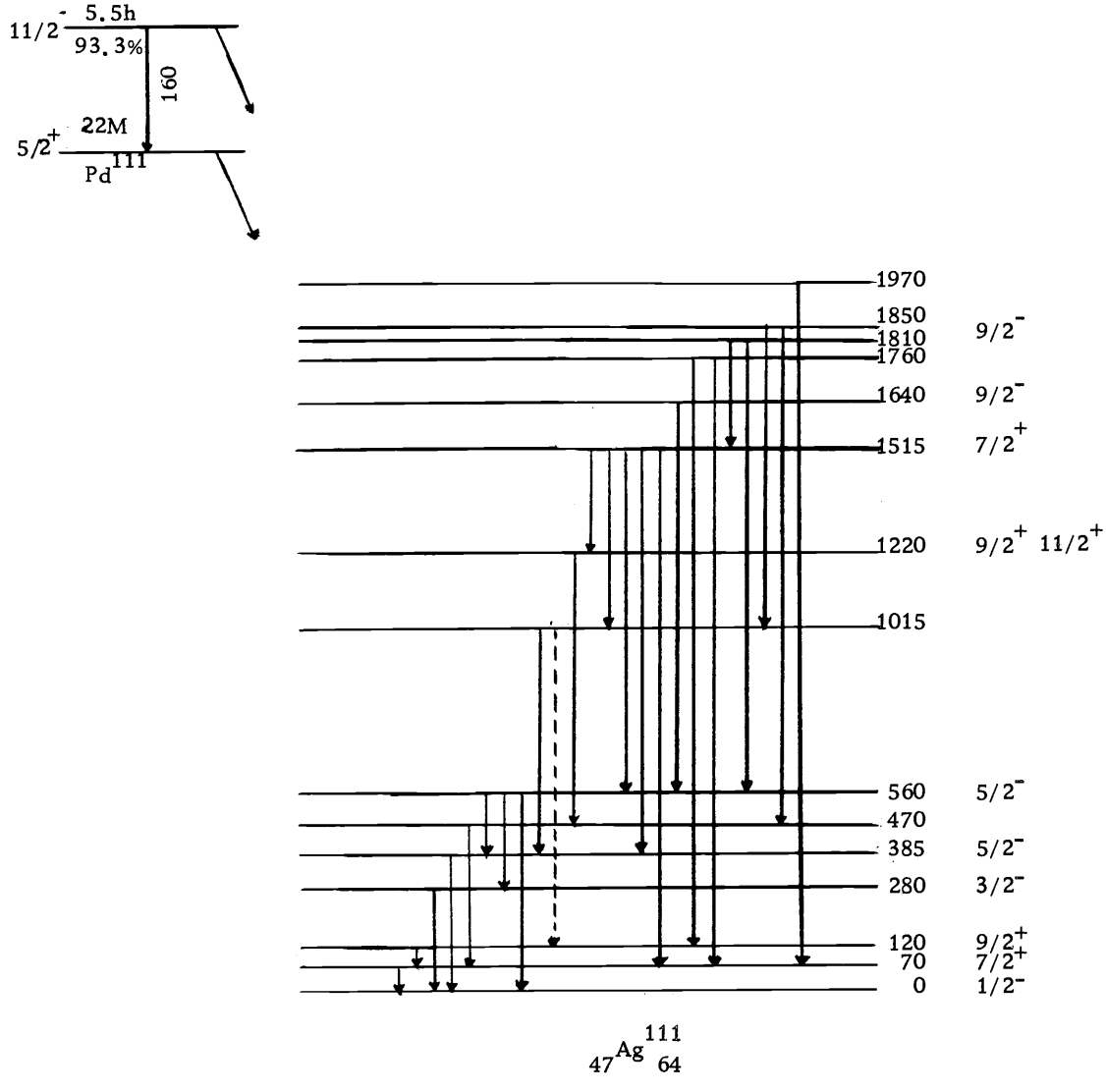

Figure 8. The decay of Pd^{111} and Pd^{111m}, adapted from Pandharipande et al. (48).

below.

Sources of Pd^{111} for this study were produced by irradiating isotopically enriched Pd^{110} (Pd^{104}, 0.5%; Pd^{105}, 0.5%; Pd^{106}, 1.0%; Pd^{108}, 10.6%; Pd^{110}, 87.5%) with thermal neutrons. Samples of 10 to 20 mg were irradiated in a flux of 10^{12} neutrons/cm^2-sec at the Oregon State University Triga Reactor for one hour periods. In total 26 irradiations were made. Natural palladium targets could not be used since the natural abundance and neutron activation cross section of Pd^{108} produce large amounts of Pd^{109}. Even with the use of targets enriched in Pd^{110} the presence of Pd^{109} in the sources tended to mask those portions of the spectrum in proximity to the more intense lines of Pd^{109}.

Most of the same procedures mentioned in the last section were used to identify radioactive contaminants in the sources. Impurities in the samples were specified by the manufacturer as follows: silver (100 ppm), calcium (200 ppm), copper (200 ppm), silicon (500 ppm). No interfering activities of these elements were detected. Contaminants which were identified were Na^{24}, Mn^{56}, and In^{116}. These contaminants did not appear in large enough amounts to make chemical purification necessary. Therefore, sources were counted after the completion of irradiation as soon as they could be transported from the reactor to the laboratory, a period of about 15 minutes.

Another "contaminant" is 7.5 day Ag^{111} which decays to Cd^{111}

with the emission of two gamma rays having energies of 245 keV and 345 keV. Re-irradiation of the several targets was alternated to prevent large accumulations of this long-lived isotope.

Thermal neutron irradiation of Pd^{110} produces both 22 minute Pd^{111g} and 5.5 hour Pd^{111m} in relative proportions that depend on the cross section for the formation of each state, 0.2 b for Pd^{111g} and 0.04b for Pd^{111m} (23), and the length of irradiation.

Gamma lines associated with the Pd^{111m} decay have a 5.5 hour half life while, because of the 172 keV isomeric transition to the Pd^{111} ground state, the half life of lines associated with the Pd^{111g} decay is initially 22 minutes increasing to 5.5 hours as equilibrium with Pd^{111m} is established. An irradiation time of one hour as used in this study produces an initial supply of Pd^{111g} large enough so that Pd^{111g} lines decay with a 22 minute half life for 1-2 hours. When equilibrium has been established, lines of the Pd^{111m} decay are generally the more prominent. It is therefore possible to study the two spectral components separately to a large extent by comparing spectra taken shortly after irradiation with those taken many hours later.

Experimental techniques used to study Pd^{111} were similar to those described in the section concerning Pd^{109} with a few exceptions. In order to follow the half lives of the various lines of the spectra, the Pd^{111} source was typically counted for four periods

of 20 minutes each. Then the source was moved closer to the detector and counted again for about six periods of 100 minutes each.

Uncertainties in energy measurements caused by count rate shifts were largely eliminated in the Pd^{111} study by the use of the contaminant lines of In^{116}, Mn^{56}, Na^{24}, Pd^{109}, and Ag^{111} as internal calibration sources. The energies of impurity lines were used both as checks on the energy values determined by external calibration sources and in other instances as calibration values themselves.

For many of the same reasons mentioned in the discussion of the Pd^{109} decay, gamma-gamma coincidence measurements were not possible. Additional difficulties in the case of Pd^{111} are its shorter half life and the greater complexity of its gamma ray spectrum.

Some gamma ray transitions depopulate levels fed only in the decay of Pd^{111m} or Pd^{111g} while others belong to both decays. In this regard it is convenient to consider the total gamma ray spectrum as the sum of two components, the Pd^{111m} and the Pd^{111g} spectra. Every line in the Pd^{111m} spectrum has a constant relative intensity in time and similarly for every Pd^{111g} line. The relative contribution of each component to the total spectrum at any given time may be determined, knowing the relative intensities of a pure Pd^{111g} and a pure Pd^{111m} line. Clearly, the 172 keV isomeric transition is a pure Pd^{111m} line. By following the decay of the major transitions

seen shortly after irradiation, the 1388 keV gamma ray was found to belong exclusively to the Pd^{111g} decay, its half life deviating only slightly from 22 minutes after 60 minutes of counting. A plot of intensity versus time for several of the more prominent lines is given in Figure 9.

Consider the area A of a peak in the gamma ray spectrum which is due to a "mixed" transition, belonging to the decay of both Pd^{111g} and Pd^{111m}. If G and M are the areas of pure Pd^{111g} and Pd^{111m} peaks in the same spectrum, then

$$A = aG + bM,$$

where a and b are the relative intensities of the mixed line in the Pd^{111g} and Pd^{111m} spectra, respectively. By finding the values of A, G, and M in a second spectrum taken at a different stage in the decay, it is possible to solve for a and b. In this way the relative intensity of each line in the Pd^{111g} and Pd^{111m} spectra may be determined.

The energies and relative intensities of the gamma rays observed in the decay of Pd^{111g} and Pd^{111m} are listed in Tables 3 and 4. Energy uncertainties are the standard error of the mean as calculated from at least ten measurements. The intensities have been normalized to the area of the 1388 keV peak in the decay of Pd^{111g} and the 172 keV peak of Pd^{111m}. Uncertainties listed for the intensities include an estimated 10% error in the efficiency curve and

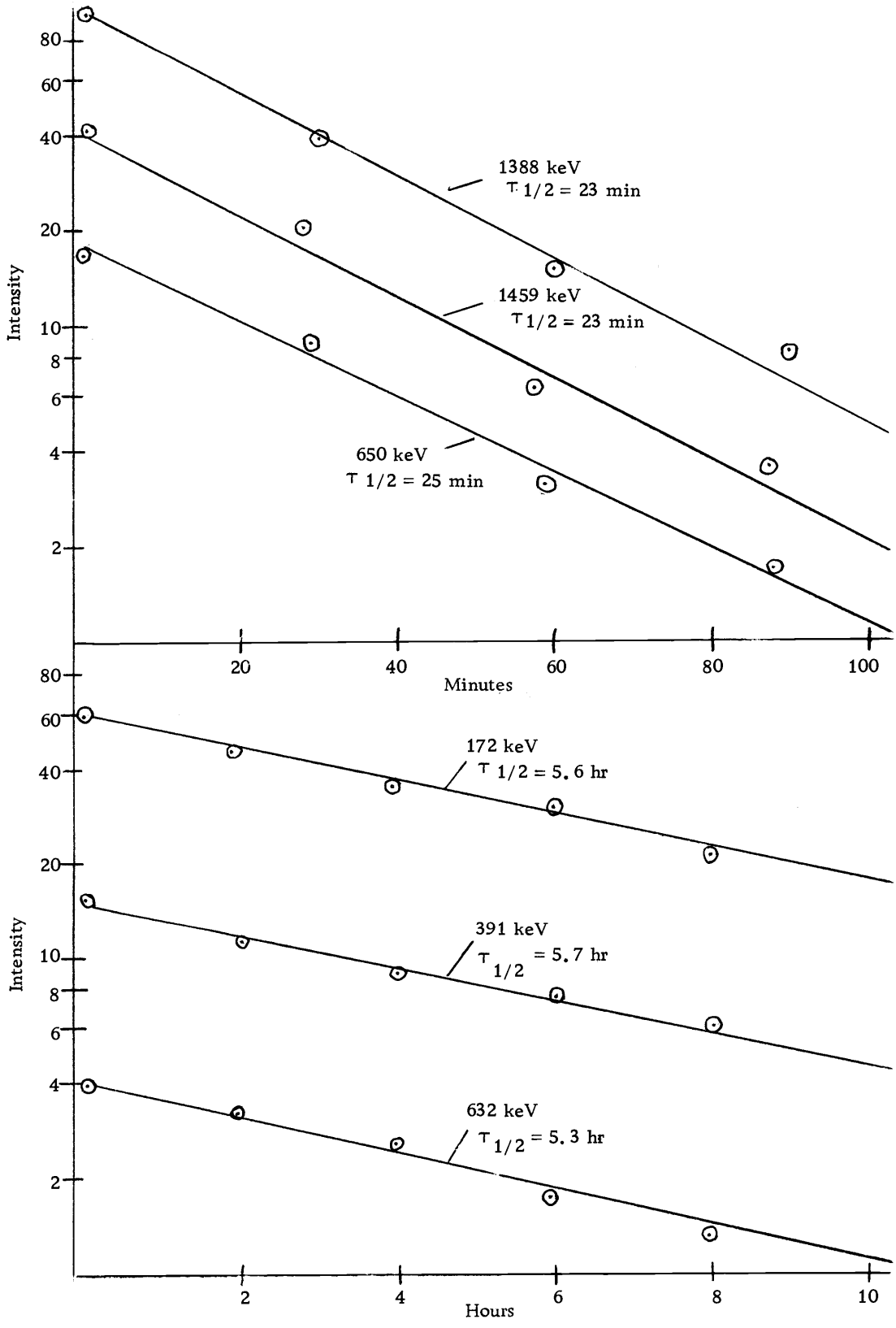

Figure 9. Intensity of major peaks of Pd^{111g} and Pd^{111m} as a function of time.

the standard error of the mean in measuring the areas of peaks.

Figures 10, 11, and 12 show the gamma ray spectrum of Pd^{111g}. The spectrum of Pd^{111m} in equilibrium with Pd^{111g} is shown in Figures 13 through 16. Many peaks are of such low intensity that a single spectrum is not sufficient to establish their identity conclusively. These peaks are labeled in the figures. Since some 26 irradiations were made and typically eight spectra per irradiation were taken, it was possible to gather sufficient evidence to determine the energies and intensities of these weaker lines.

In regions close to the more intense lines of Pd^{109} an unfolding of peaks was performed to reveal any hidden Pd^{111} gamma rays. The unfolding was accomplished by subtracting a Pd^{109} spectrum of proper energy/channel spread from the Pd^{111} spectrum. A significant portion of the 415 keV peak in Pd^{111m} was found to be due to Pd^{109}. The additional presence of an intense 417 keV peak due to 54 minute In^{116} masks this region of the Pd^{111g} spectrum. Subtraction of the 647 keV transition of Pd^{109} revealed a peak at 645 keV in the Pd^{111m} spectrum. Figures 17 and 18 show the subtracted spectra in the 415 keV and 645 keV regions.

The 415 keV peak, as shown in Figure 17, is broader than peaks of comparable energy, indicating two or more gamma transitions of nearly equal energy. Because of the smooth, symmetric appearance of the peak, it is likely to be composed of two gamma rays of

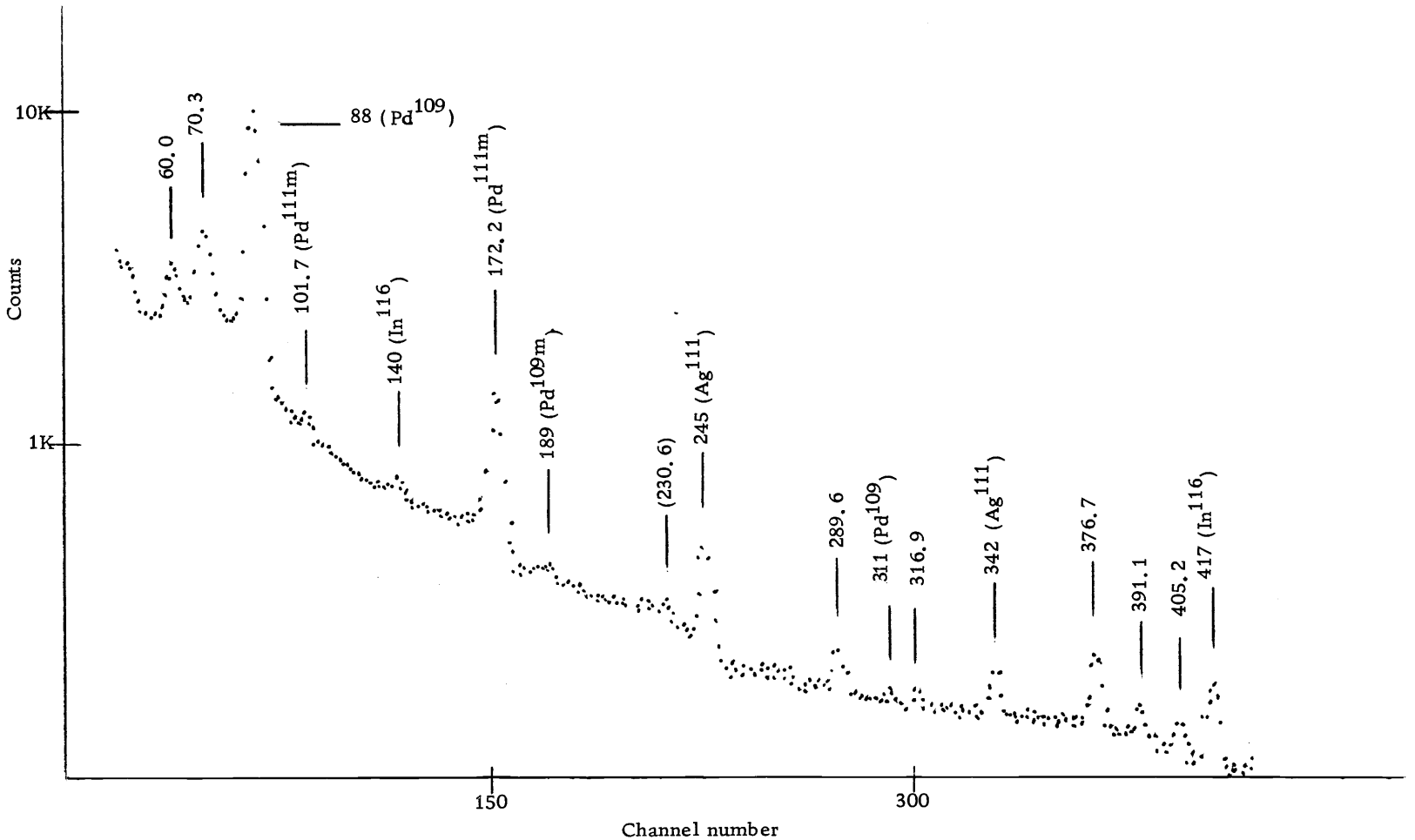

Figure 10. Low-energy gamma spectrum of Pd^{111g}. The energies given in parentheses indicate gamma rays whose presence cannot be conclusively established on the basis of this spectrum alone.

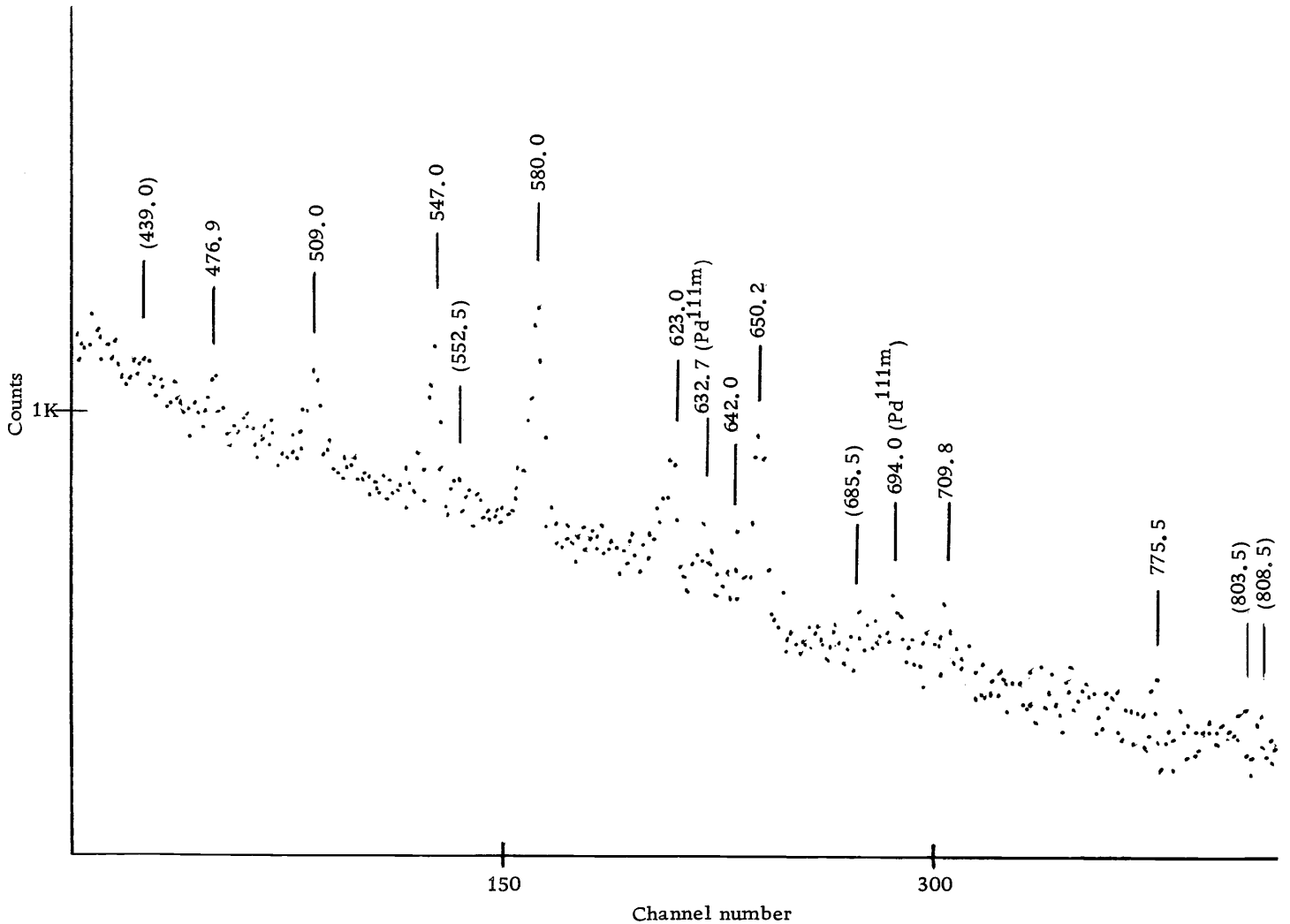

Figure 11. Intermediate-energy gamma ray spectrum of Pd^{111g}. The energies given in parentheses indicate gamma rays whose presence cannot be conclusively established on the basis of this spectrum alone.

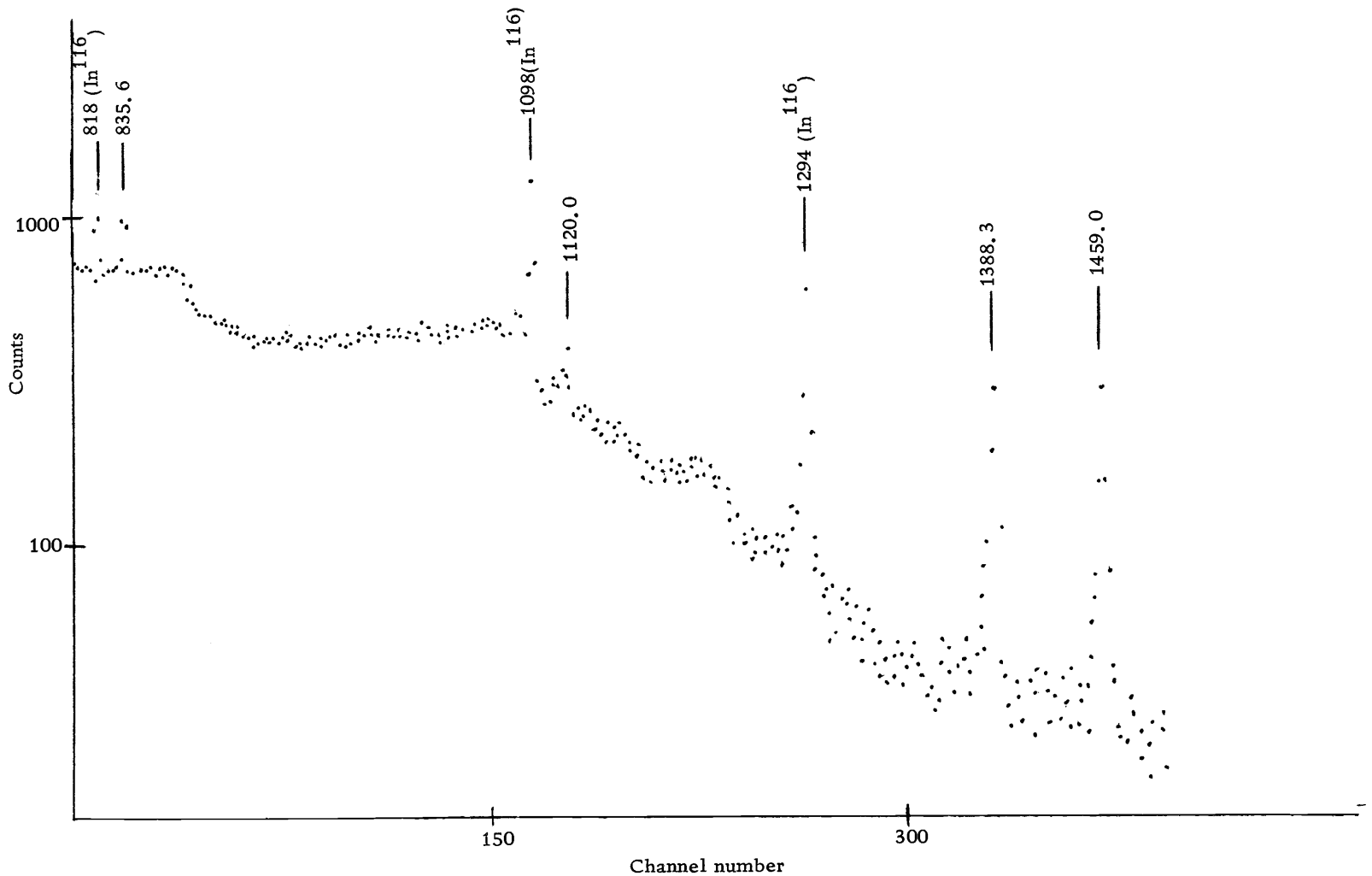

Figure 12. High-energy gamma ray spectrum of Pd^{111g}.

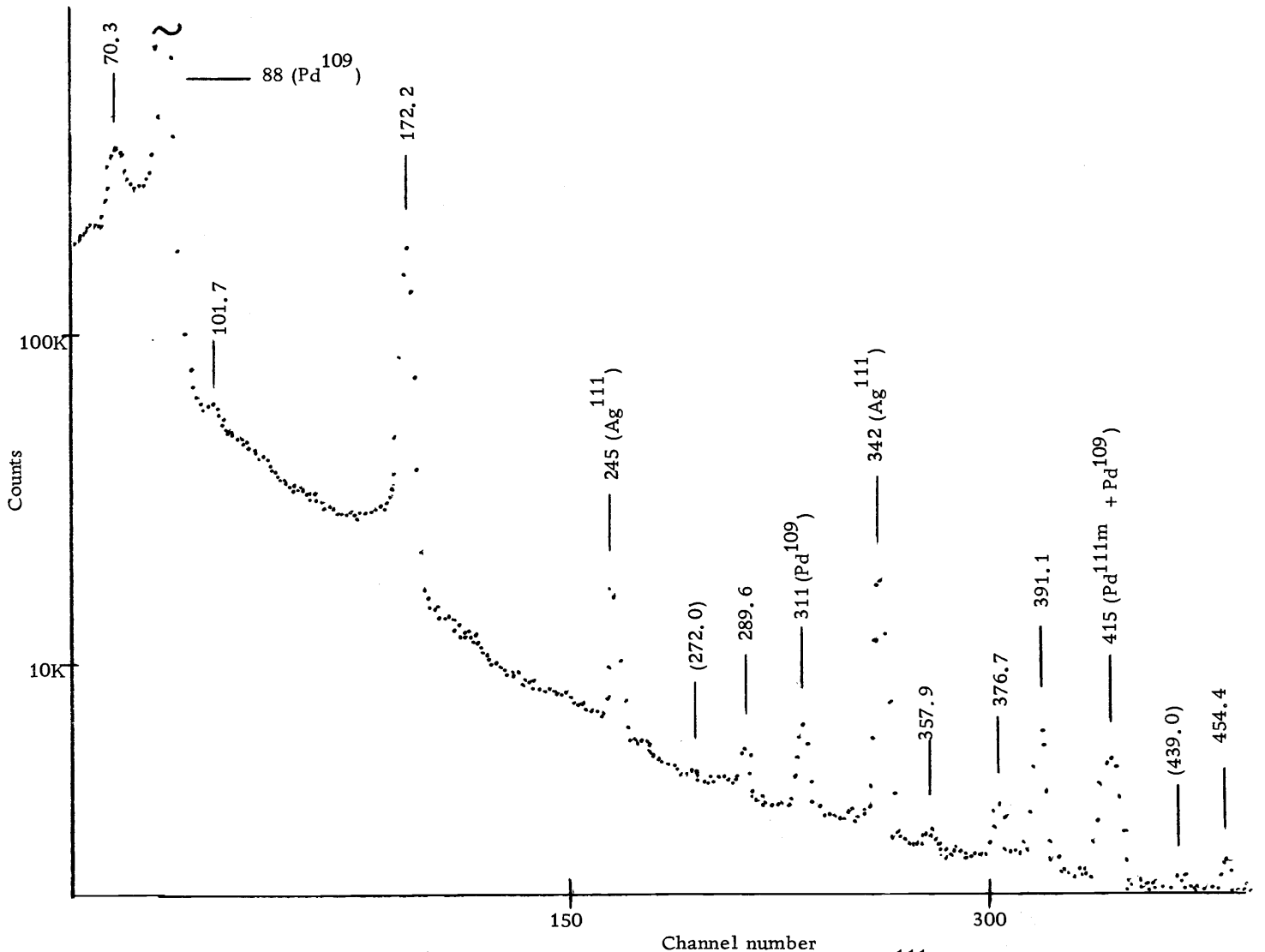

Figure 13. Low-energy gamma ray spectrum of Pd^{111m}.

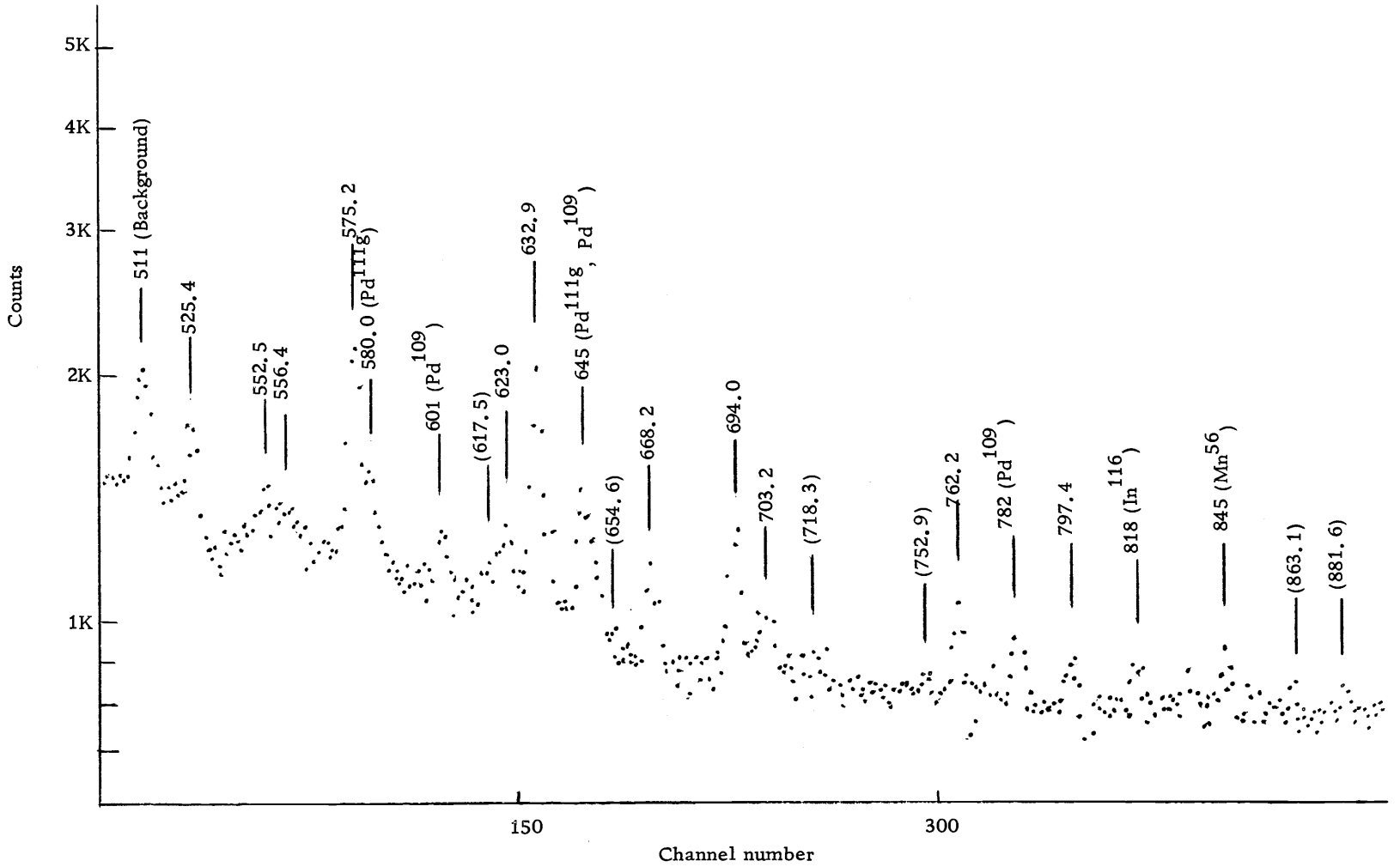

Figure 14. Intermediate-energy gamma ray spectrum of Pd^{111m}. The energies given in parentheses indicate gamma rays whose presence cannot be conclusively established on the basis of this spectrum alone.

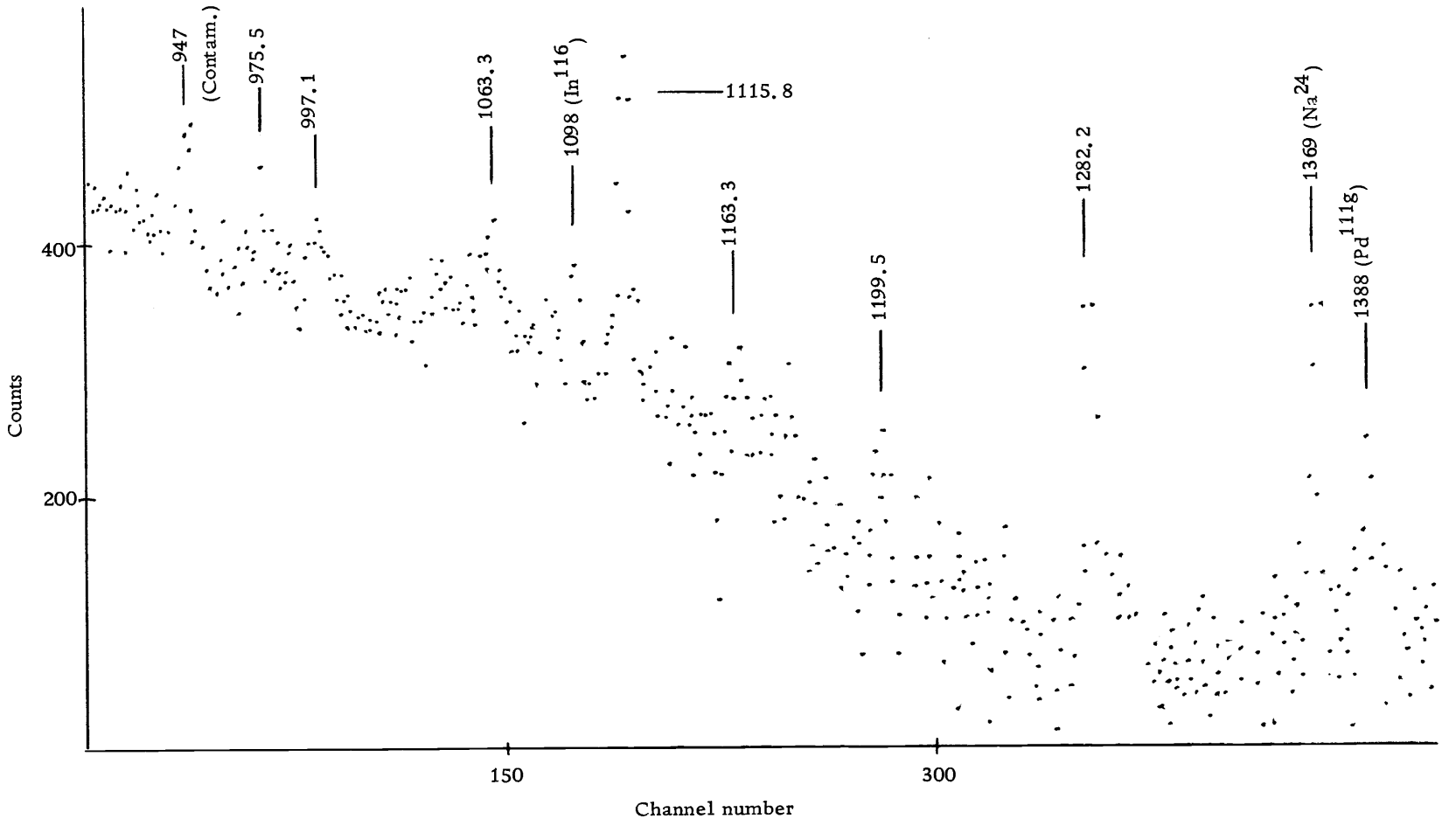

Figure 15. Intermediate-energy gamma ray spectrum of Pd^{111m}.

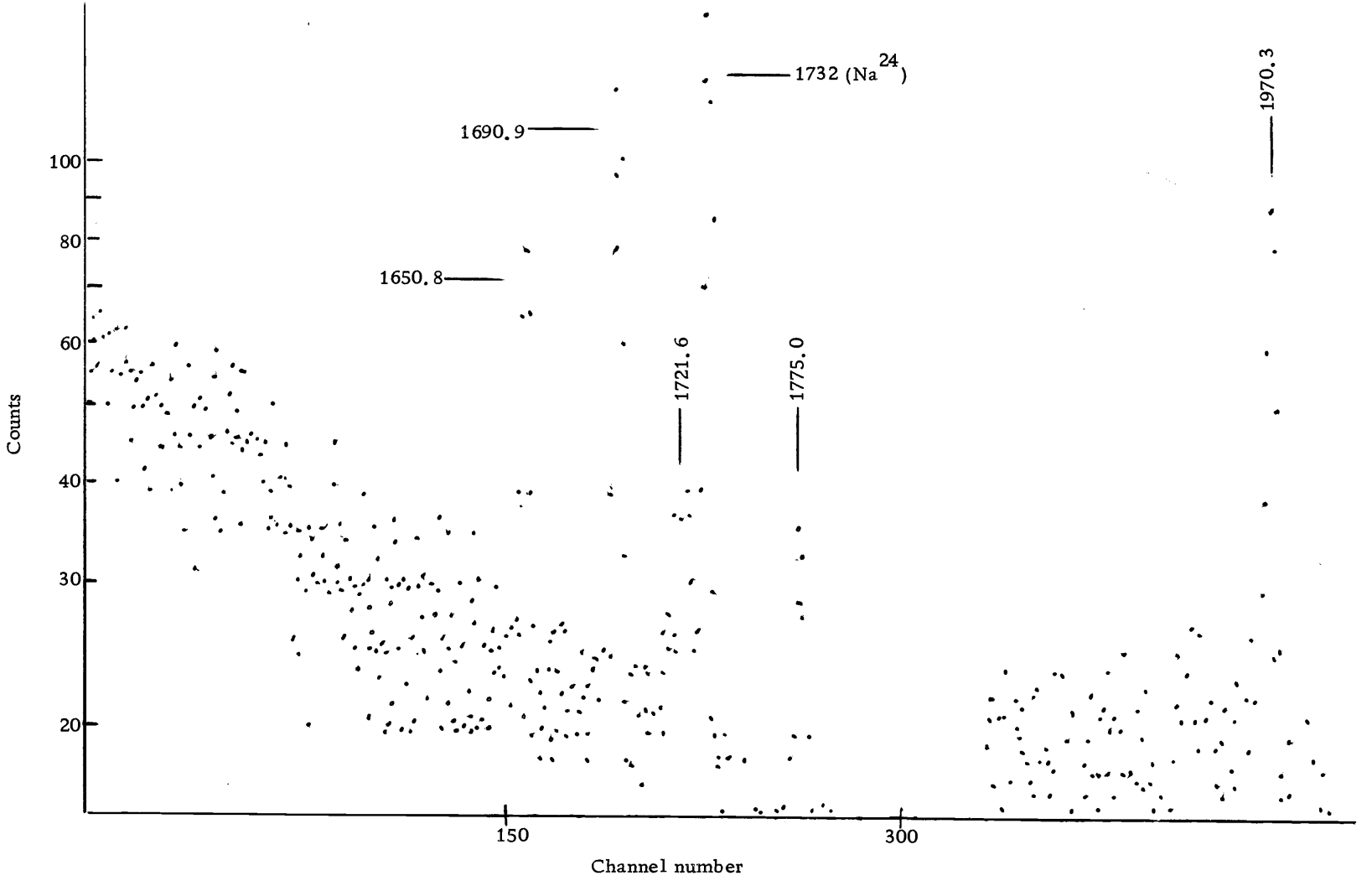

Figure 16. High-energy gamma ray spectrum of Pd^{111m}.

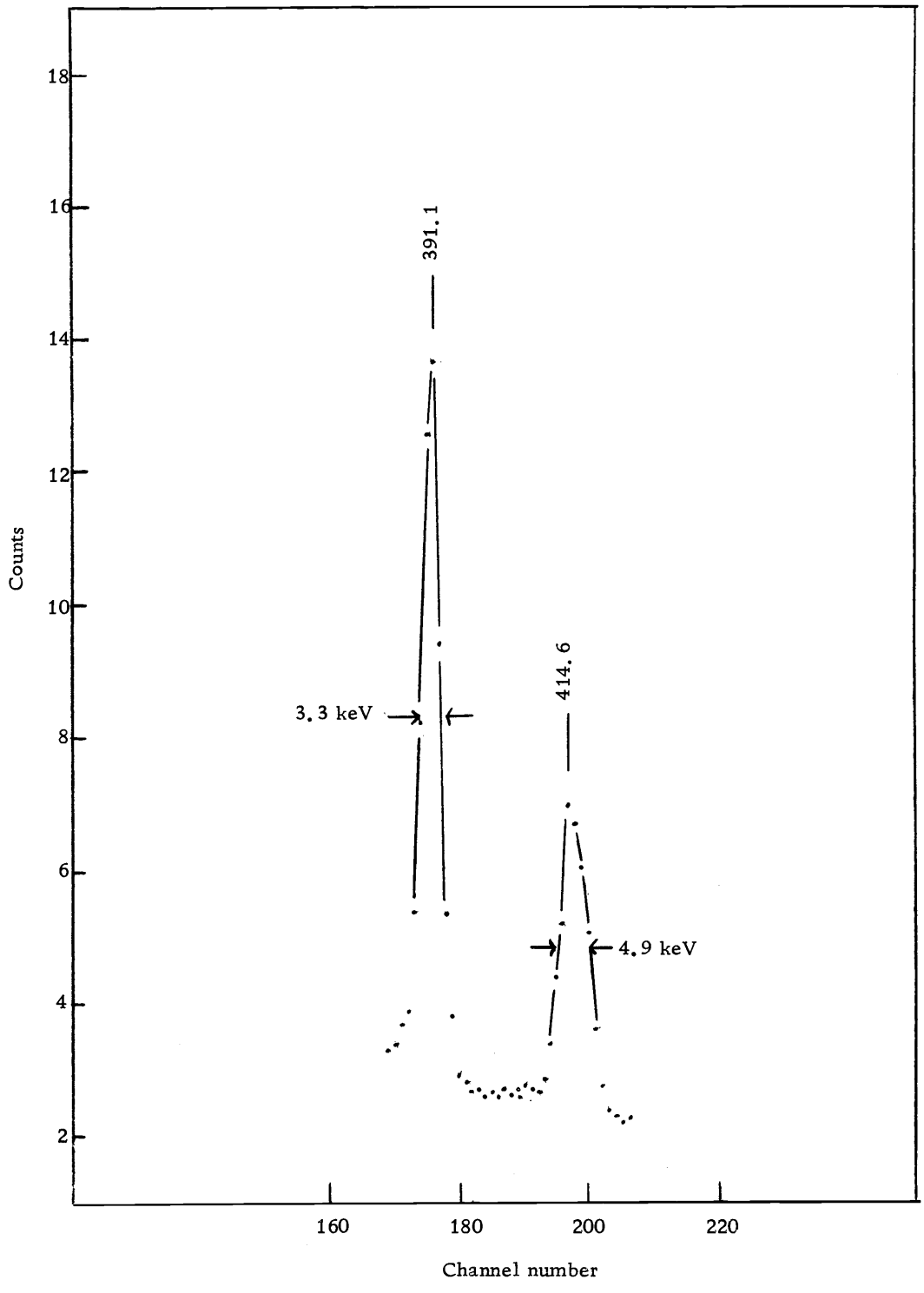

Figure 17. The complex 415 keV peak of Pd^{111m} with Pd^{109} subtracted. The contribution to the area of the 415 keV Pd^{111m} peak from Pd^{109} was approximately 30%.

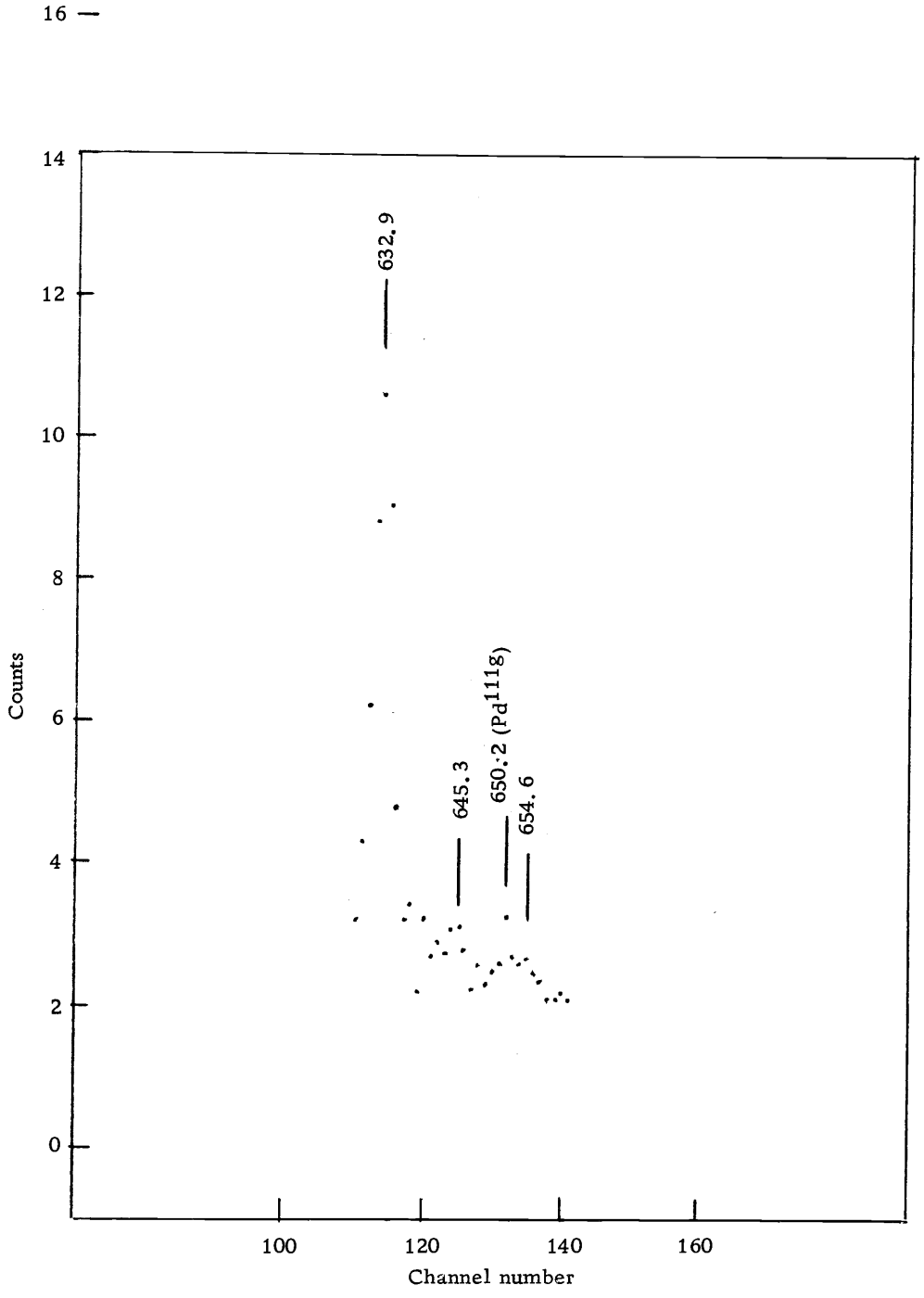

Figure 18. Gamma ray spectrum of Pd^{111m} in the region of 650 keV with Pd^{109} subtracted.

Table 3. Gamma ray energies and intensities observed in the decay of Pd^{111g}.

Energy (keV)	Relative intensity
60.0 ± 0.2	110 ± 30
70.3 ± 0.2	155 ± 40
230.6 ± 0.3	2.7 ± 0.5
289.6 ± 0.2	20 ± 2
316.9 ± 0.4	2.3 ± 0.4
376.7 ± 0.2	89 ± 9
391.1 ± 0.2	5.8 ± 0.6
405.2 ± 0.2	13 ± 1.5
439.0 ± 0.2	7.7 ± 0.8
476.9 ± 0.2	8.9 ± 1
509.0 ± 0.2	38 ± 4
547.0 ± 0.2	59 ± 6
552.5 ± 0.4	2.5 ± 0.4
580.0 ± 0.2	140 ± 15
623.0 ± 0.2	56 ± 6
642.0 ± 0.4 a)	8 ± 1
650.2 ± 0.2	90 ± 9
685.5 ± 0.3	6.3 ± 0.8
709.8 ± 0.2 a)	23 ± 2
775.5 ± 0.3	5.2 ± 0.5
803.5 ± 0.3	4.1 ± 0.4
808.5 ± 0.3	3.3 ± 0.4
835.6 ± 0.2	49 ± 5
1,002.2 ± 0.4	7 ± 1
1,120.0 ± 0.3	23 ± 2
1,388.3 ± 0.3	100
1,459.0 ± 0.3	109 ± 11

a) Not placed in the decay scheme

Table 4. Gamma ray energies and intensities observed in the decay of Pd^{111m}.

Energy (keV)	Relative intensity	Energy (keV)	Relative intensity
70.3 ± 0.2	190 ± 50	668.2 ± 0.2	19 ± 2
101.7 ± 0.4	4 ± 1	694.0 ± 0.2	39 ± 4
172.2 ± 0.2	1,000	703.2 ± 0.3	13 ± 2
272.0 ± 0.3	3.1 ± 0.5	718.3 ± 0.4 a)	2.3 ± 0.5
289.6 ± 0.2	22 ± 2	752.9 ± 0.4	2.1 ± 0.6
357.9 ± 0.3	7.9 ± 0.8	762.2 ± 0.3	20 ± 2
376.7 ± 0.2	17 ± 2	797.4 ± 0.3	17 ± 2
391.1 ± 0.2	112 ± 11	863.1 ± 0.4	2.4 ± 0.5
414.6 ± 0.5 b)	80 ± 20	881.6 ± 0.4	3.2 ± 0.5
439.0 ± 0.3	5.4 ± 0.7	975.5 ± 0.4	3.8 ± 0.5
454.4 ± 0.2	24 ± 3	997.1 ± 0.4	5.4 ± 0.6
485.7 ± 0.3	8.2 ± 0.8	1,063.3 ± 0.4 a)	5.1 ± 0.8
525.4 ± 0.2	21 ± 2	1,115.8 ± 0.3	21 ± 2
552.5 ± 0.3	5 ± 1	1,163.3 ± 0.4	4.9 ± 0.6
556.4 ± 0.4	3 ± 1	1,199.5 ± 0.4	5.4 ± 0.6
575.2 ± 0.2	67 ± 7	1,282.2 ± 0.3	23 ± 2
617.5 ± 0.4	2.3 ± 0.8	1,650.8 ± 0.3	14 ± 2
623.0 ± 0.3	11 ± 1	1,690.9 ± 0.3	23 ± 2
632.9 ± 0.2	65 ± 7	1,721.6 ± 0.4	5.0 ± 0.8
645.3 ± 0.5	4 ± 2	1,775.0 ± 0.4	7 ± 1
654.6 ± 0.4 a)	4 ± 1	1,970.3 ± 0.5	10 ± 1

a) Not placed in decay scheme

b) Complex peak

approximately equal intensity.

The Decay Scheme of Pd^{111g}

The decay scheme constructed for Pd^{111g} is shown in Figure 19.

A great deal of previously established data was available regarding the energy levels of Ag^{109}. Such is not the case for Ag^{111}. Reaction data pertaining to Ag^{111} do not exist. The only gamma-gamma coincidence study (48) was performed with scintillation detectors and because of the complexity of the decay the results are of little value.

Energy balance relationships are therefore heavily relied upon in determining the decay scheme which follows. Because of the possibility of energy relationships that are purely accidental or of ambiguities in the ordering of the gamma rays, a unique decay scheme cannot be demonstrated by energy balance considerations alone. In choosing among alternative level arrangements, preference is given to that scheme having the fewest number of levels needed to accommodate the observed transitions. Otherwise one must explain the absence of transitions connecting the additional states. Occasionally, intensity balance relationships and beta or gamma decay selection rules are helpful in making a choice.

A complete list of the Pd^{111g} gamma ray energy groupings such that the sum of the first two energies equals the third within the

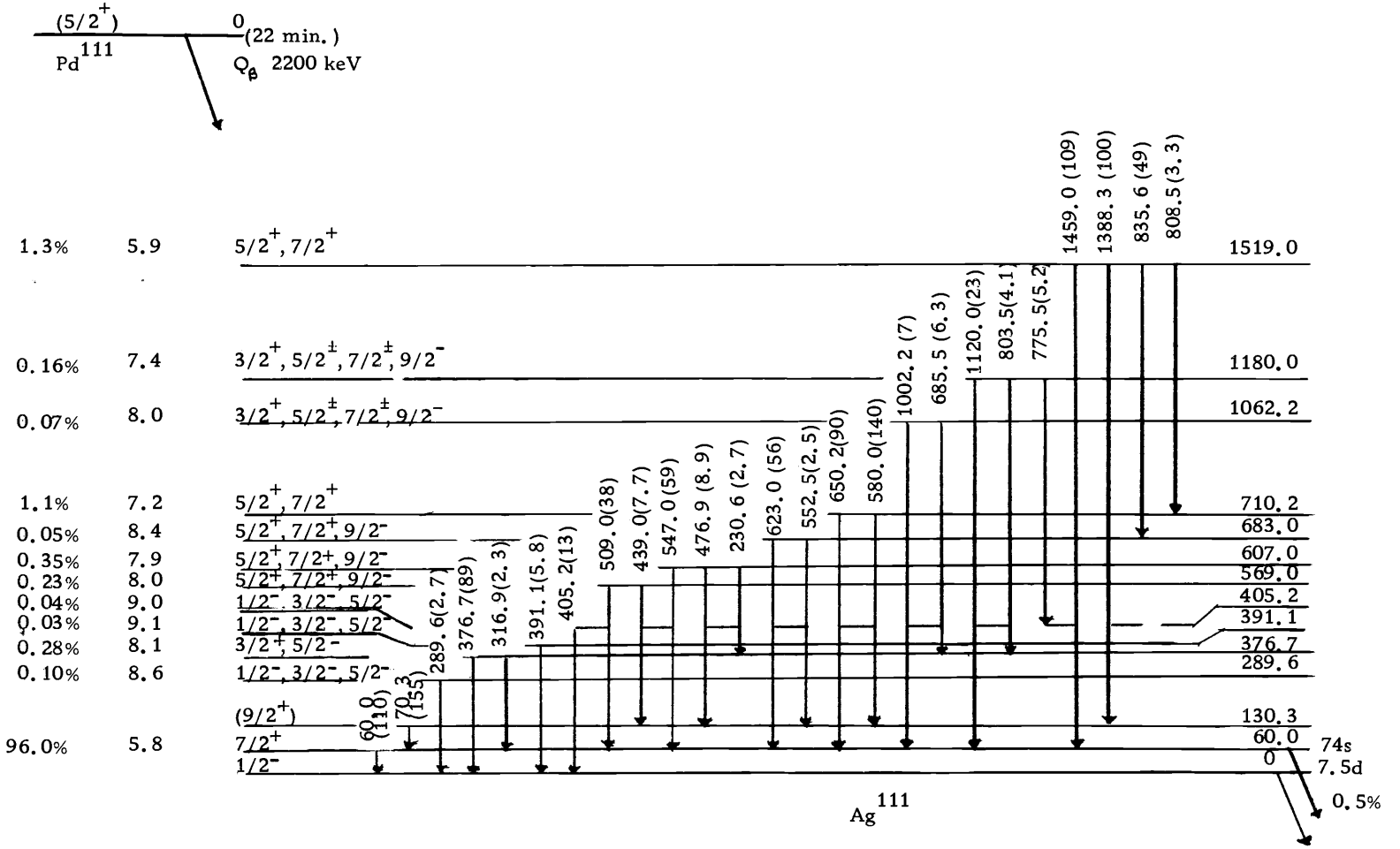

Figure 19. Decay scheme of 22 min Pd^{111g}. Relative photon intensities are given by the numbers in parentheses.

experimental error is given below. These energy balance relations indicate the possibility of two cascade gamma rays and the corresponding crossover transition in the decay of Pd^{111g}.

1) 60.0, 316.9, 376.7
2) 60.0, 650.2, 709.8
3) 60.0, 775.5, 835.6
4) 70.3, 439.0, 509.0
5) 70.3, 476.9, 547.0
6) 70.3, 552.5, 623.0
7) 70.3, 580.0, 650.2
8) 70.3, 1388.3, 1459.0
9) 230.6, 316.9, 547.0
10) 316.9, 685.5, 1002.2
11) 316.9 803.5, 1120.0
12) 552.5, 835.6, 1388.3
13) 580.0, 808.5, 1388.3
14) 623.0, 835.6, 1459.0
15) 650.2, 808.5, 1459.0

The placement of each of the low-lying levels will be discussed in detail.

The known(78)74 second 60 keV first excited state of Ag^{111} is assumed to give rise to the 60.0 keV gamma ray observed in the decay of Pd^{111g}. The lifetime of this state strongly suggests an E3 transition and a spin of $7/2^+$. The strong intensity of the 60 keV gamma line is consistent with the findings of McGinnis (43) and Pratt and Cochran (50) which show a large fraction of beta transitions feeding the 60 keV level from Pd^{111g}. In fact a calculation of the beta branching to the 60 keV level using an E3 internal conversion coefficient of 180 shows that 96% of the beta transitions proceed to the Ag^{111m} level.

The 70.3 keV gamma ray is an intense transition in both the Pd^{111g} and Pd^{111m} spectra and would be expected to lie low in the decay scheme for the following reason. The large difference in spin between the $5/2^+$ Pd^{111g} state and the $11/2^-$ Pd^{111m} state means that a level of Ag^{111} fed by an allowed transition from one of the isomers must be fed by a first forbidden unique or higher order transition from the other. Hence, any intense gamma rays common to the decay of both must be fed by gamma ray transitions from higher lying levels rather than by direct beta decay.

In analogy with the level structures of Ag^{107} and Ag^{109}, the 70.3 keV transition is taken to feed the 60 keV first excited state of Ag^{111}. As shown in Figure 20, Ag^{107} and Ag^{109} each have a first excited state of spin $7/2^+$ at 93 and 88 keV, respectively, and the corresponding first excited state in Ag^{111} is the $7/2^+$ 60 keV level mentioned above. The second excited states of Ag^{107} and Ag^{109} lie at 126 and 133 keV, respectively, and have spin $9/2^+$. Hence, a second excited state at 130 keV, as provided by the 70 keV transition, seems reasonable in view of these level systematics. It is argued below in the section on spins and parities that if indeed the 70 keV transition feeds the first excited state, its calculated internal conversion coefficient implies a $9/2^\pm$ spin assignment for the state.

A level is placed at 376.7 keV accommodating a 316.9 keV transition to Ag^{111m} and a 376.7 keV transition to the ground state

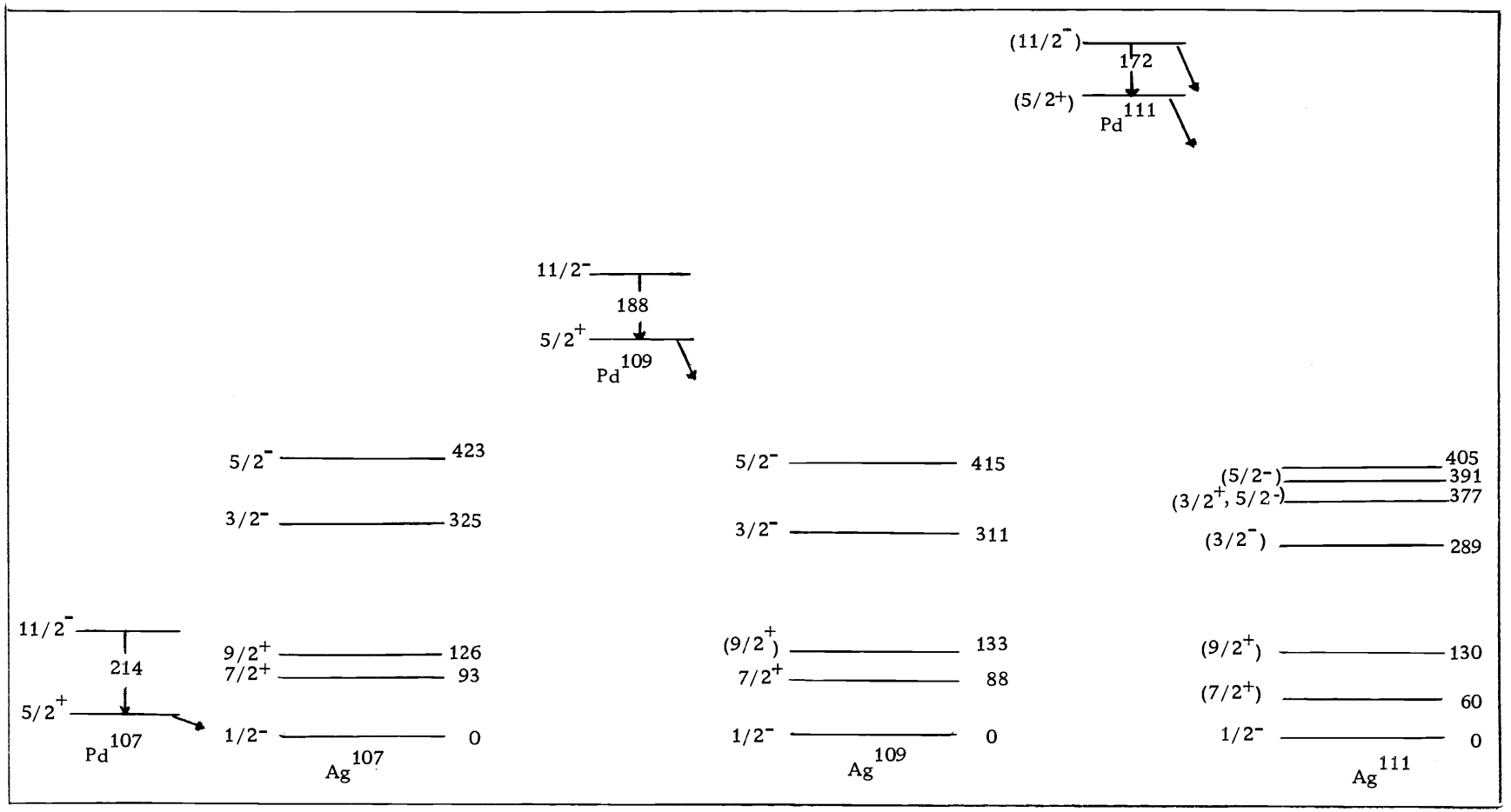

Figure 20. Comparison of the low-lying levels of the A=107, 109, 111 isotopes of Pd and Ag. The excitation energies of the Pd states are not drawn to scale. The data are taken from this study and reference 5.

on the basis of energy relation 1).

The 289.6 keV and 391 keV transitions appear prominently in both the Pd^{111g} and Pd^{111m} spectra. These transitions probably feed the same level since the 101.7 keV gamma ray observed in the Pd^{111m} spectrum suggests a 101.7-289.6 keV cascade and a 391.1 keV cross-over transition. (One would not expect to see the 101 keV line in the Pd^{111g} spectrum because of the reduced intensity of the 289 keV and 391 keV lines.) Since the intensity of the 289 keV gamma ray exceeds that of the 101 keV transition and since there is no evidence of any other transition depopulating the intermediate level, the 101 keV transition must precede the 289 keV transition.

The 289 keV and 391 keV gamma rays are placed as transitions to the ground state by the following argument. In the decay of Pd^{111m}, energy relations indicate that three gamma rays are in cascade with the 391 keV transition and two are in cascade with the 289 keV transition. In addition the levels from which these transitions proceed are themselves a part of a larger network of levels, many of which give rise to transitions which feed the low-lying levels. If the 391 keV and 289 keV gamma rays fed, for instance, the first or second excited levels rather than the ground state, one would expect gamma rays proceeding from levels in the network to these low-lying states whose energies indicated this fact. No such gamma rays are detected. It is therefore concluded that the 391 keV and 289 keV gamma rays are transitions to the ground state.

With the low-lying levels in place, it is relatively easy to construct the remainder of the level scheme using the energy

relationships. A list follows of the remaining levels and the energy relations upon which they are based.

Energy level	Depopulating transition	Energy relation
569.0	439.0, 509.0	4)
607.0	230.6, 476.9, 547.0	5), 9)
683.0	552.5, 623.0	6)
710.2	580.0, 650.2	7)
1062.2	685.5, 1002.2	10)
1180.2	803.5, 1120.0	11)
1519.0	808.5, 835.6, 1388.3, 1459.0	8), 12), 13), 14), 15)

Relations 1), 2), and 3) are not listed above. Relation 1) was discussed in connection with the low-lying levels.

Relation 2) would suggest that the 709.8 keV gamma ray feeds the $1/2^-$ ground state from the level at 710 keV. Relation 7) has the 580 keV and 650 keV transitions feeding the $9/2^+$ and $7/2^+$ first and second excited states from the 710 keV level. Both of these relations cannot be valid since it is not possible to feed states of such widely different spin with comparable intensity from the same level. The positions of the 750 keV and 580 keV transitions are substantiated by energy relations 13) and 15). Therefore, the 710 keV transition is not placed in the decay scheme since no other relations bear upon it.

Relation 3) is in contradiction to relations 12) and 14). Since the levels at 1519 keV and 683 keV seem well-established and since there is no other evidence that a state at 835 keV exists, it is concluded that relation 3) is invalid.

Two gamma rays observed in the decay of Pd^{111g} which have not been placed in the level scheme are the 775.5 keV and 405.2 keV transitions. None of the energy relations except the invalid relation 3) bears on these. It is seen, however, that the energy sum 775.5 + 405.2 = 1180.7 equals the energy of the 1180.2 keV state within the experimental error, suggesting that the two transitions form a cascade from the 1180 keV state to ground. If this were the case, the 775 keV transition would precede the more intense 405 keV transition, implying the existence of a level at 405.5 keV. Because of the scarcity of data supporting such a cascade, this level appears as a dashed line in the decay scheme.

The proposed decay scheme of Pd^{111g} is shown in Figure 19. The number in parentheses after each gamma ray energy indicates the relative intensity of the transition. The log ft values, which follow the percentage of beta branching to each state, were determined from the nomogram of Moszokowski (46). In calculating the log ft values total internal conversion coefficients of 180 and 1.15 were used for the 60.0 keV and 70.3 keV transitions respectively, based on the theoretical value for an E3 and M1 transition (28). The Pd^{111g} disintegration energy was taken to be 2.2 MeV (50).

Spin and Parities in the Pd^{111g} Decay

For the most part spins and parities have been deduced on the basis of log ft values and gamma decay selection rules. In a few cases arguments by analogy with the level structure of the neighboring odd-A isotopes of Ag and Pd have been used. Except for the isomeric transitions it will be assumed that gamma ray transitions are limited to E1, M1, and E2 multipolarity. Because of the high log ft values encountered in the decay of Pd^{109} a transition will be considered definitely allowed when the log ft value is less than 7.0 and definitely first forbidden when it exceeds 8.5.

The Pd^{111} Ground State

The spin of this state has not been directly measured. In analogy with the known (13) $5/2^+$ ground state spins of Pd^{107} and Pd^{109}, a $5/2^+$ assignment is made for Pd^{111g}. From the shell model point of view, a $5/2^+$ state would correspond to the configuration $(2d_{5/2})^5 (1g_{7/2})^8 (1h_{11/2})^2$ for 65 neutrons. The usual ground state spin for the 65 to 75 neutron region is $1/2^+$, corresponding to the $(2d_{5/2})^6 (1g_{7/2})^8 (3s_{1/2})^1$ configuration, whereas a $5/2^+$ ground state is more typical of the nonspherical 65 proton nuclei. However, a spin $\geq 5/2$ is strongly suggested for the Pd^{111g} state on the basis of intense beta feeding to the $(7/2^+)$ first excited state of Ag^{111}.

The Ag^{111} Ground State

A spin of 1/2 has been established for this state by an atomic beam experiment (80). The magnetic moment has been measured to be -0.146 nm which lies close to the $j = \ell - 1/2$ Schmidt line for $j = 1/2$, implying an odd parity.

The 60.0 keV Level

The lifetime of this level has been measured to be 74 seconds (61), which, based on the single particle estimate, indicates an E3 or M3 multipolarity. A measurement of the internal conversion coefficient of this transition has not been made. The energy and lifetime of this level are very similar to those of the first excited states of Ag^{107} and Ag^{109} whose gamma ray transitions have been established as E3 in character by internal conversion coefficient measurements (38). An E3 multipolarity is therefore strongly suggested for the 60.0 keV transition, implying a $7/2^+$ spin assignment. Beta transitions from a $5/2^+$ Pd^{111g} level to a $7/2^+$ Ag^{111m} level are consistent with the log ft value of 5.8.

The 130.3 keV Level

In the decay of Pd^{111m}, which is discussed below, several levels are fed from the $11/2^-$ Pd^{111m} state by allowed transitions,

as indicated by their associated log ft values. These levels with possible spins of $9/2^-$, $11/2^-$, or $13/2^-$ decay preferentially to the 130 keV state rather than to the $7/2^+$ isomeric state, indicating a spin higher than 7/2 for the 130 keV level. Beta transitions from Pd^{111g} to the 130 keV level are therefore at least first forbidden unique, implying little beta feeding. Under this assumption the internal conversion coefficient of the 70.3 keV transition may be calculated as the difference between the gamma intensities feeding and depopulating the 130 keV level divided by the gamma intensity of the depopulating transition. This calculation yields an internal conversion coefficient of 0.7 which is midway between the E1 value of 0.15 and the M1 value of 1.15. An E1 multipolarity would mean a $9/2^-$ state while a $9/2^+$ state would be indicated by a M1 multipolarity. Unfortunately, the uncertainties involved in the detector efficiency at low energies and in how the baseline is drawn in determining the 70.3 keV peak area do not make it possible to resolve this ambiguity. Because Ag^{107} and Ag^{109} both have second excited states at about 130 keV with $9/2^+$ spins, the $9/2^+$ assignment will be made for the Ag^{111} second excited state.

The 289.6 keV Level

Gamma transitions from this level populate the $1/2^-$ ground state but not the $7/2^+$ or $9/2^+$ first and second excited states,

implying a low spin. The log ft value of 8.6 for this state indicates a first forbidden transition, making $1/2^-$, $3/2^-$, and $5/2^-$ the possible assignments.

The 376.7 keV Level

A spin of $3/2^+$ or $5/2^-$ is indicated for this level since gamma transitions feed states of $7/2^+$ and $1/2^-$. The log ft value of 8.1 is not large enough to rule out the allowed ($5/2^+ \rightarrow 3/2^+$) transition, in view of the Pd^{109} results.

The 391.1 keV and 405.2 keV Levels

These levels have gamma transitions to the $1/2^-$ ground state, while the $7/2^+$ and $9/2^+$ levels are not fed from them. First forbidden transitions are indicated by the log ft values of 9.1 and 9.0. Therefore, spins of $1/2^-$, $3/2^-$, or $5/2^-$ are most likely for these levels.

The 569.0, 607.0, and 683.0 keV Levels

Gamma transitions from these levels feed the $7/2^+$ and $9/2^+$ first and second excited states. The log ft values of 8.0, 7.9, and 8.4 suggest allowed or first forbidden transitions. Spin assignments of $5/2^+$, $7/2^+$, and $9/2^-$ are therefore possible.

The 710.2 keV Level

A spin of $5/2^+$ and $7/2^+$ is indicated for this level on the basis of an allowed log ft value of 7.2 and gamma transitions to the $7/2^+$ and $9/2^+$ states.

The 1062.2 keV and 1180.0 keV Levels

Allowed or first forbidden beta transitions for these levels, as implied by log ft values of 8.0 and 7.4, and gamma transitions to the $7/2^+$ level indicate possible spin assignments of $3/2^+$, $5/2^\pm$, $7/2^\pm$, and $9/2^-$.

The 1519.0 keV Level

This level is fed by an allowed beta transition, the log ft value being 5.9. A gamma transition to the $9/2^+$ state rules out $3/2^+$, leaving $5/2^+$ and $7/2^+$ as possible assignments.

The Decay Scheme of Pd^{111m}

The decay scheme proposed for Pd^{111m} is shown in Figure 21.

Energy-balance relations pertaining to the gamma ray transitions observed in the decay of Pd^{111m} are:

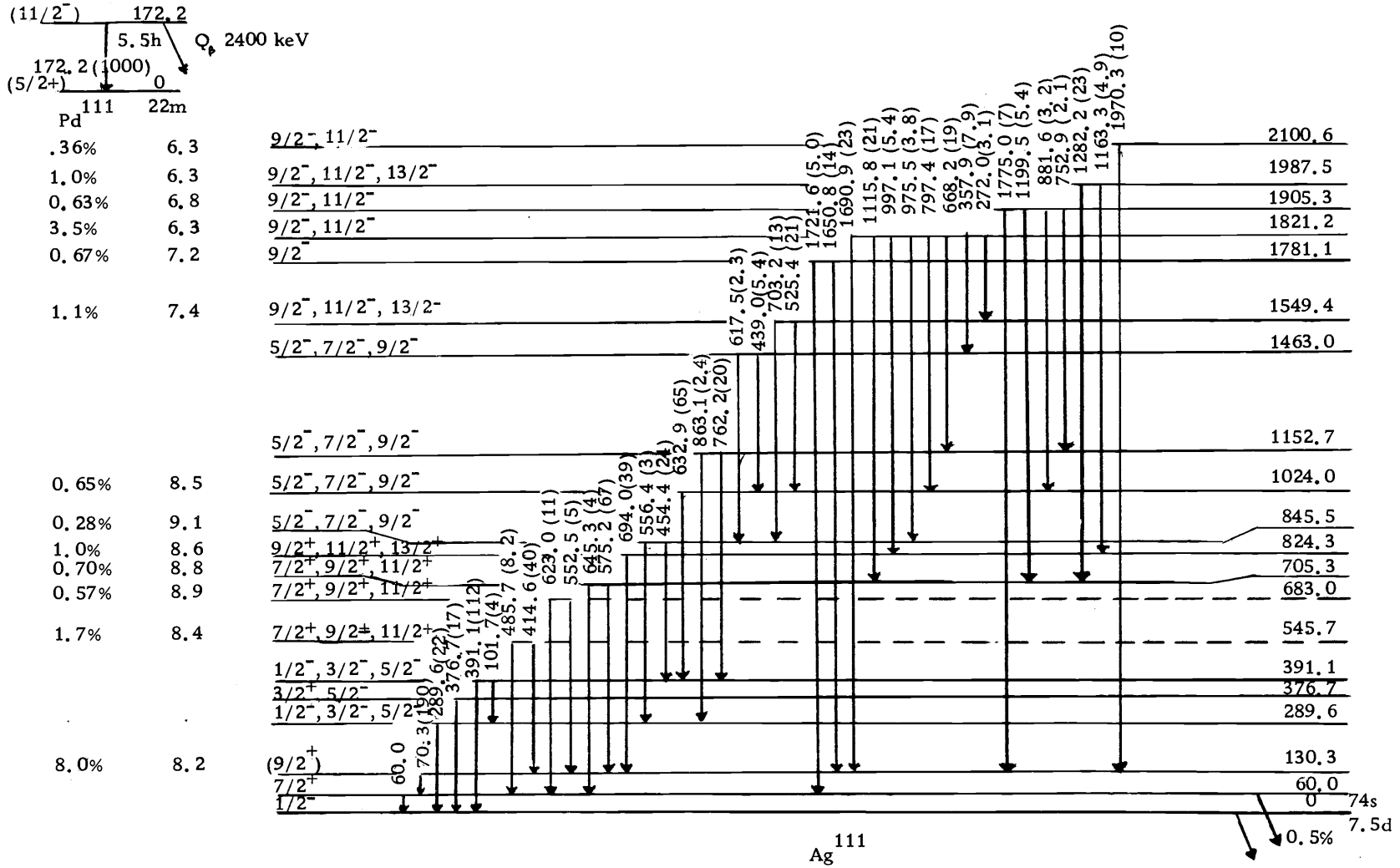

Figure 21. Decay scheme of 5.5 h Pd^{111m}. Relative photon intensities are given by the numbers in parentheses.

1)	70.3,	552.5,	623.0	10) 272.0,	703.2, 975.5
2)	70.3,	414.6,	485.7	11) 289.6,	414.6, 703.2
3)	70.3,	575.2,	645.3	12) 357.9,	439.0, 797.4
4)	70.3,	632.9,	703.2	13) 357.9,	618.4, 975.5
5)	70.3,	1650.8,	1721.6	14) 376.6,	376.6, 752.9
6)	101.7,	289.6,	391.1	15) 439.0,	1282.2, 1721.6
7)	101.7,	454.4,	556.4	16) 575.2,	1115.8, 1690.9
8)	101.7,	762.2,	863.1	17) 575.2,	1199.5, 1775.0
9)	272.0,	525.4,	797.4	18) 694.0,	997.1, 1690.9

Constructing the decay scheme of Pd^{111m} from these energy relations is not as straightforward as in the case of Pd^{111g} and so the arguments are presented in some detail.

Gamma rays of energy 70.3, 289.6, 376.7, and 391.1 keV which were discussed in connection with the decay of Pd^{111g} are also observed in the Pd^{111m} decay. Levels at 60.0, 130.3, 289.6, 376.7 and 391.1 keV are therefore indicated for the Pd^{111m} level scheme. The 60.0 keV line is not observed in the Pd^{111m} spectrum because of the absence of direct beta feeding to the Ag^{111m} level and because of the large internal conversion coefficient associated with this level.

Relations 3) and 5) suggest energy levels at 705.5 and 1781.1 keV, respectively.

Relation 6) was discussed in connection with the Pd^{111g} decay.

Relations 7) and 8) indicate the existence of levels at 845.5 keV and 1152.7 keV, respectively.

Levels at 1821.2 keV and 1905.3 keV are indicated by relations 16) and 17) in conjunction with relation 3). The 752.9 keV gamma ray has the right energy to fit between the 1905.3 keV and 1152.7 keV levels.

Relations 9), 10), 12), and 13) suggest a network of levels built around the 975.5 keV gamma ray, which has just the right energy to fit between the 845.5 keV and the 1821.2 keV levels. Because the 797.4 keV gamma ray is in common with the 357.9 keV and the 272.0 keV transitions, these latter two transitions must either both precede or both follow the corresponding members of the 358-618 and 272-703 cascades. If both precede, levels at 1549, 1463, and 1023 keV are indicated. If both follow, one expects levels at 1641, 1203, and 1118 keV. Two gamma rays which have not yet been placed in the decay scheme support the existence of a level at 1204.0 keV, thus favoring the situation in which the 272.0 keV and 357.9 keV transitions are the preceding members. These two gamma rays are the 632.9 keV transition, which has the right energy to lie between the 391.1 keV level and the proposed 1024.0 keV level, and the 881.6 keV transition whose energy equals the energy difference between the 1905.3 keV level and the proposed 1024.0 keV level.

Relation 18) suggests a 694.0-997.1 keV cascade paralleling the 1690.9 keV transition, which was shown by relation 16) to go between the 1821.2 keV and the 130.3 keV levels. An intermediate level exists at either 1127 keV or 824 keV depending on whether the 694.0 keV or the 997.1 keV transition precedes. A level at 824.3 keV is the more likely in view of the fact that the 1163.3 keV and 1282.2 keV gamma rays have the right energy to fit between a level at 1987.5 keV and the 824.3 keV and 705.5 keV levels, respectively.

A 414-289 keV cascade and a 703.2 keV crossover transition are implied by relation 11). That a member of the 414 keV complex feeds the 289.6 keV level seems improbable for several reasons. There is no additional evidence supporting a level 414 keV above the 289.9 keV level. The 703.2 keV transition fits logically between the 1549 keV and the 845 keV levels in accordance with relation 10). Furthermore, a 414-289 keV cascade is ruled out if the intensity of the 414 keV transition exceeds that of the 289 keV transition, which is likely. It is therefore concluded that relation 11) is invalid.

Relation 4) has the 632.9 keV transition feeding the second excited level with the 703.2 keV gamma ray as the crossover transition. This relation is invalid for the following reasons. The 632.9 keV transition fits between the well-established levels at 391.1 keV and 1024.0 keV so that an additional level need not be postulated. The intensity balance at the 1024.0 keV level cannot be explained without

the presence of the depopulating 632.9 keV transition. Finally, additional gamma ray transitions whose energies indicate the presence of a level 633 keV above the second excited state are not present.

A 376-376 keV cascade is implied by relation 14). However, the 376.7 keV peak does not appear to be complex. There is no additional evidence of transitions feeding or depopulating a level at 753 keV. Furthermore, the 753 keV gamma ray fits between the 1905 keV and 1153 keV levels without the assumption of an additional level. It is therefore concluded that relation 14) is invalid.

Relation 15) has the 439.0 keV and 1282.2 keV gamma rays in cascade and the 1721.6 keV gamma ray as the crossover transition. However, additional levels for which there is no other supporting evidence would be required to satisfy this relation, while a more reasonable placement for these transitions is given by relations 5) and 12).

The placement of the 1970.3 keV transition in the decay scheme is not indicated by any of the energy relations. Since the beta disintegration energy of Pd^{111m} is 2400 keV, the 1970 keV transition may feed any of the five lowest lying levels. However, the maximum log ft value associated with a level depopulated by a gamma ray of this energy and intensity is 6.9, implying an allowed transition. Hence, the level has possible spins of $9/2^-$, $11/2^-$, $13/2^-$ and will feed preferentially the $9/2^+$ second excited state or, less probably,

the $7/2^+$ first excited state. The 1970.3 keV transition is therefore taken to depopulate a level at 2100.6 keV.

The proposed decay scheme of Pd^{111m} is shown in Figure 21. In calculating the log ft values theoretically derived internal conversion coefficients of 180, 1.15, and 1.2 were used for the E3 60.0 keV, the M1 70.3 keV, and the E3 172.2 keV transitions respectively. The beta disintegration energy was taken to be 2.4 MeV (50).

Spins and Parities in the Decay of Pd^{111m}

Levels at 0, 60.0, 130.3, 376.7, and 391.1 keV have been discussed in connection with the decay of Pd^{111g}.

The Pd^{111m} Isomeric Level

The spin of this level is taken to be $11/2^-$ in analogy with the measured (13) spins of the 214 keV and 189 keV isomeric levels of Pd^{107} and Pd^{109}. Such an assignment is explained from a shell model point of view as the $(2d_{5/2})^6(1g_{7/2})^8(1h_{11/2})^1$ configuration, which would be expected to lie close in energy to the $(2d_{5/2})^5(1g_{7/2})^8(1h_{11/2})^2$ ground state configuration.

The 545.7, 683.0, 705.3, and 824.3 keV Levels

These levels have similar gamma decay modes, feeding the $7/2^+$ and $9/2^-$ first and second excited states, and log ft values

ranging from 8.4 to 8.9. Noting that an allowed transition cannot be ruled out for the 545.7 keV level and that the $7/2^+$ state is not fed from the 824.3 keV level, we have the following possible spin assignments for these levels: 545.7 $(7/2^+, 9/2^\pm, 11/2^+)$; 683.0 $(7/2, 9/2, 11/2)^+$; 705.3 $(7/2, 9/2, 11/2)^+$; 824.3 $(9/2, 11/2, 13/2)^+$.

The 845.5, 1024.0, 1152.7, and 1463.0 keV Levels

Gamma ray transitions from the first three of these four levels feed exclusively the low-spin $(1/2, 3/2, 5/2)^-$, odd-parity levels at 289.6 keV and 391.1 keV. The 1463.0 keV transition in turn feeds the 845.5 keV and 1024.0 keV levels. The spins of these four levels cannot be lower than $5/2^-$ since all four are fed from higher lying states having allowed log ft values. Nor can the spin be greater than 9/2, since levels of spin 5/2 or less are fed. The four levels most likely have odd parity, since they do not decay to the $7/2^+$ and $9/2^+$ excited states. So possible spin assignments of $5/2^-$, $7/2^-$, $9/2^-$ are indicated by the gamma decay selection rules.

Second forbidden or, in the case of the $9/2^-$ assignment, allowed log ft values are expected to be associated with these levels. The 1152.7 keV and 1463.0 keV levels indeed receive no detectable beta feeding. The 845.5 keV and 1024.0 keV levels have first forbidden log ft values of 9.1 and 8.5, respectively, which probably signal the presence of low intensity gamma ray transitions which

were not observed in the spectra or the gamma rays not placed in the decay scheme (see Table 4) feeding these levels.

The Levels at 1549.4, 1781.1, 1821.2, 1905.3, 1987.5, and 2100.6 keV

These levels have log ft values indicating allowed beta transitions and, hence, spins of $9/2^-$, $11/2^-$, or $13/2^-$. The $13/2^-$ possibility is ruled out for the 1781.1, 1821.2, 1905.3, and 2100.6 keV levels because of gamma decay to states of spin $9/2^+$ or lower. The level at 1781.1 keV is restricted to a spin of $9/2^-$ since the $11/2^-$ and $13/2^-$ possibilities are excluded by a gamma transition to the $7/2^+$ level. Thus, the spin assignments are 1549.4 $(9/2, 11/2, 13/2)^-$; 1781.1 $(9/2^-)$; 1821.2 $(9/2, 11/2)^-$; 1905.3 $(9/2, 11/2)^-$; 1987.5 $(9/2, 11/2, 13/2)^-$; 2100.6 $(9/2, 11/2)^-$.

DISCUSSION OF RESULTS

A comparison of the Pd^{109} and Pd^{111} decay schemes of Figures 7, 19, and 21 with those of radioactive decay studies made prior to the start of this investigation (Figures 1 and 8) shows many significant differences. Many new gamma ray transitions have been identified, different assignments of previously reported gamma rays have been made, and new energy levels have been proposed.

In this discussion little emphasis will be placed on these earlier studies. Rather, the discussion will be concerned with the very recent data provided by Coulomb excitation (5, 54,) and Ge(Li) decay scheme measurements (27, 4, 57, 3).

Coulomb excitation studes of Pd^{109} by Black and Gruhle (5) and Robinson et al. (54) have already been mentioned in connection with the Pd^{109} decay scheme. The levels of Ag^{109} observed by Black and Gruhle are shown in Figure 1. In these studies isotopically enriched targets of Ag^{109} are bombarded with 45 MeV oxygen ions, populating the odd-parity levels of Ag^{109} by E2 excitations of the $1/2^-$ ground state. De-excitation gamma rays are then studied with Ge(Li) detectors. The comparison of gamma ray energies and branching ratios given in Table 2 indicates that the 311, 415, 702, and 862 keV levels are populated both in Coulomb excitation and in the Pd^{109} decay. Gamma ray energies and intensities are generally

in good agreement. An exception is the ratio of intensities for the 415 keV and 104 keV transitions. Robinson et al. (54) report a 20/1 ratio, compared to the 8/1 ratio of this study and the 11/1 ratio of Black and Gruhle (5). A similar discrepancy regarding the intensity of the 104 keV gamma ray occurs in the beta decay studies, as is mentioned below.

The 728 and 915 keV levels seen by Black and Gruhle are apparently not the same as the 724.1 and 910.2 keV levels of this study, since different sets of gamma ray transitions are involved. Black and Gruhle also report a 781 keV gamma ray of low intensity which they are unable to definitely place in their decay scheme. If the 781.2 keV gamma ray seen in this study is identical with it, then it must proceed from an odd-parity state rather than from the $5/2^+$ state at 869.0 keV proposed in this study. There is no evidence, such as a 557-311 keV or 454-415 keV coincidence relationship, which would suggest a level at 869 keV populated in the Coulomb excitation experiments. Rather, the 781 keV gamma ray of Black and Gruhle may arise from a level at 1092 keV, in which case the two transitions are not identical since the companion 677 keV line would have been observed in this study.

Three Ge(Li) detector studies of the decay of Pd^{109} have appeared since the present study was begun (27, 4, 57). In all three studies activities were produced by neutron irradiation of Pd^{108}.

Graeffe and Gordon ([27]) obtained gamma-gamma coincidence results with a Ge(Li)-NaI(Tl) coincidence spectrometer. Berzins, Bunker, and Starner ([4]) used a Ge(Li)-Ge(Li) system to perform coincidence measurements. Schick and Talbert ([57]) on the other hand, relied on singles spectra in their investigation of the Pd^{109} decay.

The energy and intensity values of the gamma rays associated with the Pd^{109} decay are compared in Table 5. All intensities have been normalized to a value of 21 for the 602 keV peak to facilitate comparison. There is generally good agreement between this and the other studies. The energy values of this study tend to lie several tenths of a keV lower than do those of the other studies. With a few exceptions intensity measurements agree closely in all studies. The intensity values of Berzins et al. ([4]) for gamma rays of 311 keV energy and less lie about 30% lower than those of this study. Their intensity measurement for the 104 keV gamma ray is only one-fifth that of this study. It may be mentioned in this regard that Berzins et al. ([4]), as well as Graeffe and Gordon ([27]), observed the 104 keV transition only in coincidence spectra. Intensity measurements made from singles spectra, as in this study, avoid the complications of variations in coincidence efficiency with energy and the subtraction of chance coincidences.

The 967 keV and 1010 keV gamma rays observed in this study are also seen by Berzins et al. ([4]) but with half the intensity. They

Table 5. Comparison of gamma ray energies and intensities observed in the decay of Pd^{109}.

This study		Graeffe and Gordon a)		Berzins et al. b)		Schick and Talbert c)	
Energy d) (keV)	Intensity	Energy (keV)	Intensity*	Energy (keV)	Intensity*	Energy (keV)	Intensity*
		44.8 ± 0.2 g)	3.5 ± 1	44.7 ± 0.2 5)	2.7		
87.8	9700 ± 1000	88.2 ± 0.5	8650 ± 790	88.1 ± 0.2	7180 ± 720	88.04 ± 0.05	9460 ± 860
103.7	3.2 ± 1	103.6 ± 0.7 g)	2.2 ± 0.6	103.7 ± 0.2 g)	0.62	103.9 ± 0.4	2.5 ± 0.5
133.8	3.2 ± 0.5	134.7 ± 0.7 g)	3.1 ± 0.9	134.3 ± 0.2	2.3	134.2 ± 0.2	3.4 ± 0.7
144.7	2.5 ± 0.7	145.9 ± 0.7 g)	2.6 ± 0.8	145.4 ± 0.3	1.6	145.1 ± 0.2	3.0 ± 0.5
						286.3 ± 0.5	0.37 ± 0.1
				309.3 ± 0.5	5.7 ± 0.5	309.1 ± 0.5	12.3 ± 3.7
311.0	100	311.5 ± 0.5	99	311.3 ± 0.1	52.6 ± 5.3	311.4 ± 0.1	84 ± 7
390.2	2.3 ± 0.3	390.9 ± 0.8	2.5 ± 0.5	390.5 ± 0.3	1.8	390.6 ± 0.2	2.5 ± 0.5
						395.6 ± 0.5	0.17 ± 0.07
414.3 e)	47 ± 5	413.5 ± 1.0	25.4 ± 7.7	413.0 ± 0.1	14 ± 1	413.0 ± 0.4	17 ± 2.5
		415.2 ± 0.6	22 ± 7	415.0 ± 0.1	28 ± 3	415.2 ± 0.3	28 ± 2.5
423.8	1.6 ± 0.2	424.7 ± 0.8	1.7 ± 0.4	423.9 ± 0.3	2.3	423.9 ± 0.2	2.5 ± 0.5
447.2	1.8 ± 0.3	448.2 ± 0.8	2.5 ± 0.6	447.5 ± 0.2	2.0	447.6 ± 0.2	2.2 ± 0.5
454.1	0.9 ± 0.2			454.3 ± 0.2	1.5	454.3 ± 0.3	1.4 ± 0.6
551.1	1.9 ± 0.2	551.3 ± 0.8	1.4 ± 0.5	551.3 ± 0.2	1.6	551.4 ± 0.4	1.6 ± 0.4
557.8	6.4 ± 0.7	557.8 ± 0.5	6.2 ± 0.7	558.1 ± 0.1	6.0 ± 0.6	558.1 ± 0.2	6.4 ± 0.7
602.4	21 ± 2	602.4 ± 0.5	21 ± 2	602.5 ± 0.1	21 ± 2	602.5 ± 0.1	21 ± 1
						609.5 ± 0.5 f)	0.37 ± 0.02
636.3	31 ± 3	636.1 ± 0.5	26.4 ± 3.0	636.4 ± 0.2	25 ± 2	636.3 ± 0.1	26 ± 1
647.2	64 ± 6	647.3 ± 0.6	64 ± 5	647.3 ± 0.1	61 ± 6	647.3 ± 0.1	64 ± 5
701.6	9 ± 1	701.8 ± 0.8	8.4 ± 1	702.0 ± 0.2	9.3 ± 0.9	701.9 ± 0.2	8.2 ± 0.7
706.7	3.8 ± 0.5	707.3 ± 0.8	4.4 ± 0.5	706.9 ± 0.3	4.2 ± 0.4	707.0 ± 0.2	4.2 ± 0.5
				724.6 ± 0.3	0.7	724.7 ± 0.3	0.49 ± 0.1
736.5	4.4 ± 0.5	736.7 ± 0.7	4.9 ± 0.5	737.7 ± 0.2	4.9 ± 0.5	736.7 ± 0.2	4.4 ± 0.5
				778.3 ± 0.5	2.5	778.3 ± 0.5	3.9 ± 1
781.2	34 ± 3	781.8 ± 0.7	32 ± 3	781.4 ± 0.2	32 ± 3	781.4 ± 0.2	29 ± 3

Table 5. Continued.

This study		Graeffe and Gordon a)		Berzins et al. b)		Schick and Talbert c)	
Energy d) (keV)	Intensity	Energy (keV)	Intensity*	Energy (keV)	Intensity*	Energy (keV)	Intensity*
822.4	0.47 ± 0.06			822.9 ± 0.3	0.49	822.9 ± 0.4	0.49 ± 0.07
862.6	0.44 ± 0.06		<0.5	862.8 ± 0.5	0.37	862.5 ± 0.4	0.35 ± 0.07
						868.8 ± 1.0 f)	0.1 ± 0.05
967.1±1 f)	0.12 ± 0.03			966.3 ± 0.5	0.06		
1011.8±1 f)	0.11 ± 0.03			1010.5 ± 0.5	0.06		

a) Reference 27. b) Reference 4. c) Reference 57.

d) All errors are ± 0.5 keV unless otherwise indicated.

e) Known multiplet.

f) Assignment to Pd^{109} decay is uncertain.

g) Determined from coincidence spectra.

* Renormalized to 21 for the 602 keV transition.

take these transitions to depopulate a level of 1099 keV on the basis of energy balance considerations. A $5/2^+$ or $7/2^+$ spin-parity assignment is indicated by the log ft value and gamma decay modes. By partially resolving the 415 keV peak in their singles spectra, Berzins et al. (4) confirm the existence of a doublet there. In addition they find that the lines at 311 keV and 781 keV have weak, lower energy companions at 309 keV and 778 keV. On the basis of these additional lines and a reported 496.9 keV transition, they propose levels at 911.0 keV and 912 keV. The former of these, which corresponds to the 910.2 keV level suggested in this study, is given a possible $5/2^+$ or $7/2^+$ spin assignment. The latter level is seen in Coulomb excitation and is assigned a $1/2^-$ or $7/2^-$ spin by Robinson et al. (54).

Schick and Talbert (57) report the additional presence of 286.3, 395.6, 609.5, and 868.8 keV gamma rays. The first two of these feed the 415 keV and the 311 keV levels respectively. The latter two cannot be assigned to the Pd^{109} decay with certainty. Schick and Talbert (57) are unable to confirm or deny the existence of gamma rays at 966 keV and 1010 keV. Their level scheme is very similar to the one proposed in this study. They place the 707 keV gamma ray as a ground state transition on the basis of observing a 395.6 keV gamma ray, which has the right energy to fit between the 707 and 311 keV levels.

Graeffe and Gordon[27] claim a 707-45 keV coincidence relationship which would suggest the existence of a level at 840 keV. However, this relationship is not confirmed by Berzins et al. [4]. In all other respects the Graeffe and Gordon decay scheme closely resembles that of this investigation.

Table 6 compares the energies, log ft values, and spin-parity assignments of the levels populated in the decay of Pd^{109}. Schick and Talbert [57] warn that odd-parity levels might not be observed in Coulomb excitation if E2 transitions to the ground state were sufficiently retarded, as in the case of transitions between single-particle levels. They therefore list both odd and even parity assignments for the 707, 724, 735, 869, and 911 keV levels.

Since the start of this investigation, two studies of the Pd^{111} decay have appeared. Berzins, Bunker, and Starner [3] produced sources of Pd^{111} by neutron bombardment of natural and enriched palladium and by the (d, p) reaction on Pd^{110}. Spectra were recorded with a Ge(Li) detector and a Ge(Li)-Ge(Li) coincidence spectrometer. Some of the low-energy singles spectra were taken with a Si(Li) detector. Schick and Talbert [57] used Ge(Li) and Ge(Li)-NaI(Tl) detector systems to investigate the Pd^{111} decay. Their sources were reactor-produced from palladium targets enriched in Pd^{110}.

A comparison of the gamma ray energy and intensity measurements associated with the decay of Pd^{111g} and Pd^{111m} appears in

Table 6. Comparison of experimental data on the energy levels of Ag^{109}.

This study			Graeffe and Gordon a)			Berzins et al. b)			Schick and Talbert c)		
Energy (keV)	*log ft	Spin-parity	Energy (keV)	*log ft	Spin-parity	Energy (keV)	*log ft	Spin-parity	Energy (keV)	*log ft	Spin-parity
0		$1/2^-$	0		$1/2^-$	0		$1/2^-$	0		$1/2^-$
87.8	6.2	$7/2^+$	88.2	6.2	$7/2^+$	88.1	6.3	$7/2^+$	88.0	6.1	$7/2^+$
132.6		$(9/2^+)$	133.0		$(9/2^+)$	132.8		$(9/2^+)$	132.8		$(9/2^+)$
311.0	9.4	$3/2^-$	311.5	9.3	$3/2^-$	311.3	9.8	$3/2^-$	311.4	9.4	$3/2^-$
415	9.5	$5/2^-$	415.2	9.6	$5/2^-$	415.0	9.6	$5/2^-$	415.3	9.8	$5/2^-$
701.6	9.0	$3/2^-$	701.8	9.1	$3/2^-$	701.9	9.1	$3/2^-$	701.9	9.0	$3/2^-$
						706.9 e)	9.5	$(3/2^+)$	707.0	9.4	$5/2^+, 3/2^\pm$
724.1	8.4	$3/2^+, 5/2^+$	724.3	8.3	$5/2^+, 3/2^+$	724.5	8.5	$(5/2^+)$	724.4	8.3	$3/2^+, 5/2^-$
735.0	8.1	$(5/2^+)$	735.5	8.1	$5/2^+, 7/2^+$	735.3	8.2		735.3	8.1	$5/2^+, 7/2^-$
			840.3	8.9							
794.5 d)	9.2										
862.6	8.8	$5/2^-$	863.2	8.7	$5/2^-$	862.6	9.0	$5/2^-$	862.7	8.8	$5/2^-$
869.0	7.7	$(5/2^+)$	870.0	7.6	$5/2^+, 7/2^+$	869.4	7.8	$(5/2^+)$	869.5	7.7	$5/2^+, 7/2^-$
910.2 d)	9.4					911.0	8.8	$5/2^+, 7/2^+$	911.0	8.5	$5/2^+, 7/2^\pm$
						912	9.8	$1/2^-, 7/2^-$			
						1099	6.9	$5/2^+, 7/2^+$			

a) Reference 27. b) Reference 4. c) Reference 57.

d) Existence of level uncertain.

e) Or 795.0 keV

* Missing log ft values imply no significant amount of beta feeding to the level.

Tables 7 and 9. The intensity values of Berzins et al. (3) and Schick and Talbert (57) have been renormalized to 140 and 65 for the 580 keV and 633 keV transitions of Pd^{111g} and Pd^{111m} respectively. For those gamma rays whose intensities were not below the limit of detection of this study, there is excellent agreement in general between the results of the other studies and the results of this work. As in the case of Pd^{109}, the intensity values of Berzins et al. (3) lie generally lower for the low energy transitions. This discrepancy can no doubt be attributed to a systematic error in one or more of the detector efficiency curves at low energies.

Of the gamma rays associated with the Pd^{111g} decay several of moderate intensity are listed by Schick and Talbert (57) but not by Berzins et al. (3). These are the gamma rays at 245.5, 507.0, 620.0, and 752.9 keV. Peaks of these energies are also seen in the spectra of this study. However, these transitions may arise from the beta decay of the 60 keV Ag^{111m} first excited state to levels of Cd^{111}. If such were the case, the peaks would initially decay with the 22 minute Pd^{111g} half-life, since the life-time of the Ag^{111m} state is only 74 seconds. Gamma transitions of these energies and intensities have been observed in the Coulomb excitation of Cd^{111} (41). Further, performing a rapid chemical separation of Ag from Pd^{111}, Berzins et al (3) were able to report the presence of gamma rays having energies of 170, 203, 245, 342, 413, 509, 620, and 753

Table 7. Comparison of gamma ray energies and intensities observed in the decay of Pd^{111g}.

This study		Berzins et al. a)		Schick and Talbert b)	
Energy (keV)	Intensity	Energy (keV)	Intensity*	Energy (keV)	Intensity*
60.0 ± 0.2	110 ± 30	59.9 ± 0.1	88 ± 7	59.8 ± 0.1 f)	115 ± 27
70.3 ± 0.2	155 ± 40	70.5 ± 0.2	112 ± 7	70.4 ± 0.1	147 ± 27
		101.7 ± 0.5	0.3 ± 1		
		141.8 ± 0.5	0.07 ± 0.03		
		166 ± 1	1.4 ± 1	165.8 ± 1.0	~ 2.5
		169 ± 0.5 d, e)	8.4 ± 3	168.8 ± 1.0	~ 4.8
		202.1 ± 0.5 d)	1.0 ± 0.3	202.2 ± 0.4	1.5 ± 0.4
230.6 ± 0.3	2.7 ± 0.5	230.5 ± 0.5	2.8 ± 0.3	230.5 ± 0.3	4.2 ± 0.8
				245.5 ± 0.1 f)	81 ± 4
		278.8 ± 1.0 d)	0.8 ± 0.4	278.9 ± 0.3	2.3 ± 0.6
289.6 ± 0.2	20 ± 2	289.8 ± 0.5	14 ± 0.7	289.8 ± 0.1	17 ± 2
		308 ± 1	1.0 ± 0.4	307.6 ± 0.5	1.7 ± 0.6
316.9 ± 0.4	2.3 ± 0.4	316.9 ± 0.5	2.5 ± 0.3	316.9 ± 0.3	3.6 ± 0.6
				336.3 ± 0.5 c)	0.8 ± 0.4
		352.6 ± 0.5	1.8 ± 0.4	352.3 ± 0.4	1.3 ± 0.4
376.7 ± 0.2	89 ± 9	376.7 ± 0.3	77 ± 3	376.7 ± 0.1	80 ± 6
391.1 ± 0.2	5.8 ± 0.6	391.3 ± 0.5	5.6 ± 1	391.2 ± 0.1	5.0 ± 1.5
405.2 ± 0.2	13 ± 1.5	404.9 ± 0.5	12 ± 1.4	404.9 ± 0.2	13 ± 1.1
		415 d)	14 ± 3	415.3 ± 0.3	10 ± 3
		418 ± 1	0.7 ± 0.4		
439.0 ± 0.2	7.7 ± 0.8	438.7 ± 0.5	8.8 ± 1.4	438.4 ± 0.3	8.8 ± 0.8
476.9 ± 0.2	8.9 ± 1	476.7 ± 0.5	11 ± 3	476.6 ± 0.3	~ 8.5
		478.5 ± 1	3 ± 1	478.5 ± 0.5	~ 1.9
		485.9 ± 0.5	5.6 ± 1	485.8 ± 0.2	5.4 ± 1.3
		494.2 ± 1	1.4 ± 0.7	494.1 ± 0.5 c)	1.5 ± 0.8
				507.0 ± 1.0 c, g)	4.8 ± 2
509.0 ± 0.2	38 ± 4	508.9 ± 0.5 d)	39 ± 3	508.9 ± 0.2	32 ± 4
		516.5 ± 0.5	2.8 ± 1	516.6 ± 0.5	2.9 ± 0.8
		519.2 ± 1.0	1.4 ± 0.7	519.2 ± 0.7 c)	1.1 ± 0.6
		514 ± 1	2.5 ± 0.7	540.9 ± 0.4	3.5 ± 1

Table 7. Continued.

This study		Berzins et al. a)		Schick and Talbert b)	
Energy (keV)	Intensity	Energy (keV)	Intensity*	Energy (keV)	Intensity*
547.0 ± 0.2	59 ± 6	547.1 ± 0.5	62 ± 3	547.0 ± 0.1	65 ± 4
552.5 ± 0.4	2.5 ± 0.4	552.9 ± 0.5	2.8 ± 1	552.5 ± 0.4	3.4 ± 2
		572 ± 1 e)	1.4 ± 0.7		
580.0 ± 0.2	140 ± 15	580.1 ± 0.5	140	580.1 ± 0.1	140 ± 8
		603 ± 1 e)	1.4 ± 0.7		
		611.4 ± 0.5	2.1 ± 0.7	611.1 ± 0.4 c)	2.5 ± 0.6
				620.0 ± 0.4 c, g)	17 ± 2
623.0 ± 0.2	56 ± 6	623.2 ± 0.5	55 ± 4	623.2 ± 0.2	53 ± 4
		624 ± 1 e)	2.8 ± 0.7		
		635 ± 1 e)	0.6 ± 0.3		
642.0 ± 0.4 c)	8 ± 1	642 ± 0.5 d)	8.0 ± 1	642.0 ± 0.2	9.0 ± 1
650.2 ± 0.2	90 ± 9	650.6 ± 0.5	95 ± 6	650.5 ± 0.1	88 ± 6
		657.7 ± 0.5	2.4 ± 0.7	657.4 ± 0.4	2.7 ± 0.6
685.5 ± 0.3	6.3 ± 0.8	685.7 ± 0.5	6.3 ± 1	685.6 ± 0.2	7.1 ± 0.8
709.8 ± 0.2 c	23 ± 2	710.0 ± 0.5	21 ± 3	709.9 ± 0.2	20 ± 2
		743 ± 1	2.0 ± 0.7	742.6 ± 0.5 c)	1.5 ± 0.6
		746.0 ± 1	2.0 ± 0.7	746.1 ± 0.5	1.7 ± 0.6
				752.9 ± 0.4 c, g)	6.2 ± 1
		773 ± 1 e)	0.7 ± 0.3		
775.5 ± 0.3	5.2 ± 0.5	775.6 ± 0.5	6.4 ± 1	775.4 ± 0.3	7.6 ± 1.4
		794 ± 1	2.1 ± 1	793.9 ± 0.5 c)	3.3 ± 0.8
803.5 ± 0.3	4.1 ± 0.4	803.9 ± 0.7	5.6 ± 0.2	803.6 ± 0.5	5.5 ± 1.6
808.5 ± 0.3	3.3 ± 0.4	808.5 ± 1 d)	4.2 ± 0.2	808.2 ± 0.5	5.0 ± 1.6
		816.5 ± 1	1.3 ± 0.7		
		828 ± 1	0.7 ± 0.4		
		833 ± 1 e)	1.4 ± 0.7		
835.6 ± 0.2	49 ± 5	835.8 ± 0.5	48 ± 3	835.7 ± 0.3	46 ± 3
		890 ± 1 e)	0.7 ± 0.3		
		920.5 ± 0.7	1.3 ± 0.7	920.6 ± 1.0 c)	1.5 ± 0.8
		937.3 ± 1	1.1 ± 0.6	937.4 ± 1.0 c)	1.2 ± 0.6

Table 7. Continued.

This study		Berzins et al. a)		Schick and Talbert b)	
Energy (keV)	Intensity	Energy (keV)	Intensity*	Energy (keV)	Intensity*
		950.0 ± 1	1.4 ± 0.6		
		955.1 ± 0.7	5.6 ± 1	955.1 ± 0.4	6.5 ± 1.3
1002.2 ± 0.4	7 ± 1	1002.2 ± 0.7	8.4 ± 3	1002.2 ± 0.5	8.2 ± 1.3
		1015 ± 1 e)	1.4 ± 0.7	1014.5 ± 1.0 c)	1.0 ± 0.6
		1022 ± 1 e)	1.1 ± 0.6		
		1026.6 ± 1	1.4 ± 0.7	1026.8 ± 1.0	1.3 ± 0.6
				1050.5 ± 1.0 h)	0.8 ± 0.6
		1053 ± 1 e)	0.7 ± 0.4		
		1059.8 ± 1	2.1 ± 0.7	1060.2 ± 1.0 c)	1.7 ± 0.8
		1067.1 ± 0.5 e)	2.1 ± 0.7	1066.8 ± 1.5 c, h)	1.2 ± 0.6
		1098 ± 1 e)	1.1 ± 0.5		
1120.0 ± 0.3	23 ± 2	1120.2 ± 0.5	25 ± 7	1120.7 ± 0.3	23 ± 2
				1147.2 ± 1.0 c)	1.3 ± 0.8
		1246 ± 1 e)	0.6 ± 0.3		
		1269.7 ± 0.5	1.4 ± 0.4		
		1311.2 ± 1	1.3 ± 0.7	1311.5 ± 1.0 c)	1.0 ± 0.6
				1346.6 ± 1.5 c, h)	0.4 ± 0.4
1388.3 ± 0.3	100	1388.4 ± 0.5	119 ± 11	1388.5 ± 0.2	82 ± 4
		1395 ± 1 e)	0.7 ± 0.4		
1459.0 ± 0.3	109 ± 11	1458.7 ± 0.5	123 ± 11	1458.9 ± 0.2	90 ± 4
		1506 ± 1	0.1 ± 0.1		
		1542.4 ± 1	3.9 ± 0.7	1542.7 ± 0.4 c)	3.1 ± 0.8
		1549 ± 1	0.8 ± 0.4	1547.2 ± 0.4	3.3 ± 0.8
		1574.1 ± 1	5.2 ± 1		
		1644.3 ± 1	3.2 ± 0.7	1645.0 ± 0.7	1.9 ± 0.6
		1705 ± 1	0.1 ± 0.1		
		1863.2 ± 1	0.4 ± 0.3	1864.3 ± 1.5 c, h)	0.4 ± 0.2
		1933 ± 1	0.1 ± 0.1		

a) Reference 3 b) Reference 57 c) Not placed in decay scheme d) known multiplet e) Observed in coincidence data only
f) Observed in the decay of Ag^{111m}. g) Possibly due to the decay of Ag^{111m}. h) Existence of gamma ray is uncertain.
* Renormalized to 140 for the 580 keV transition.

keV which decay with the Ag^{111m} half-life. No intensities were reported. Schick and Talbert (57) were similarly able to show that the 245 keV gamma ray is associated with the decay of Ag^{111m}.

The approximate beta branching of the Ag^{111m} state may be found assuming that the intensity of the 245 keV line due to the Pd^{111g} decay equals the total beta feeding from the Ag^{111m} level. The 22 minute portion of the 245 keV intensity is 96, which is at least four times the combined intensity of the other Ag^{111m} lines. Using an internal conversiton coefficient of 180 for the 60 keV transition, we obtain a beta branching of 0.5% for Ag^{111m}. This result is comparable to the 0.5% and 0.3% values of Schick and Talbert (57) and Berzins et al. (3).

Berzins et al. (3) deduced the Pd^{111g} decay scheme largely from Ge(Li)-Ge(Li) coincidence data and to a lesser degree from energy balance considerations. Schick and Talbert (57), on the other hand, relied mainly on gamma ray energy relationships. The proposed levels populated in the Pd^{111g} decay, their associated log ft values and spin-parity assignments are compared in Table 8.

The Pd^{111g} decay schemes of these studies are consistent in most respects with the decay scheme of this study. Major gamma ray transitions are similarly placed in all level schemes. However, Berzins et al. (3) have divided the intensity of some lines between two or more levels either because they found the lines to be complex

Table 8. Comparison of experimental data on the energy levels populated in the decay of Pd^{111g}.

This study			Berzins et al. a)			Schick and Talbert b)		
Energy (keV)	*log ft	Spin-parity	Energy (keV)	*log ft	Spin-parity	Energy (keV)	*log ft	Spin-parity
0		$1/2^-$	0		$1/2^-$	0		$1/2^-$
60.0	5.8	$7/2^+$	59.9	5.9	$7/2^+$	59.8	5.8	$7/2^+$
130.3		$(9/2^+)$ d)	130.4		$(9/2^+)$ d)	130.2		$(9/2^+)$ d)
289.6	8.6	$1/2^-, 3/2^-, 5/2^-$	289.8	9.2	$(3/2^-)$ d)	289.8	8.7	$(3/2^-)$ d)
376.7	8.1	$3/2^+, 5/2^-$	376.7	8.2	$3/2^+, 5/2^-$	376.7	8.2	$3/2^+, 5/2^-$
391.1	9.1	$1/2^-, 3/2^-, 5/2^-$	391.3	9.1	$(5/2^-)$ d)	391.2	8.9	$(5/2^-)$ d)
405.2 c)	9.0	$1/2^-, 3/2^-, 5/2^-$	404.9		$1/2^+, 3/2^\pm, 5/2^-$	404.9		
			546.0	8.3	$5/2^+, 7/2^\pm$	545.6	8.5	$7/2^+, 5/2^+$
569.0	8.0	$5/2^+, 7/2^+, 9/2^-$	568.8	8.0	$5/2^+, 7/2^-$	568.7	8.0	$5/2^+, 7/2^-$
607.0	7.9	$5/2^+, 7/2^+, 9/2^-$	607.1	7.7	$5/2^+, 7/2^\pm$	606.9	7.7	$5/2^+, 7/2^+$
			642.4	9.1	$3/2^-, 5/2^-$			
683.0	8.4	$5/2^+, 7/2^+, 9/2^-$	683.2	8.6	$7/2^\pm$	683.0	8.4	
710.2	7.2	$5/2^+, 7/2^+$	710.5	6.7	$5/2^+, 7/2^+$	710.3	7.3	$5/2^+, 7/2^\pm$
			809	9.0	$5/2^-$			
			876.4		$7/2^\pm, 9/2^\pm, 11/2^+$	876.3	8.6	
			959		$9/2^\pm, 11/2^\pm$			
1062.2	8.0	$3/2^+, 5/2^\pm, 7/2^\pm, 9/2^-$	1062.5	7.8	$3/2^+, 5/2^\pm$	1062.3	8.0	
			1085.4	8.0	$5/2^+, 7/2^\pm$	1085.3	8.0	
			1086.7	7.6	$3/2^\pm, 5/2^\pm, 7/2^\pm$	1086.5	7.6	
			1119.8	7.7	$3/2^+, 5/2^\pm, 7/2^+$			
			1170	8.2	$3/2^\pm, 5/2^\pm, 7/2^\pm$			
1180.0	7.4	$3/2^+, 5/2^\pm, 7/2^\pm, 9/2^-$	1180.4	7.4	$3/2^\pm, 5/2^\pm, 7/2^-$	1180.4	7.3	$5/2^+, 7/2^\pm$
			1210.2	8.2	$3/2^\pm, 5/2^\pm, 7/2^-$			
			1506.1	8.3	$3/2^\pm, 5/2^-$			
1519.0	5.9	$5/2^+, 7/2^+$	1518.8	5.8	$5/2^+, 7/2^+$	1518.7	5.9	$5/2^+, 7/2^+$

a) Reference 3 b) Reference 57

c) Existence of level uncertain.

d) From analogy with Ag^{109}.

* Missing log ft values imply no significant amount of beta feeding to the level.

Table 8. Continued.

This study			Berzins et al. a)			Schick and Talbert b)		
Energy (keV)	*log ft	Spin-parity	Energy (keV)	*log ft	Spin-parity	Energy (keV)	*log ft	Spin-parity
			1622	7.6	$3/2^{\pm}, 5/2^{\pm}, 7/2^{\pm}$			
			1674.4	7.2	$3/2^{\pm}, 5/2^{\pm}, 7/2^{\pm}$			
			1705	6.6	$5/2^{+}, 7/2^{+}$	1704.6	6.6	$5/2^{+}, 7/2^{+}$
			1994 c)	6.8	$(5/2^{+})$			

or because there was an unresolved ambiguity in the placement. These are the lines of energy 476, 623, 642, 775, 808, 835, and 1120 keV. Spin-partiy assignments and log ft values are in general agreement, although the observation of additional gamma ray transitions has enabled in some instances the other investigators to narrow the range of spin-parity choices. It may be mentioned that the unique assignments for the 289 and 391 keV levels made in the other studies are based primarily on analogy with the Ag^{109} level scheme.

Tables 9 and 10 compare the results of Berzins et al. (3), Schick and Talbert (57), and this study concerning the gamma ray transitions and energy levels populated in the decay of Pd^{111m}. Berzins et al. (3) used Ge(Li)-Ge(Li) coincidence measurements in deducing a decay scheme, whereas Schick and Talbert (57) used a Ge(Li)-NaI(Tl) coincidence spectrometer. While all studies agree in basic respects on the details of the Pd^{111m} decay, there are several discrepancies upon which the results of this study have a bearing.

The 1463 keV level

This level is proposed by Berzins et al. (3) and by this study but not in the investigation of Schick and Talbert (57). Major transitions suggested as being associated with this level have energies of 358, 439, 617, and 654 keV, the latter gamma ray not placed in the

Table 9. Comparison of gamma ray energies and intensities observed in the decay of Pd^{111m}.

This study		Berzins et al. a)		Schick and Talbert b)	
Energy (keV)	Intensity	Energy (keV)	Intensity*	Energy (keV)	Intensity*
		59.9 ± 0.1	13 ± 3	59.8 ± 3	
70.3 ± 0.2	190 ± 50	70.5 ± 0.2	136 ± 10	70.4 ± 0.1	185 ± 40
101.7 ± 0.4	4 ± 1	101.7 ± 0.5	5 ± 1	~ 101	
		119.1 ± 1.0	1.1 ± 0.5	118.9 ± 0.5	1 ± 0.5
		167.0 ± 0.5 e)	1 ± 1	168.8 ± 1.0	
		169.4 ± 0.5 e)	14 ± 3		
172.2 ± 0.2	1000	172.2 ± 0.5	600 ± 20	172.0 ± 0.1	905 ± 50
		178 ± 1	0.5 ± 0.3		
				259.5 ± 0.5 c)	1.5 ± 0.5
		263.0 ± 1	0.4 ± 0.2		
272.0 ± 0.3	3.1 ± 0.5	272.0 ± 0.5	2.4 ± 0.5	271.9 ± 0.2	2.3 ± 0.8
289.6 ± 0.2	22 ± 2	289.8 ± 0.5	14 ± 2	289.8 ± 0.1	19 ± 2
		307.5 ± 1	2.4 ± 1		
		316.9 ± 0.5 e)	0.3 ± 0.1		
357.9 ± 0.3	7.9 ± 0.8	358.1 ± 0.5	7.8 ± 2	358.1 ± 0.2	8.8 ± 1
376.7 ± 0.2	17 ± 2	376.7 ± 0.3	14 ± 3	376.7 ± 0.1	17 ± 4
				381.0 ± 0.5 c)	0.8 ± 0.4
391.1 ± 0.2	112 ± 11	391.3 ± 0.5	97	391.2 ± 0.1	104 ± 5
				413.3 ± 0.3	34 ± 6
414.6 ± 0.5 d)	80 ± 20	415 d)	66 ± 10	415.3 ± 0.3	29 ± 6
		418 ±1	1 ± 0.5		
439.0 ± 0.3	5.4 ± 0.7	439.2 ± 0.5	4.7 ± 1	439.1 ± 0.7	4.3 ± 1.8
				443.9 ± 0.5 c)	2.9 ± 1
454.4 ± 0.2	24 ± 3	454.6 ± 1 d)	24 ± 2	454.4 ± 0.1	25 ± 2
				465.7 ± 1.0 c)	1.8 ± 0.8
				467.2 ± 1.0 c)	
		476	1		
485.7 ± 0.3	8.2 ± 0.8	485.9 ± 0.5	11 ± 1.5	485.8 ± 0.2	10 ± 1
		504 ± 1	1 ± 0.5	505.5 ± 1.0 c, h)	~ 1
		519.2 ± 0.5	2 ± 1	519.1 ± 0.3 c)	3.9 ± 1

Table 9. Continued.

This study		Berzins et al. a)		Schick and Talbert b)	
Energy (keV)	Intensity	Energy (keV)	Intensity*	Energy (keV)	Intensity *
525.4 ± 0.2	21 ± 2	525.6 ± 0.5 d)	24 ± 3	525.5 ± 0.1	27 ± 2
552.5 ± 0.3	5 ± 1	552.5 ± 0.7 d)	5.0 ± 1.5	552.3 ± 0.4	5.2 ± 2
556.4 ± 0.4	3 ± 1	556.3 ± 0.7	3.2 ± 1.5	556.5 ± 0.7	3.9 ± 1
575.2 ± 0.2	67 ± 7	575.1 ± 0.5	67 ± 5	575.0 ± 0.1	60 ± 5
		584	5	583.5 ± 0.5 c)	4.7 ± 1
				595.5 ± 0.3 c)	2.9 ± 0.8
617.5 ± 0.4	2.3 ± 0.8	617 ± 1	1.4 ± 0.5	618.0 ± 1.0 c)	~1.6
623.0 ± 0.3	11 ± 1	623.2 ± 0.5	4.8 ± 1		
632.9 ± 0.2	65 ± 7	632.7 ± 0.5	65 ± 7	632.6 ± 0.1	65 ± 5
645.3 ± 0.5	4 ± 2	645.6 ± 0.5 e)	1.9 ± 1		
654.6 ± 0.4 c)	4 ± 1	654.0 ± 1.0	3.4 ± 1	654.5 ± 0.5 c)	1.8 ± 0.5
668.2 ± 0.2	19 ± 2	668.3 ± 0.5	20 ± 2	668.2 ± 0.1	18 ± 2
694.0 ± 0.2	39 ± 4	694.1 ± 0.5	38 ± 3	694.1 ± 0.1	38 ± 3
		697 ± 1 e)	1 ± 0.5		
703.2 ± 0.3	13 ± 2	703.6 ± 0.7	12 ± 3	703.6 ± 0.3	13 ± 3
		716 ± 1	0.8 ± 0.4	715.4 ± 0.7	0.9 ± 0.4
718.3 ± 0.4 c)	2.3 ± 0.5	718.9 ± 1	3.4 ± 0.5	718.6 ± 0.4 c)	3.4 ± 1
		724.6 ± 0.5	4.5 ± 0.5	724.4 ± 0.3	4.2 ± 1
		746.3 ± 0.7	2.0 ± 1.0	746.4 ± 0.4 c)	3.1 ± 1
752.9 ± 0.4	2.1 ± 0.6	752.7 ± 0.5 d)	1.4 ± 1.0	752.6 ± 0.3	2.1 ± 1
762.2 ± 0.3	20 ± 2	762.0 ± 0.5	20 ± 2	761.9 ± 0.1	21 ± 2
				785.7 ± 0.7	0.6 ± 0.4
797.4 ± 0.3	17 ± 2	797.6 ± 0.5	17 ± 2	797.6 ± 0.1	17 ± 2
		808.5 ± 1	1.0 ± 0.5		
		816.8 ± 1	1.7 ± 0.5	816.6 ± 0.5 c)	1.5 ± 0.4
		828 ± 1 d)	2 ± 1	828.6 ± 0.4	2.6 ± 0.8
				844.7 ± 1.0	0.4 ± 0.3
863.1 ± 0.4	2.4 ± 0.5	863.1 ± 1 d)	2.4 ± 1.0	863.1 ± 0.5	2.1 ± 0.5
881.6 ± 0.4	3.2 ± 0.5	882.0 ± 1 d)	3.8 ± 1.0	882.0 ± 0.4	3.4 ± 0.8
				893.9 ± 0.7	0.6 ± 0.3

Table 9. Continued.

This study		Berzins et al. a)		Schick and Talbert b)	
Energy (keV)	Intensity	Energy (keV)	Intensity*	Energy (keV)	Intensity*
				896.7 ± 1.0 c, h)	0.4 ± 0.2
		916.6 ± 1	1.0 ± 0.5	916.4 ± 1.0 h)	0.6 ± 0.3
				941.5 ± 1.0 h)	0.8 ± 0.5
		945.0 ± 1	2.0 ± 1	945.0 ± 1.0 c)	2.4 ± 0.8
975.5 ± 0.4	3.8 ± 0.5	975.6 ± 1	3.8 ± 1.5	975.6 ± 0.4	3.1 ± 0.8
				984.9 ± 1.0 c)	0.5 ± 0.3
997.1 ± 0.4	5.4 ± 0.6	997.0 ± 1	4.8 ± 2	997.0 ± 0.4	4.2 ± 0.8
		1001 ± 1	2.0 ± 1	1001.2 ± 1.0	2.1 ± 1
		1022.9 ± 1	2.0 ± 1	1023.4 ± 0.5	2.7 ± 0.8
		1029.3 ± 1	1.3 ± 1	1028.8 ± 1.0	1.3 ± 0.5
		1045.5 ± 1	1.4 ± 1	1045.5 ± 0.7	1.3 ± 0.5
1063.3 ± 0.4 c)	5.1 ± 0.8	1063.4 ± 1	3.8 ± 1.5	1063.5 ± 0.7	2.6 ± 0.8
		1076 ± 1	0.8 ± 0.4		
		1088.3 ± 1	4.9 ± 1	1088.3 ± 0.5	3.1 ± 0.8
		1098.5 ± 1	2.2 ± 1		
1115.8 ± 0.3	21 ± 2	1115.6 ± 0.7	20 ± 3	1116.2 ± 0.2	22 ± 2
		1140 ± 2 d)	2 ± 1	1140.4 ± 1.5 h)	0.4 } 0.8
				1142.7 ± 1.0	1.2 }
1163.3 ± 0.4	4.9 ± 0.6	1163.1 ± 0.5	5.7 ± 1.5	1163.5 ± 0.3	6.0 ± 0.5
1199.5 ± 0.4	5.4 ± 0.6	1200.0 ± 1	5.7 ± 1.5	1200.5 ± 0.3	5.5 ± 0.5
		1223.6 ± 1	0.9 ± 0.5	1222.8 ± 0.5 c)	1.6 ± 0.5
				1258.5 ± 1.0 h)	0.5 ± 0.3
				1269.9 ± 1.5 c, h)	0.4 ± 0.2
1282.2 ± 0.3	23 ± 3	1282.6 ± 1	22 ± 3	1282.7 ± 0.2	19 ± 1
		1309 ± 1	1 ± 0.5		
				1351.2 ± 2.0 c, h)	0.5 ± 0.3
		1381 ± 1	0.7 ± 0.4		
		1418 ± 1	1.7 ± 0.5	1418.6 ± 0.5	1.8 ± 0.5
				1428.3 ± 1.5 c)	0.5 ± 0.3
1650.8 ± 0.3	14 ± 2	1651.1 ± 0.5	17 ± 2	1651.4 ± 0.2	13 ± 1

Table 9. Continued.

This study		Berzins et al. a)		Schick and Talbert b)	
Energy (keV)	Intensity	Energy (keV)	Intensity*	Energy (keV)	Intensity*
1690.9 ± 0.3	23 ± 2	1691.1 ± 0.5	26 ± 2	1691.0 ± 0.2	21 ± 1
1721.6 ± 0.4	5.0 ± 0.8	1721.8 ± 0.5	5.2 ± 1	1721.7 ± 0.3	4.9 ± 0.5
				1762.1 ± 1.0 g)	0.4 ± 0.2
1775.0 ± 0.4	7 ± 1	1775.2 ± 0.5	9.0 ± 2	1775.1 ± 0.3	7.5 ± 0.8
		1904.7 ± 1	1.5 ± 0.5	1904.9 ± 1.0	1.1 ± 0.4
		1939.0 ± 1	1.5 ± 0.5	1940.0 ± 1.0	1.1 ± 0.4
1970.3 ± 0.5	10 ± 1	1970.6 ± 1	13 ± 1.5	1970.7 ± 0.5	10 ± 1
		2064.1 ± 1	0.5 ± 0.3	2063.7 ± 1.5 c)	0.4 ± 0.2
		2086.1 ± 1	0.5 ± 0.3	2086.2 ± 1.5	0.7 ± 0.3

a) Reference 3. b) Reference 57.
c) Not placed in decay scheme.
d) Known multiplet.
e) Observed in coincidence data only.
f) Intensity could not be reliably determined.
g) Peak is possibly due to summation.
h) Existence of gamma ray is uncertain.
* Renormalized to 65 for the 633 keV transition.

Table 10. Comparison of experimental data on the energy levels populated in the decay of Pd^{111m}.

This study			Berzins et al. a)			Schick and Talbert b)		
Energy (keV)	*log ft	Spin-parity	Energy (keV)	*log ft	Spin-parity	Energy (keV)	*log ft	Spin-parity
0		$1/2^-$	0		$1/2^-$	0		$1/2^-$
60.0		$7/2^+$	59.9	8.6	$7/2^+$	59.8		$7/2^+$
130.3	8.2	$(9/2^+)$ d)	130.4	8.2	$(9/2^+)$ d)	130.2	8.2	$(9/2^+)$ d)
289.6		$1/2^-, 3/2^-, 5/2^-$	289.8		$(3/2^-)$ d)	289.8		$(3/2^-)$ d)
376.7		$3/2^+, 5/2^-$	376.7		$3/2^+, 5/2^-$	376.7		$3/2^+, 5/2^-$
391.1		$1/2^-, 3/2^-, 5/2^-$	391.3		$(5/2^-)$ d)	391.2		$(5/2^-)$ d)
545.7 c)	8.4	$7/2^+, 9/2^\pm, 11/2^+$	546.0		$5/2^+, 7/2^\pm$	545.6	9.1	$7/2^+, 5/2^+$
683.0 c)	8.9	$7/2^+, 9/2^+, 11/2^+$	683.2		$7/2^\pm$			
705.3	8.8	$7/2^+, 9/2^+, 11/2^+$	705.5	9.0	$7/2^+, 9/2^+, 11/2^+$	705.2	8.9	$11/2^\pm, 13/2^\pm$
			809.0		$5/2^-$			
824.3	8.6	$9/2^+, 11/2^+, 13/2^+$	824.5	8.5	$9/2^\pm, 11/2^\pm$	824.4	8.5	$11/2^\pm, 13/2^\pm$
845.5	9.1	$5/2^-, 7/2^-, 9/2^-$	846.0		$5/2^-, 7/2^-$	845.6	8.9	$7/2^-, 9/2^-$
			876.7	9.6	$7/2^+, 9/2^\pm, 11/2^+$			
						903.9	9.0	
			959	8.1	$9/2^\pm, 11/2^\pm$	958.8	8.2	
			986.8		$5/2^-, 7/2^-$			
1024.0	8.5	$5/2^-, 7/2^-, 9/2^-$	1024.0		$5/2^-, 7/2^\pm, 9/2^-$	1023.7	8.5	$(9/2^-)$
1152.7		$5/2^-, 7/2^-, 9/2^-$	1153.3		$(7/2^-)$	1153.1		$(7/2^-)$
			1159.7	8.5	$9/2^\pm, 11/2^\pm, 13/2^\pm$			
1463.0		$5/2^-, 7/2^-, 9/2^-$	1463.1	8.5	$9/2^-$			
			1543	8.2	$9/2^\pm, 11/2^\pm, 13/2^\pm$			
1549.4	7.4	$9/2^-, 11/2^-, 13/2^-$	1549.6	7.4	$9/2^\pm, 11/2^\pm$	1549.1	7.3	$11/2^\pm, 9/2^\pm$
			1706	7.4	$9/2^\pm, 11/2^\pm$			
			1748.6	7.8	$9/2^\pm, 11/2^\pm, 13/2^\pm$			
1781.1	7.2	$(9/2^-)$	1781.6	6.9	$9/2^-$	1781.6	7.1	$9/2^-$
1821.2	6.3	$9/2^-, 11/2^-$	1821.5	6.2	$9/2^-, 11/2^-$	1821.3	6.3	$11/2^-$

Table 10. Continued.

This study			Berzins et al. a)			Schick and Talbert b)		
Energy (keV)	*log ft	Spin-parity	Energy (keV)	*log ft	Spin-parity	Energy (keV)	*log ft	Spin-parity
1905.3	6.8	$9/2^-, 11/2^-$	1905.7	6.6	$9/2^-, 11/2^-$	1905.6	6.9	$(11/2^-)$
						1933.9	7.4	
						1964.6	7.4	$9/2^{\pm}; 11/2^-$
1987.5	6.3	$9/2^-, 11/2^-, 13/2^-$	1987.8	6.2	$9/2^-, 11/2^-, 13/2^-$	1987.9	6.2	$(13/2^-)$
			2069.6	6.8	$9/2^-, 11/2^-$	2069.5	7.0	$(11/2^-)$
			2087	6.7	$9/2^-, 11/2^-, 13/2^-$			
2100.6	6.3	$9/2^-, 11/2^-$	2101	5.9	$9/2^-, 11/2^-$	2101.2	6.1	$(11/2^-)$
						2216.7	6.3	$11/2^-; 9/2^-$

a) Reference 3. b) Reference 57.

c) Existence of level uncertain.

d) From analogy with Ag^{109}.

* Missing log ft values imply no significant amount of beta feeding to the level.

decay scheme of this study. Several arguments may be put forth favoring the existence of the 1463 keV level over the 903 keV level:

1. Schick and Talbert (57) mention that the energy fits of the four gamma rays accommodated by the 903 keV level are relatively poor.
2. The energy of the three gamma rays accommodated by the 1463 keV level in this study, on the other hand, agree with the level differences to within 0.3 keV.
3. Berzins et al. do not confirm the existence of a 358-414 keV coincidence. Instead, they report that the 358 keV transition is in coincidence with the 391, 439, 519, 617, 633, and 654 keV gamma rays, strongly favoring the existence of a level at 1463 keV. The Ge(Li)-Ge(Li) coincidence spectrometer of Berzins et al. (3) would be expected to give the more reliable results by virtue of its superior resolution.
4. The 618 keV transition which Schick and Talbert (57) cannot place in the decay scheme is logically accommodated by the 1463 keV level in this study. Moreover, Berzins et al. are able to assign three additional gamma rays, which Schick and Talbert (57) do not place in the decay scheme, to the 1463 keV level.

The 552 keV Gamma Ray

The only other disagreement over the placement of gamma rays seen in this study concerns the 552 keV transition. Schick and Talbert (57) on the basis of energy balance place it between the 2101 keV and 1549 keV levels, while it is taken to lie between the 683 keV and 130 keV levels in this study. Berzins et al. (3) place part of the intensity between the 683 and 130 keV levels and the remainder between levels at 1706 and 1153 keV. An argument for placing at least part of the 552 keV intensity between the 683 keV and 130 keV levels is that the 623 keV and 552 keV lines, which are known to depopulate a level at 683 keV in the Pd^{111g} decay, are seen also in the decay of Pd^{111m}. Furthermore, the energy fit in this study of the 552 keV line between the 683 and 130 keV levels is much superior to that between the 2101 and 1549 keV levels.

The 623 keV and 645 keV Gamma Rays

The existence of gamma rays at 623 keV and 645 keV, which are observed by Berzins et al. (3) but not by Schick and Talbert (37), is confirmed in the spectra of this study. The 645 keV peak was previously seen only in the coincidence spectra of Berzins et al. (3).

Log ft values and spin-parity assignments for the levels populated in the Pd^{111m} decay are not in as good agreement as were the

Pd^{109} and Pd^{111g} results. The log ft values found in this study for the levels at 545 keV and 683 keV are low because it was not possible to place transitions feeding these levels. The log ft values of this study associated with the 845 and 1024 keV levels should also probably be higher, as was discussed in an earlier section. Spin-parity assignments, although often not identical, generally overlap among the studies. Where there are differences, the assignments of Berzins et al. (3) are generally in closer agreement with those of this study.

The odd-A silver isotopes are especially interesting from a theoretical point of view. Interpretations of the nuclear properties of these isotopes have been made in terms of the particle-core weak coupling model of de-Shalit, the pairing-plus-quadrupole model, and the Nilsson model. The predictions of each of these models will be compared with the experimental findings of this and other studies.

The even-even mass nuclei adjacent to Ag^{109} and Ag^{111} have energy levels which may be interpreted in terms of the vibrational model. In this model the nucleus is taken to perform small oscillations about a spherical equilibrium shape. The normal modes of the oscillations are labeled by their multipole order λ, the lowest member being of quadrupole type since a deformation of order $\lambda = 1$ is equivalent to a translation of the whole system. The nuclear energy levels then have excitation energies $\Sigma_\lambda N_\lambda \hbar\omega_\lambda$, where the integer N_λ is the number of excitation quanta or phonons of order λ in the

excited state. A phonon of order λ carries an angular momentum of λ units and parity $(-)^{\lambda}$. The first excited state has one quadrupole phonon present and is a 2^+ state. Since it is found experimentally that $2\omega_2 \approx \omega_3$, the second excited state is either the two-quadrupole-phonon triplet of states or the one-octupole-phonon state. In the former case we have three states degenerate in energy with spins 0^+, 2^+, 4^+ which are formed by coupling two angular momenta of two units. The latter case would be a 3^- state.

The vibrational model has enjoyed some success in explaining the energies, spins, and E2 transition probabilities of the states in the even-A isotopes of palladium and cadmium. The recent observation of large static electric quadrupole moments of the first 2^+ state in many of these nuclei (63) and ratios of B(E2) values which are lower than those predicted by theory (45, 55) have cast doubt on the validity of a simple vibrational explanation. However, Tamura and Udagawa (71) have demonstrated that even these experimental results may be explained within the vibrational framework if one is willing to accept rather large admixtures of the one- and two-quadrupole phonon states.

The odd-A silver isotopes differ from the even-mass Pd and Cd isotopes by the addition or subtraction of a single proton. A possible explanation of the energy levels of the odd-A silver isotopes might therefore be in terms of a coupling of the odd proton with the vibrational excitations of the even core. For instance the ground

state would consist of the odd proton in the lowest single-particle state of the average potential created by the core nucleons. If the next single-particle state were high compared to the lowest excitation energy of the core, the excited states would result from core excitations coupled to the odd proton in its lowest state. Calling J_c and j the total angular momenta of the collective core and the odd particle outside the core respectively, we then have for each state J_c a multiplet of states with spins $|J_c - j| \leq J \leq J_c + j$.

Such a model was proposed by de-Shalit in 1961 (16), and it probably provides the best interpretation of the negative-parity levels of $Ag^{107, 109, 111}$. In de-Shalit's formulation no detailed assumptions are made about the nature of the core excitations other than to identify them with the observed states in the neighboring even nuclei. The interaction between the odd particle and the core is taken to be the scalar product of two tensors, one operating on the core degrees of freedom and the other operating on the degrees of freedom of the particle. A straightforward calculation then shows that the center of gravity of each multiplet of states arising from a particular J_c lies at roughly the same energy as the state J_c of the neighboring even-mass nuclei.

Figure 22 compares the negative-parity level structures of Ag^{107}, Ag^{109}, and Ag^{111} with those of the adjacent even nuclei of Pd. The ground state of the odd-A silver isotopes is the $2p_{1/2}$

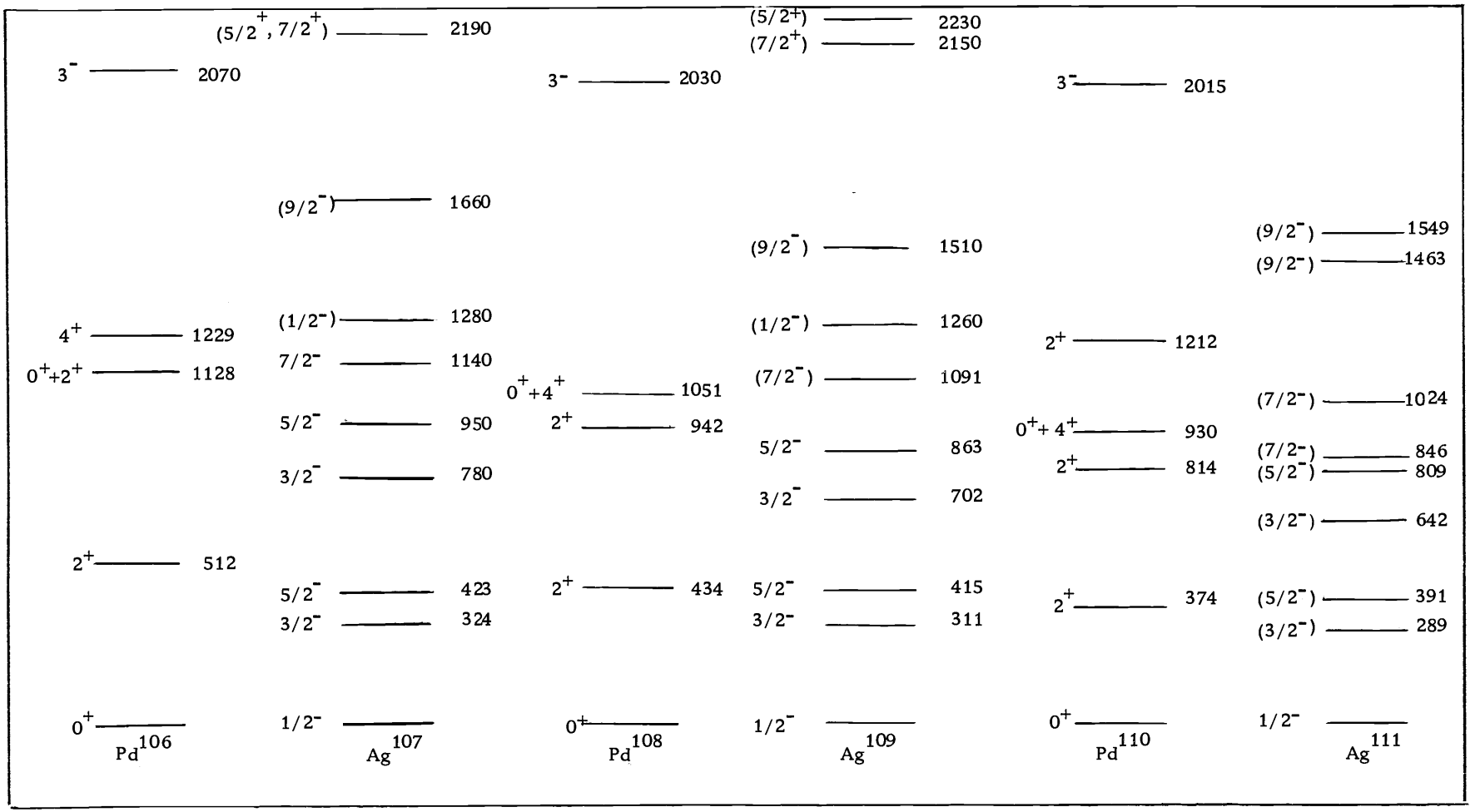

Figure 22. Comparison of selected negative-parity levels of Ag^{107}, Ag^{109}, and Ag^{111} with levels of the neighboring even-mass Pd isotopes. The data are compiled from this study and references 21 and 3.

single-particle state. We therefore expect to observe a doublet of states with spins $3/2^-$ and $5/2^-$ centered at about the energy of the first 2^+ state in the neighboring even-mass nuclei. Indeed, the $3/2^-$ and $5/2^-$ states at 324 and 423 keV in Ag^{107} (5) and at 311 and 415 keV in Ag^{109} have energies only slightly below the 512, 434, and 374 keV 2^+ states of the even Pd nuclei. In Ag^{111} the states at 289 and 391 keV have similar energies and gamma decay modes, suggesting that they too may arise from coupling of the $p_{1/2}$ single-particle state to the 2^+ core excitation.

The even-mass Pd isotopes exhibit a 0^+, 2^+, 4^+ triplet of states at about 1 MeV which may be interpreted as the two-quadrupole-phonon states. According to the de-Shalit model, we expect to see five states in the odd-A silver isotopes ranging in spin from $1/2^-$ to $9/2^-$, which are due to the coupling of the $p_{1/2}$ state with the two-phonon triplet. Five states with these spin-parities have been found in Ag^{107} (20) at energies ranging from 780 to 1660 keV. In Ag^{109} the $3/2^-$ state at 702 keV and the $5/2^-$ state at 863 keV are possible members of this multiplet. The recent (p,p') scattering data of Ford et al. (21) have identified in addition $7/2^-$, $1/2^-$, and $9/2^-$ states at 1091, 1260, and 1570 keV respectively in Ag^{109} which are presumably the remaining members of the multiplet.

Identifying the two-quadrupole-phonon levels in Ag^{111}, if indeed any do exist, is more difficult because of the large number of levels

from which to choose and the lack of definitive spin-parity assignments. Judging from the systematic level ordering in Ag^{107} and Ag^{109}, we expect states in Ag^{111} of spin $3/2^-$, $5/2^-$, $7/2^-$, $1/2^-$, and $9/2^-$ lying at energies of approximately 700, 800, 1000, 1200, and 1500 keV respectively. These states should preferentially gamma decay to other members within the group. No level is seen in this study which can reasonably be identified with the $3/2^-$ member of the multiplet. However, Berzins et al. (3) report a weakly populated level at 642 keV which decays to the 289 keV state, a member of the one-quadrupole-phonon doublet, and which has either spin $3/2^-$ or $5/2^-$. The 846 keV level observed in this study and the 809 keV level reported by Berzins et al. (3) are likely candidates for the $5/2^-$ member, judging from their energy, spin-parity, and gamma decay to the one-phonon doublet. The $7/2^-$ member of the multiplet could possibly be the 1024 keV or 1153 keV level. A third possibility is the 986 keV level observed by Berzins et al. (3) Each of these levels has a possible $7/2^-$ spin and decays to the one-phonon doublet. Both the 1463 and 1549 keV levels appear to be good candidates for the $9/2^-$ member, decaying to the 1024 and 845 keV levels which were considered possible $7/2^-$ and $5/2^-$ candidates. Not surprisingly, no $1/2^-$ state besides the ground state is seen in this or the other studies. Beta transitions to such a state from Pd^{111g} would be at least first forbidden unique and the state would be only weakly populated by

gamma feeding from higher-lying levels.

It is therefore apparent that many of the negative parity levels in Ag^{107}, Ag^{109}, and, more speculatively, in Ag^{111} can be explained by the de-Shalit weak coupling model. Additional evidence for the applicability of this approach is provided by the results of Coulomb excitation. The de-Shalit model predicts that the B(E2) value for the transition from each state of a multiplet to the ground state equals the B(E2) value for the corresponding transition in the neighboring even-mass nuclei. Also, $N = \pm 1$ for E2 transitions, where N is the phonon number, so that transitions from an N=2 multiplet to ground is forbidden. The B(M1) values for transitions to the ground state are predicted to be zero if there is no configuration mixing.

The Coulomb excitation data of Black and Gruhle (5) and Robinson et al. (54) for Ag^{107} and Ag^{109} show that the B(E2) values for the first excited state of Pd^{106}, the first $3/2^-$ and $5/2^-$ excited states of Ag^{107}, the first excited state of Cd^{108}, and the first $3/2^-$ and $5/2^-$ excited states of Ag^{109} are all nearly equal, as predicted. Further, the measured M1 strengths (54) for transitions from the first $3/2^-$, $5/2^-$ states of Ag^{107} and Ag^{109} to ground show that these transitions are strongly hindered. As for the "two-phonon states" in the 1 MeV region, the de-Shalit model predicts that the B(E2; N=2 $\rightarrow$ 1) value should be similar to the B(E2; N=1 $\rightarrow$ ground state) value. All of the higher-lying negative-parity states have B(E2) values which

are an order of magnitude smaller than those of the "one-phonon states." However, many of these levels do exhibit B(E2) values which are enhanced over the single-particle estimates and many have a strong preference for decaying through the N=1 states, suggesting a collective nature.

The study of proton and alpha particle scattering from Ag^{107} and Ag^{109} has further demonstrated the applicability of the de-Shalit model to these isotopes. Applied to direct reactions, the de-Shalit theory predicts (7) that the inelastic cross section for excitation of the member of the multiplet with spin J is just $(2J+1)/(2J_o+1)(2J_c+1)$ times the cross section of the state with spin J_c in the adjacent even-mass nuclei, where J_o is the ground state spin of the odd-A nucleus. The sum of the cross sections for the excitation of the states in the multiplet then equals the cross section for excitation of the core state. Further, the angular momentum transferred to the target equals the spin J_c of the core state even when other angular momentum transfers are permitted by angular momentum conservation. Therefore, the angular distributions for populating the states of a multiplet should all have the same shape as the angular distribution for populating the corresponding core state in the neighboring even-mass nuclei.

Ford et al. (20, 21) measured the differential cross sections for the elastic and inelastic scattering of 13 MeV protons from Ag^{107}

and Ag^{109}. For the states which appear to be due to coupling of the odd proton to the one-phonon states of the even core, the cross sections were fitted by distorted-wave theory. For states with excitation energies suggesting coupling of the odd particle to the two-quadrupole-phonon core states, the differential cross sections were fitted by coupled-channel calculations, since two-phonon core states may be populated by multiple excitation which cannot be treated by first-order distorted-wave theory. The shapes and relative magnitudes of the measured cross sections were then compared to those for neighboring even-mass nuclei. Their results show that the cross sections of the first $3/2^-$ and $5/2^-$ states in Ag^{107} and Ag^{109} are consistent with coupling the odd particle to the first 2^+ state of the core.

By adjusting the theoretical cross sections to the data, the partial deformations $\beta_\lambda^p(J)$ for these levels are found. Deformation parameters obtained in this way agree with those obtained from Coulomb excitation (44, 54) and inelastic alpha particle scattering (68). If the de-Shalit model is valid, the partial deformation for exciting the level with spin J is related to the total deformation β_λ of the even core by (67)

$$\beta_\lambda^p(J) = [(2J+1)/(2J_0+1)(2J_c+1)]^{1/2}\,\beta_\lambda .$$

It is found that the partial deformations of the low-lying $3/2^-$ and $5/2^-$

states in $Ag^{107, 109}$ are in satisfactory agreement with this prediction if the experimental β_2 values for the first 2^+ states in the neighboring even-mass nuclei are used.

Angular distributions of the scattered protons for several states in the 1 MeV region suggest that these states are formed by coupling the odd proton to the 0^+, 2^+, 4^+ two-quadrupole-phonon triplet. In Ag^{107}, states with energy and spin-parity of $780(3/2^-)$, $950(5/2^-)$, $1140(7/2^-)$, $1280(1/2^-)$, and $1660(9/2^-)$ keV each have an angular distribution resembling that of its associated 0^+, 2^+, 4^+ state in the neighboring even nuclei. The analogous states in Ag^{109} are the $702(3/2^-)$, $863(5/2^-)$, $1091(7/2^-)$, $1260(1/2^-)$, and $1510(9/2^-)$ keV states. Coupled-channel fits to the angular distributions can only be made, however, if an admixture of the one- and two-quadrupole phonon states are allowed. The beta parameters thus determined are in reasonable agreement with the values found for the even-mass nuclei $Pd^{106, 108, 110}$. However, the relative magnitudes of the cross sections for these states do not generally agree with theoretical predictions. One must make assumptions concerning admixtures of one-phonon states or of single-particle states to account for the observed strengths.

Ford et al. (20, 21) also report states of Ag^{107} and Ag^{109} at about 2 MeV which have angular distributions and energies similar to those for the 3^- one-octupole-phonon states of the adjacent even

nuclei. However, the total strength of these levels is only half that expected.

The inelastic scattering of 42 MeV alpha particles from Ag^{107} and Ag^{109} by Stewart et al. (68) has given results very similar to those found from proton scattering. The shapes and magnitudes of the angular distributions and the derived partial-deformation parameters for the first $3/2^-$ and $5/2^-$ states were found to be consistent with the coupling of an odd proton to a core quadrupole vibration. Other of the states observed by Ford et al. (20, 21) were seen with the proper excitation strengths to classify them as two-quadrupole-phonon states. In both isotopes a state was observed at an excitation energy of 2.17 MeV whose angular distribution indicated that it was a member of a possible octupole doublet.

Several difficulties exist in applying the de-Shalit weak coupling model to the odd-A silver isotopes. Discrepancies regarding the magnitudes of the cross sections predicted by theory have already been mentioned. Another problem is the additional states found in these isotopes which have no simple explanation in terms of the model. For example, Ag^{109} has at least three negative-parity states which cannot be attributed to coupling of the $p_{1/2}$ particle to excitations of the core. The situation is worse for Ag^{111} which has a multitude of negative-parity levels. Several explanations could be advanced for the existence of these states. The $p_{1/2}$ and $f_{5/2}$

single-particle levels are expected to lie rather close to the $p_{1/2}$ level. In fact the relatively small B(E2) values associated with the 787 keV state in Ag^{107} and the 702 keV state in Ag^{109} (5) may indicate a significant amount of $p_{3/2}$ admixture in these states. Other negative-parity levels should result from the coupling of these single-particle states with quadrupole phonons.

Regarding the positive-parity states, the only low-lying single-particle level of positive-parity expected in the region immediately below the 50 proton closed shell is the $g_{9/2}$ level. Presumably, the 126, 133, and 130 keV levels of Ag^{107}, Ag^{109}, and Ag^{111} are these $g_{9/2}$ states. The de-Shalit model then predicts a multiplet of five states with spins ranging from $5/2^+$ to $13/2^+$ whose center of gravity lies at about 500 keV. Instead, one finds a $7/2^+$ state lying below the $g_{9/2}$ level in all three isotopes and no other positive parity levels in Ag^{107} and Ag^{109} below 700 keV. Above 700 keV Ag^{107} has only two known (5) positive-parity levels, each with spin $5/2^+$ whereas Ag^{109} has possibly five with spins ranging from $3/2^+$ to $7/2^+$. States of spin higher than $7/2^+$ probably would not be observed since beta feeding is from a $5/2^+$ state in the decay of Cd^{107} and Pd^{109}. Ag^{111} has a large number of positive-parity states spread across the entire energy spectrum, and it would be difficult to identify their origin. In sum, although the de-Shalit weak coupling model appears to interpret correctly many of the properties of the negative-parity states in $Ag^{107, 109, 111}$, particularly of the first $3/2^-$ and $5/2^-$ states, a more sophisticated model

may be required to explain the positive-parity states of these isotopes.

Another method which has been used to treat spherical nuclei is the pairing-plus-quadrupole model. In these calculations the Hamiltonian of the system is composed of three parts

$$H = H_S + H_P + H_Q.$$

H_S is a spherically symmetric single-particle Hamiltonian, and the other two parts, H_P and H_Q, constitute the residual interaction. H_P represents a short-range pairing force which is effective only for shell-model pairs coupled to zero angular momentum. When neutrons and protons are filling different levels, the pairing force is assumed to exist only for protons and neutrons separately and to be approximately the same for each. H_Q represents a long-range quadrupole interaction. This force is important for particles in different orbits and is therefore effective among neutron-proton pairs as well as neutron and proton pairs separately. It is the quadrupole force which gives rise to the collective effects in the nucleus. The Hamiltonian is first written in terms of the creation and annihilation operators for shell-model particles. A canonical transformation is then performed to introduce the so-called "quasi-particle" creation and annihilation operators. Eigenfunctions of $H_P + H_S$ are the quasi-particle states so that quasi-particles have the property

of not interacting except through the quadrupole force, which is treated as a perturbation. Quasi-particles can be shown to behave like fermions. In the treatment of the quadrupole force, phonons and their interaction with the quasi-particles are introduced.

In applying the pairing-plus-quadrupole theory to the prediction of energy levels, Kisslinger and Sorensen (35) determined the pairing and quadrupole force strength parameters from data taken from single-closed shell nuclei. They limited their considerations to one-quasi-particle and zero-, one-, and two-phonon excitations. Their theoretical predictions for Ag^{109} and Ag^{111} are compared to the findings of this study in Figure 23. It is seen that the low-lying $9/2^+$, $3/2^-$, and $5/2^-$ states are correctly predicted. The higher-lying 5/2 and 7/2 states might be identified with any of several observed levels.

A serious failure of the theory, however, is its inability to predict the low-lying $7/2^+$ level. A more recent calculation by Kisslinger (33) includes three-quasi-particle states. It is found that when a high-spin level (such as the $g_{9/2}$) lies close in energy to several low-spin levels of the opposite parity, then, when the level is about half full, an extra state of spin j-1 may appear at low energies. Talmi and Unna (70) have also shown in a shell model calculation that the j-1 seniority three state of the $(g_{9/2})^3$ configuration in 47-neutron Sr^{85} is particularly lowered by residual interactions. This "intruder" state is a three-quasi-particle level whose energy

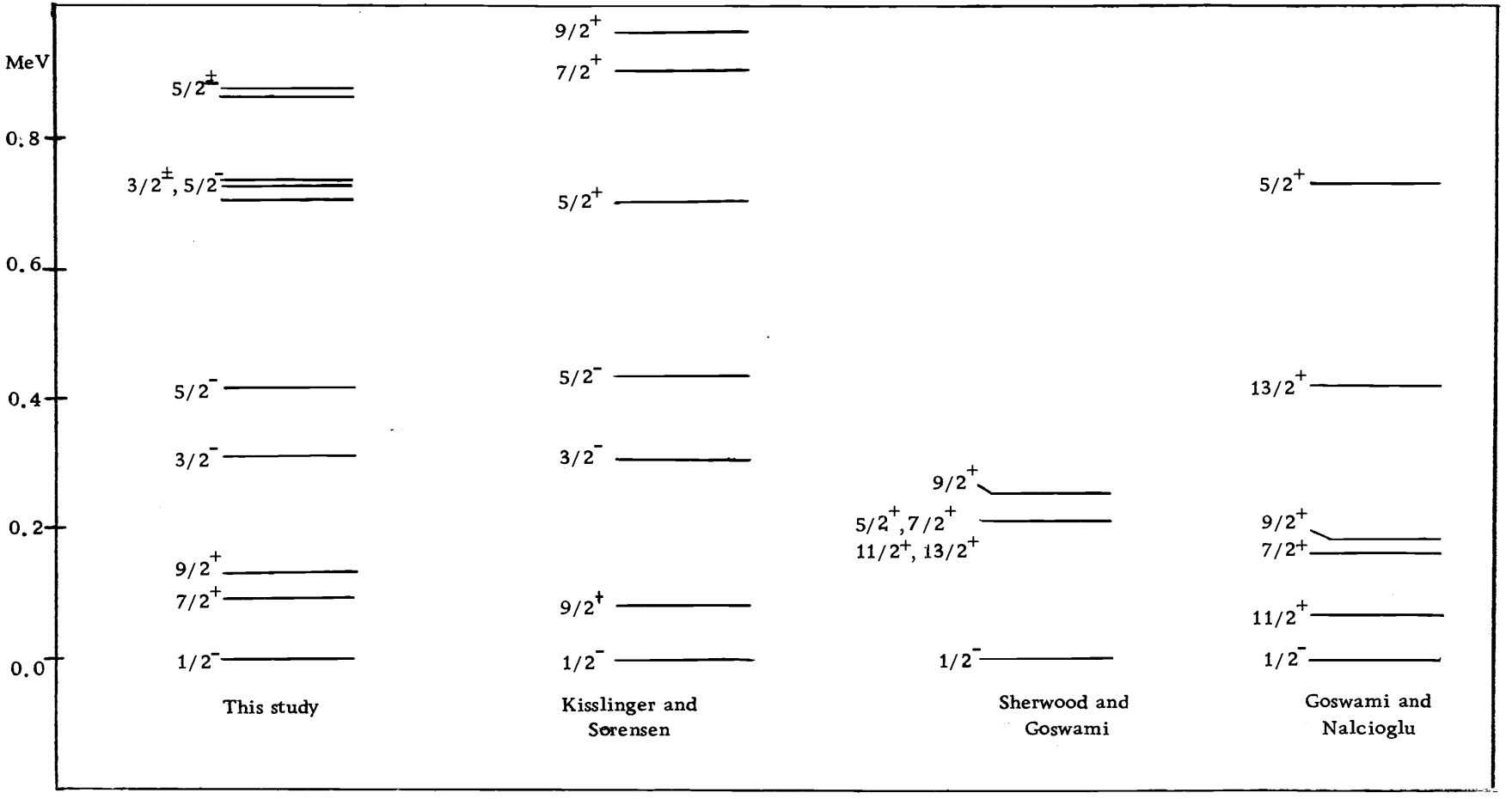

Figure 23. Comparison of Ag^{109} energy levels: the experimental results of this study and the theoretical predictions of Kisslinger and Sorensen (35), Sherwood and Goswami (59), and Goswami and Nalcioglu (24).

has been greatly lowered by the quadrupole interaction. Thus, the low-lying $7/2^+$ level in the odd-mass Ag, Tc, and Rh isotopes may be explained as a greatly lowered state of three $g_{9/2}$ quasi-particles coupled to a spin of 7/2. The low-lying $9/2^-$ state in the Te and Xe isotopes may similarly arise from incomplete filling of the $h_{11/2}$ shell in the 50-82 neutron region. A predicted feature of the intruder state is the complete absence of an M1 transition from it to the one quasi-particle state. This transition is a J=1, no parity change, so that either M1 or E2 transitions are normally possible. No measurements of E2/M1 ratios have been made for the $9/2^+ \rightarrow 7/2^+$ transitions in $Ag^{107, 109, 111}$. However, analogous transitions in such isotopes as Tc^{97}, Tc^{99}, and Rh^{103} have been shown (6, 72, 26) to be largely M1. Additional difficulties with this explanation are that the calculations cannot bring the $7/2^+$ state below the $9/2^+$ level and that lowered $5/2^+$ states in nuclei similar to the Ag isotopes are not accounted for.

Ikegami and Sano (31) have suggested that the inclusion of more orbits in the pairing-plus-quadrupole calculations may generate low-lying $7/2^+$ and $5/2^+$ levels. Taking into account 40 shell-model orbits, they predict a $5/2^+$ state lying below the $7/2^+$ state. However, no $5/2^+$ states of low energy have been observed in the odd-mass Ag isotopes, even though they would be populated by allowed beta transitions.

Whereas the Kisslinger and Sorenson calculations (35) assumed

only a part of the quasi-particle Hamiltonian to be important, the effects of the full quasi-particle interaction Hamiltonian are considered by Sherwood and Goswami (59), thereby including certain correlation effects in the core state. These effects are found to be particularly significant in the Tc, Rh, and Ag isotopes where the $g_{9/2}$ shell is about half filled. Rather than to lower the $7/2^+$ state, the result of these calculations is to raise the $9/2^+$ state to the vicinity of the multiplet of levels with spins from $5/2^+$ to $13/2^+$, which are due to the coupling of the $5/2^+$ state with the first 2^+ state of the even core. Figure 23 compares the predicted level sequence of Sherwood and Goswami for Ag^{109} with the experimental results of this study. While the $7/2^+$ and $9/2^+$ states are indeed brought together in this way, we also expect to see $5/2^+$, $11/2^+$, and $13/2^+$ states at low energies. However, no $5/2^+$ state is observed in Ag^{109} below 700 keV, nor are low-lying $11/2^+$ and $13/2^+$ states populated in the decay of Pd^{111m}.

The discovery of large, negative quadrupole moments in Cd^{114} and Cd^{116} (69, 60, 63) has led Goswami and Nalcioglu (24) to include the effect of coupling to the quadrupole moment of the core in calculations similar to those of Sherwood and Goswami. In Ag^{109} the effect of the new coupling is to lower the $11/2^+$ level below the $9/2^+$ and $7/2^+$ levels and to raise the $5/2^+$ state about 500 keV, as is seen in Figure 23. This indeed gives the correct level ordering for the $7/2^+$, $9/2^+$, and $5/2^+$ states. But the absence of low-lying

$11/2^+$ and $13/2^+$ states in Ag^{111} again proves to be a serious discrepancy.

It was suggested as early as 1953 (8, 1) that the odd-mass Ag isotopes may exhibit rotational spectra, which are characteristic of an equilibrium deformation of the nucleus. However, the absence of any systematic evidence for deformations in nuclei with mass $40 \leqslant A \leqslant 120$ has led later workers to favor descriptions in terms of a spherical equilibrium shape. Very recent experimental results may encourage a re-examination of the rotational interpretation. In^{115} and In^{117} have been found to have excited states whose energy spacing and transition rates are indicative of a $1/2^+$ rotational band (49, 42, 2). Cd^{114} and Cd^{116}, which have typically vibrational spectra, nevertheless have been found to possess large static electric quadrupole moments in their first 2^+ state (63, 69, 60, 22). Such quadrupole moments are expected to be zero in an ideal vibrational nucleus (71). Although it is possible to account for quadrupole moments within the framework of the vibrational model by allowing admixtures of states (71), it has also been suggested that the moments may arise because nuclear shapes in this region are transitional between spherical and strongly deformed (11, 34, 42, 13).

With these thoughts in mind, we now consider the possible applicability of the Nilsson model of the deformed nucleus to Ag^{109} and Ag^{111}. In the Nilsson model an axially symmetric oscillator potential

with spin-orbit coupling is used. The interaction of one nucleon with the nuclear field is represented by the following Hamiltonian

$$H = H_0 + C \vec{\ell} \cdot \vec{s} + D \vec{\ell}^2$$

where $H_0 = -\frac{\hbar^2}{2m}\nabla^2 + \frac{m}{2}(\omega_x^2 x^2 + \omega_y^2 y^2 + \omega_z^2 z^2)$

with x, y, z being the coordinates of a particle in a coordinate system fixed in the nucleus. If $\vec{J}$ and $\vec{j}$ are the total and particle angular momenta, and K and Ω, respectively, are their components along the axis of symmetry, then $K = \Omega$. Calling Λ and Σ the components of $\vec{\ell}$ and $\vec{s}$, respectively, along the axis of symmetry, then we also have $\Omega = \Sigma + \Lambda$. One other quantum number is N, the total number of quanta of vibration along each of the three axes.

Nilsson solved numerically the single-particle wave equation for the axially symmetric case in terms of a distortion parameter δ such that

$$\omega_x = \omega_y = \omega_o (1 + 1/3\,\delta), \quad \omega_z = \omega_o (1 - 2/3\delta)$$

with $\omega_o = \frac{2k}{m}$. His results are given in graphs which show the energy of each state as a function of the distortion δ. Each state is labeled by the value of Ω, the parity, and the triad $[N\ n_z \Lambda]$. The levels of distorted odd-A nuclei are understood as single-particle states and rotational bands built on them. The relative energies in a given band are given as

$$E_J = \frac{\hbar^2}{2I} [J(J+1) + a\,(-)^{J+1/2}(J+1/2)\,\delta_{K,\,1/2}]$$

where J = K, K+1 . . . . The second term vanishes except when K = 1/2. a is called the decoupling parameter since it corresponds to a partial decoupling of the particle motion from the rotating core. I is the moment of inertia of the nucleus.

According to the Nilsson diagram (75), the ground states of the Ag isotopes have quantum numbers $1/2^-[301]$. It is apparent that the $1/2^-, 3/2^-, 5/2^-$ sequence of levels in $Ag^{107, 109, 111}$ might constitute a K=1/2 rotational band. Fitting the energies of the first two excited states to the E_J formula, we get $\frac{\hbar^2}{2I}$ = 58 keV and a = 0.65 for the three Ag isotopes. The remaining members of the band should then have the following energies and spins: $1070(7/2^-)$, $1250(9/2^-)$, $2310\,(11/2^-)$. Ag^{107} and Ag^{109} are known (42, 43) to have $7/2^-$ states at 1140 and 1090 keV, respectively, which might be identified with the $7/2^-$ member. However, the lowest-lying $9/2^-$ states observed in Ag^{107} and Ag^{109} (20, 21) have energies of 1660 and 1510 keV, which are much higher than predicted. In Ag^{111} states at 1024 and 1158 keV are possible candidates for the $7/2^-$ and $9/2^-$ members of the rotational band.

Using the B(E2) values found from Coulomb excitation (5) between the ground state and the lowest $3/2^-$ and $5/2^-$ states in Ag^{107} and Ag^{109}, it is possible to deduce the deformation δ of the nuclei.

Under the assumption that the nuclei are indeed deformed, we use the formula (51)

$$B(E2;\ JK \rightarrow J'K) = \frac{5}{16\pi} e^2 Q_0^2 \left| < J\ 2\ K\ O | J'K > \right|^2$$

where the intrinsic quadrupole moment Q_0 is

$$Q_0 = \frac{3}{\sqrt{5\pi}}\ Z\ R_0^2\ \delta\ (1 + 0.36\ \delta)$$

and $R_0 = 1.2A^{1/3}$ fm is the nuclear radius. For B(E2) = 40, we have $\delta \approx 0.2$, which is a moderate deformation matching the values found for In^{115} and In^{117} (2).

Additional negative-parity states expected in the Nilsson model are the $3/2^-[301]$ and $5/2^-[303]$ single-particle states and rotational bands built upon them. Although the $3/2^-$ state at 702 keV in Ag^{109} has been shown to have a single-particle nature (5), there is little evidence for the existence of these states in the three Ag isotopes.

As far as positive-parity levels are concerned, the low-lying $7/2^+$ state is explained in the Nilsson formulation as a $7/2^+[413]$ state. The $9/2^+$ state at about 130 keV in the three isotopes would be interpreted as a mixture of the expected $9/2^+[404]$ single-particle state and the $9/2^+$ member of the rotational band built upon the aforementioned $7/2^+[413]$ state. Because these two intrinsic states lie close together, mixing of the two bands due to Coriolis coupling is to be expected (10) so that a simple J(J+1) spectrum would not be

observed.

In conclusion, it may be said with some confidence that certain sets of levels in the odd-mass Ag isotopes possess collective characteristics, as indicated by their selective mode of decay, enhanced B(E2) values, and ease of excitation by charged particle bombardment. It is the exact nature of these collective motions which is uncertain. The inelastic proton scattering experiments of Ford et al. (20, 21) provide persuasive evidence that many of the negative-parity levels can be explained by a simple particle-core weak coupling model. Their discussion is in terms of vibrational excitations of a spherical core, although it should be noted that the de-Shalit model makes no detailed assumptions about the nature of the core excitations.

Recent experimental data, indicating large quadrupole moments and possible rotational bands in the excited states of nuclei which have long been thought to be spherical, have suggested the possibility of nuclear deformations. However, evidence for rotational bands in the odd-mass Ag isotopes is at present essentially limited to the fact that certain sets of energy levels can be fit with the use of parameters which are not unreasonable. Conclusions are especially hampered by the lack of definitive spin-parity assignments for the energy levels of Ag^{111}, whose shape is the most likely to be deformed. What is clear is that none of the present models is capable of explaining successfully a very large fraction of the levels

observed and that a great deal of experimental and theoretical work remains to be done.

BIBLIOGRAPHY

1. Alder, K. et al. Study of nuclear structure by electromagnetic excitation with accelerated ions. Reviews of Modern Physics 28:432-542. 1956.

2. Backlin, A. and B. Fogelberg. Possible deformed states in ^{115}In and ^{117}In. Nuclear Physics A96:539-560. 1967.

3. Berzins, G., M. E. Bunker and J. W. Starner. The decay of ^{111}Pd and ^{111m}Pd. Nuclear Physics A126:273-299. 1969.

4. Berzins, G., M. E. Bunker and J. W. Starner. Ge(Li)-Ge(Li) coincidence studies of the decay of ^{109}Pd. Nuclear Physics A114:512-528. 1968.

5. Black, John L. and Wolfgang Gruhle. The excited states of ^{107}Ag and ^{109}Ag. Nuclear Physics A93:1-30. 1967.

6. Black, J. L. et al. The low-lying excited states of ^{103}Rh. Nuclear Physics A125:545-567. 1969.

7. Blair, J. S. Nuclear spectroscopy with direct reactions. 1964. (Argonne National Laboratory Report ANL-6878).

8. Bohr, A. and B. R. Mottelson. Collective and individual-particle aspects of nuclear structure. Det Kongelige Danske Videnskabernes Selskab 27, no. 16. 1953.

9. Brandhorst, H. W. and J. W. Cobble. Decay of Ru^{105}, Pd^{109}, and Rb^{86}. Physical Review 125:1323-1328. 1962.

10. Brockmeier, R. T. et al. Coriolis coupling between rotational bands in the nucleus W^{183}. Nuclear Physics 63:102-130. 1965.

11. Bromley, D. A. and J. Weneser. New experiments and ideas in the "vibrational" nuclei. Comments on Nuclear and Particle Physics 1:75-79. 1967.

12. Cauchois, Yvette, M. Boivin, and Y. Heno. Photoactivation nucleaire de l'argent naturel. Comptes Rendus des Seances de l'Academie des Sciences 262B:503-506. 1966.

13. Cohen, B. L., J. B. Moorhead and R. A. Moyer. Nuclear-structure studies with (d, p) reactions on Pd^{106} and Pd^{108}. Physical Review 161:1257-1265. 1967.

14. Cohen, Bernard L. and R. E. Price. Survey of inelastic scattering of deuterons by heavy elements. Physical Review 123: 283-294. 1961.

15. Cujec, Bibijana. Nuclear structure studies in the palladium isotopes with (d, p) and (d, t) reactions. Physical Review 131: 735-744. 1963.

16. de-Shalit, A. Core excitations in nondeformed, odd-A, nuclei. Physical Review 122:1530-1536. 1961.

17. Donnelly, D. P. et al. The calibration of a Ge(Li) gamma-ray spectrometer for energy and relative intensity measurements. Nuclear Instruments and Methods 57:219-226. 1967.

18. Eccles, S. F. Gamma ray spectroscopy of ^{107}Cd, ^{109}Pd and ^{111}Pd. Physica 28:251-261. 1962.

19. Fairstein, E. and J. Hahn. Nuclear pulse amplifiers--fundamentals and design practice (Part 3). Nucleonics 23:50-55. 1965.

20. Ford, J. L. C. et al. Elastic and inelastic proton scattering from ^{107}Ag and the phonon-core model. Physical Review 158: 1194-1205. 1967.

21. Ford, J. L. C. et al. Elastic and inelastic proton scattering from ^{109}Ag. Nuclear Physics A142:525-544. 1970.

22. Glenn, J. E. and J. X. Saladin. Static quadrupole moment of the first 2^+ state in ^{114}Cd measured by Coulomb excitation. Physical Review Letters 19:33-36. 1967.

23. Goldberg, M. D. et al. Neutron cross sections. 2d ed. 1966. (Brookhaven National Laboratory Report BNL 325, Supplement No. 2).

24. Goswami, A. and O. Nalcioglu. Quadrupole moment of the 2^+ phonon and the structure of the odd mass spherical nuclei. Physics Letters 26B:353-356. 1968.

25. Goulding, F. S. Semiconductor detectors for nuclear spectrometry, I. Nuclear Instruments and Methods 43:1-54. 1966.

26. Graeffe, G. The decay of ^{97}Ru. Nuclear Physics A127:65-70. 1969.

27. Graeffe, G. and G. E. Gordon. Decay of 13.5h ^{109g}Pd to levels of ^{109}Ag. Nuclear Physics A107:67-80. 1967.

28. Hager, R. S. and E. C. Seltzer. Internal conversion tables part 1: K-, L-, M-shell conversion coefficient for Z=30 to Z=103. Nuclear Data A4:1-235. 1968.

29. Hatch, Kenneth. Aspects of resolution degradation in a nuclear pulse analyzer system. IEEE Transactions on Nuclear Science NS-15(1):303-314. 1968.

30. Hogdahl, Ove T. The radiochemistry of palladium. Washington, D. C. National Academy of Sciences - National Research Council, 1961. 62 p. (Nuclear Science Series. Publication no. NAS-NS 3052).

31. Ikegami, H. and M. Sano. Effect of collective vibrational motion on the anomalous coupling states. Physics Letters 21: 323-325. 1966.

32. Jackson, D. A. and H. Kuhn. The hyperfine structure and Zeeman effect of the resonance lines of silver. Proceedings of the Royal Society of London A158:372-383. 1937.

33. Kisslinger, L. S. A note on coupling schemes in odd-mass nuclei. Nuclear Physics 78:341-352. 1966.

34. Kisslinger, L. S. and K. Kumar. Static quadrupole moment of vibrational, even nuclei and the coupling scheme for odd nuclei. Physical Review Letters 19:1239-1243. 1967.

35. Kisslinger, L. S. and R. A. Sorensen. Spherical nuclei with simple residual forces. Reviews of Modern Physics 35:853-915. 1963.

36. Klein, Claude A. Semiconductor particle detectors: a reassessment of the Fano factor situation. IEEE Transactions on Nuclear Science NS-15(3):214-225. 1968.

37. Lark, N. L. et al. Excited states of Ag^{107}. Nuclear Physics 35:582-592. 1962.

38. Lederer, C. Michael, J. M. Hollander and I. Perlman. Table of isotopes. 6th ed. New York, Wiley, 1967. 594 p.

39. Levy, A. J. and R. C. Ritter. Linearity of a Ge(Li) detector in the range 0.5 to 10 MeV. Nuclear Instruments and Methods 49:359-360. 1967.

40. Mariscotti, M. A. J. et al. Phenomenological analysis of ground-state bands in even-even nuclei. Physical Review 178: 1864-1887. 1969.

41. McDonald, J. and D. Porter. Excited states in ^{111}Cd. Nuclear Physics A109:529-538. 1968.

42. McDonald, J. et al. Excited states in ^{115}In. Nuclear Physics A104:177-188. 1967.

43. McGinnis, Carl L. Radioactivity of Pd^{111}. Physical Review 87:202. 1952.

44. McGowan, F. K. and P. H. Stelson. Yields, angular distributions, and polarization of gamma rays from Coulomb excitation. Physical Review 109:901-916. 1958.

45. McGowan, F. K. et al. Coulomb excitation of states in the even-mass ruthenium nuclei with ^{16}O and ^{4}He ions. Nuclear Physics A113:529-542. 1968.

46. Moszkowski, S. A. A rapid method of calculating log(ft) values for beta-transitions. Physical Review 82:35-37. 1951.

47. Palms, J. M., P. V. Rao and R. E. Wood. An ultra-high resolution Ge(Li) spectrometer for singles and coincidence X-ray and gamma-ray studies. Nuclear Instruments and Methods 64:310-316. 1968.

48. Pandharipande, V. R., R. M. Singru and R. P. Sharma. Decay of Pd^{111} and Pd^{111m}. Physical Review 140:B1488-1496. 1965.

49. Pandharipande, V. R. et al. Level structure of ^{117}In from the decay of ^{117}Cd. Nuclear Physics A109:81-93. 1968.

50. Pratt, W. W. and R. G. Cochran. Beta- and gamma-ray spectra of Pd^{111}. Physical Review 118:1313-1315. 1960.

51. Preston, M. A. Physics of the nucleus. Reading, Mass., Addison-Wesley. 1962. 661 p.

52. Radeka, Veljko. Low-noise preamplifiers for nuçlear detectors. Nucleonics 23:52-55. 1965.

53. Rall, Wilfred. Mass assignments of some radioactive isotopes of Pd and Ir. Physical Review 70:112. 1946.

54. Robinson, R. L. et al. Coulomb excitation of Ag^{109}. 1966. (Oak Ridge National Laboratory Report ORNL-4082).

55. Robinson, R. L. et al. Gamma-gamma angular correlations following Coulomb excitation. Nuclear Physics A123:193-204. 1969.

56. Sastry, V. V. G., et al. The radioactive decay of Ag^{111}. Nuclear Physics 56:140-146. 1964.

57. Schick, W. C. and W. L. Talbert. Gamma-ray decay schemes of ^{109g}Pd, ^{111g}Pd and ^{111m}Pd. Nuclear Physics A128:353-387. 1969.

58. Sen, S. K. and I. O. Durosinmi-Etti. Measurement of α_K, α_{total}, and K/(L+M) for electron capture transitions in ^{113m}In and ^{109m}Ag with a solid state detector. Physics Letters 18:144-146. 1965.

59. Sherwood, A. I. and A. Goswami. Extended quasi-particle-phonon coupling theory for odd-mass spherical nuclei. Nuclear Physics 89:465-480. 1966.

60. Shilling, G. et al. Static quadrupole moment of the 2^+ state in ^{114}Cd. Physical Review Letters 19:318-321. 1967.

61. Shindewolf, U. L., J. W. Winchester and C. D. Coryell. Decay properties of 74-second Ag^{111m}. Physical Review 105: 1763-1765. 1956.

62. Siegbahn, Kai. E. Kondaiah and S. Johansson. Decay of Pd-109. Nature 164:405-406. 1949.

63. Simpson, J. J. et al. A determination of quadrupole moments in ^{114}Cd, ^{130}Ba, ^{148}Sm, and ^{150}Sm. Nuclear Physics A94: 177-191. 1967.

64. Slater, David N. Gamma-rays of radionuclides in order of increasing energy. London, Butterworths, 1962. 201 p.

65. Sperduto, A., M. Mazari, and W. W. Buechner. (p, p') and (d, p) reactions from Silver. Bulletin of the American Physics Society 4:287. 1959.

66. Starner, J. W. Decay of Pd^{109} and Pd^{109m}. Bulletin of the American Physical Society 4:99. 1959.

67. Stelson, P. H. et al. Excitation of collective states by the inelastic scattering of 14 MeV neutrons. Nuclear Physics 68: 97-140. 1965.

68. Stewart, W. M. et al. Core excitations in ^{107}Ag, ^{109}Ag, ^{113}In, ^{115}In, ^{127}Sb, and ^{123}Sb resulting from inelastic scattering of 42-MeV alpha particles. Physical Review 171:1316-1324. 1968.

69. Stokstad, R. G. et al. The determination of the static quadrupole moments of the first 2^+ states in ^{114}Cd and ^{116}Cd by higher order effects in Coulomb excitation. Nuclear Physics A92:319-344. 1967.

70. Talmi, I. and I. Unna. Energy levels and configuration interaction in Zr^{90} and related nuclei. Nuclear Physics 19:225-242. 1960.

71. Tamura, Taro and T. Udagswa. Static quadrupole moment of the first 2^+ state of vibrational nuclei. Physical Review 150: 783-790. 1966.

72. Van Eyk, C. W. E. et al. The decay of ^{99}Mo. Nuclear Physics A121:440-462. 1968.

73. Vonach, W. G. and A. B. Smith. Elastic and inelastic scattering of fast neutrons from Ag, In, and Cd. Nuclear Physics 78: 389-408. 1966.

74. Walker, Donald Arthur. The decay of ^{61}Cu and ^{59}Cu--energy levels of ^{61}Ni and ^{59}Ni. Doctoral dissertation. Corvallis, Oregon State University, 1968. 136 numb. leaves.

75. Wapstra, A. H. Nuclear spectroscopy tables. Amsterdam, North-Holland. 1959. 135 p.

76. Wapstra, A. H. and W. Van der Eyk. The decay of ^{109}Cd, ^{109}Ag and ^{109}Pd. Nuclear Physics 4:325-329. 1957.

77. Way, K. et al. Nuclear data sheet NRC60-2-54. Washington, D. C., National Academy of Sciences. 1960.

78. Way, K. et al. Nuclear data sheet NRC60-2-82. Washington, D. C., National Academy of Sciences. 1960.

79. White, Gladys. X-ray attenuation coefficients from 10 keV to 100 MeV. Washington, D. C., National Bureau of Standards, 1957. 54 p. (National Bureau of Standards. Circular 583).

80. Woodgate, G. K. and R. W. Hellworth. Hyperfine structure of radioactive silver ^{111}Ag. Proceedings of the Physical Society (London) 69A:581-587. 1956.